

Development of an oral redox nanotherapeutics for
treatment of colitis and colon cancer

Vong Binh Long

Doctoral Program in Materials Science

Submitted to the Graduate School of

Pure and Applied Sciences

in Partial Fulfillment of the Requirements

for the Degree of Doctor of Philosophy in Engineering

at the

University of Tsukuba

Preface

- The present thesis is the collection of studies carried out during 3-year PhD course (March 2012 to March 2015) at University of Tsukuba. The studies are concerned with the development novel oral redox nanotherapeutics for treatment of inflammatory bowel disease and cancer. Such research and design of the biomaterial devices should have great potential and contribution to science as well as clinical applications. I would like to take this opportunity to thank many people who have made this thesis successful.

- First, I would like to express my sincerest and the grateful gratitude to my advisor, Professor Yukio Nagasaki, for providing me the opportunity to pursue Ph.D. degree and your valuable guidance, beneficial comments, and kind supports throughout the duration of the present study. Under the guidance, you also allow me the freedom to think and conduct this research independently, which improved my research skills very much.

- I am also grateful to my thesis committee members, Professor Masashi Kijima, Professor Takao Aoyagi and Professor Gouping Cheng, for your constructive comments crucial feedback to improve my thesis.

- I wish express my gratitude to Professor Hirofumi Matsui and Professor Kazuya Morikawa for your instructive guidance, kind supports and for the successful collaboration.

- The author would like to thank from the bottom of the heart to Dr. Toru Yoshitomi, for your encouragements and helpful discussions to improve this work.

- I am deeply grateful to Dr. Yutaka Ikeda, Dr. Yukuchi Horiguchi and Dr. Chonpathompikunlert Pennapa for your hearty encouragements, valuable advices for this study and my life.

- Although, I cannot list anyone I have come to contact with, I greatly appreciate to all members of Nagasaki Laboratory for your warm assistance, time, advices, and making friendly environment.

- I would like to thank to many of my friends, giving me valuable comments, the

encouragement and motivation in my research as well as my life.

- I also would like to express my sincere appreciation for the Research Fellowship of the Japan Society for the Promotion of Science (JSPS) for Young Scientists.

- I would like to thank the Department of Materials Science, University of Tsukuba, for accepting me into the PhD program.

- I also would like to thank all of my teachers and colleagues in Department of Biochemistry, University of Science Ho Chi Minh City-Vietnam National University, where I have completed my Bachelor and Master courses.

- Finally, I sincerely express my profound appreciation to my family members, especially my parents as well as my wife, Trinh Nhu Thuy, for your assistance and encouragements, giving me strength and motivation during my study.

Vong Binh Long

Graduate School of Pure and Applied Sciences

University of Tsukuba

February 2015

List of Contents

Preface

Chapter 1: General Introduction

- 1.1. Inflammatory bowel disease and colitis associated colon cancer
- 1.2. Current drugs for inflammatory bowel disease
- 1.3 Nitroxide radicals
- 1.4. Drug delivery system
 - 1.4.1. *Nanomedicine*
 - 1.4.2. *Gastrointestinal (GI) tract and oral drug delivery*
- 1.5. Objective of this study
- 1.6. References

Chapter 2: Preparation of Redox polymer and Redox nanoparticle

Abstract

- 2.1. Introduction
- 2.2. Materials and Methods
 - 2.2.1. Materials
 - 2.2.2. Synthesis of MeO-PEG-*b*-PCMS
 - 2.2.3. Synthesis of redox polymer (MeO-PEG-*b*-PMOT)
 - 2.2.4. Preparation of redox nanoparticles (RNP⁰)
- 2.3. Results
 - 2.3.1. Synthesis of MeO-PEG-*b*-PCMS
 - 2.3.2. Synthesis of redox polymer (MeO-PEG-*b*-PMOT)
 - 2.3.3. Preparation of redox nanoparticles (RNP⁰)
- 2.4. Discussions and Conclusion
- 2.5. References

Chapter 3: The specific accumulation of orally administered redox nanoparticles in inflamed colon and therapeutic effect on colitis mice

Abstract

3.1. Introduction

3.2. Materials and Methods

3.2.1. Preparation of RNP^O

3.2.2. Preparation of rhodamine-labeled RNP^O

3.2.3. Preparation of ¹²⁵I-labeled RNP^O

3.2.4. Preparation of different sized polystyrene latex particles with nitroxide radicals

3.2.5. Animals

3.2.6. Localization of RNP^O in the colon

3.2.7. Accumulation of RNP^O in the colon

3.2.8. Biodistribution of RNP^O

3.2.9. Induction of colitis by DSS and drug administration

3.2.10. Evaluation of colitis severity by disease activity index (DAI) and colon length

3.2.11. Histological assessment

3.2.12. Myeloperoxidase (MPO) activity

3.2.13. Interleukin IL-1 β measurement

3.2.14. Measurement of colon superoxide production in vivo

3.2.15. Intravital observation by in vivo live imaging

3.2.16. Survival rate experiment

3.2.17. Statistical analysis

3.3. Results

3.3.1. Specific accumulation of RNP^O in colonic mucosa and inflamed colon area

3.3.2. Distribution and non-absorption into bloodstream of RNP^O after oral administration

3.3.3. Stability of RNP^O in GI tract

3.3.4. Therapeutic effect of RNP^O on DSS-induced colitis in mice

3.3.5. *RNP^O suppresses pro-inflammatory mediators and enhances survival rate in mice*

3.4. Discussion and Conclusions

3.5. References

Chapter 4: Effect of redox nanoparticle on intestinal microflora

Abstract

4.1. Introduction

4.2. Materials and Methods

4.2.1. *Preparation of redox polymer and RNP^O*

4.2.2. *Animals*

4.2.3. *Murine model of DSS-induced colitis and experimental groups*

4.2.4. *Microbiological assay and medium*

4.2.5. *Statistical analysis*

4.3. Results

4.3.1. *Effect of RNP^O on DSS-induced colitis mice*

4.3.2. *Effect of RNP^O on microflora in normal and DSS-induced colitis mice*

4.4. Discussion and Conclusions

4.5. References

Chapter 5: Therapeutic effect redox nanoparticle on colitis-associated colon cancer

Abstract

5.1. Introduction

5.2. Materials and Methods

5.2.1. *Preparation of RNP^O*

5.2.2. *Cell lines and cultures*

5.2.3. *Cellular uptake of RNP^O in vitro*

5.2.4. *Animal*

5.2.5. *Cellular internalization of RNP^O in vivo*

5.2.6. Induction of colitis and CAC by AOM and DSS

5.2.7. Endoscopic imaging and tumor scoring

5.2.8. Iri-induced intestinal mucositis in mice

5.2.9. Statistical analysis

5.3. Results

5.3.1. Accumulation of free drinking RNP^O in the GI tract and its non-toxicity

5.3.2. Specific cellular internalization of RNP^O in cancer tissues

5.3.3. RNP^O prevents AOM/DSS-induced CAC by suppressing inflammation

5.3.4. Therapeutic effect of free drinking RNP^O against AOM/DSS-induced CAC

5.3.5. RNP^O improves the anticancer efficacy of Iri and reduces its adverse effects

5.4. Discussion and Conclusions

5.5. References

Chapter 6: Summary and Conclusion

List of Publications

List of Presentations

Chapter 1

General Introduction

1.1. Inflammatory bowel disease and colitis associated colon cancer

- Inflammatory bowel disease (IBD) comprises two types of disorders, Crohn's disease (CD) and ulcerative colitis (UC), which are chronic intractable diseases. Millions of patients in the world are suffering from these diseases.¹ While CD involves any part of the gastrointestinal (GI) tract, the inflammation of UC merely exists at colon area (**Figure 1.1**).^{2,3} Although the exact etiology and pathogenesis of IBD remain uncertain, it is incriminated in a complex interaction of environmental, genetic, and immune-regulatory factors.⁴ It has been reported that the intestinal mucosa of patients with IBD is characterized by reactive oxygen species (ROS) overproduction and an imbalance of important antioxidants, leading to oxidative damage.⁵ ROS are highly reactive molecules containing oxygen, which cause strong oxidative damage to biomolecules such as lipid, protein, DNA, and other macromolecules. Self-sustaining cycles of oxidant production may amplify inflammation and mucosal injury.⁶⁻⁹

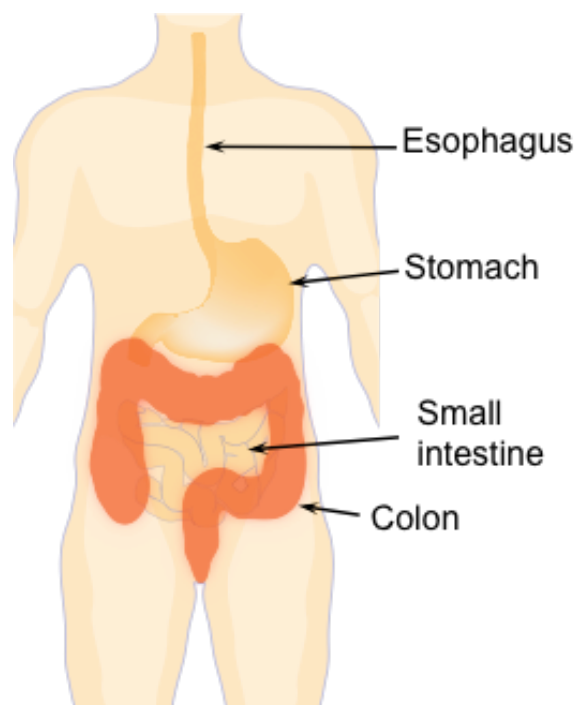


Figure 1.1: Human gastrointestinal (GI) tract

- On the other hand, the intestinal microflora also plays critical role in IBD. Human GI tract hosts a huge number of microflora. In particular, the number of bacteria in large intestine can reach upward of $10^{13} - 10^{14}$ bacteria, with more than 500 different bacterial species.¹⁰ In the normal conditions, these intestinal microflora contribute to the development of immune system, produce some key nutrients, and regulate the energy metabolism in intestine.¹¹ However, the increase in a number of pathogenic bacteria has been assumed in development of IBD. It has been reported that antibiotics show some effect to IBD patients, and intestinal microflora causes the inflammation to develop colitis mice models.^{12, 13}

- In addition, IBD patients have high risk to develop colitis-associated cancer (CAC), an subtype of colon rectal cancer, which is difficult to treat and has high mortality. Colon rectal cancer is the 2nd most common cause of cancer deaths in United States and other developed countries. More than 20% of IBD patients develop CAC within 30 years of disease onset, and 50% of these will die from CAC.^{14,15} In the UC patients, the inflammatory environment in colon can promote the accumulation of additional mutations and epigenetic changes. For example, overproduced ROS by activated inflammatory cells can induce DNA damage, genetic instability and mutations.¹⁶

1.2. Current drugs for inflammatory bowel disease

- For many decades, a large number of drugs have been developed for treatment of patients with IBD. These drugs include anti-inflammatory drugs, immunosuppressants, biological agents, and antibiotics. Due to the significant advances in therapy for IBD, many new medications are now under investigation. Although they are effective in treating IBD in some extent, their severe side effects have raised significant concerns among both physicians and patients, and limited their use.^{17,18}

- Mesalamine (or 5-aminosalicylic acid [5-ASA]) is an anti-inflammatory drug used to treat

the patient with mild to moderate active UC and for maintaining remission. Orally administered mesalamine has anti-inflammatory effect by moderating the production of pro-inflammatory cytokines, lipid mediators, and ROS. Sulfasalazine, a prodrug first developed in 1942, consists of mesalamine linked by an azo bond to sulfapyridine. Sulfasalazine is converted to sulfapyridine and mesalamine by bacterial enzyme in the colon, thus, orally administered sulfasalazine will delay the release of mesalamine in colon area.¹⁹ Corticosteroids are also anti-inflammatory agents, which have been used for more than 50 years, for moderate to severe both UC and CD. Corticosteroids can suppress the interleukin transcription, and the activation of nuclear factor kappa B (NF- κ B), which inhibit the inflammatory responses. However, depending on the dose, these anti-inflammatory may cause some adverse effects such as headache, nausea, diarrhea, dyspepsia, etc...

- Since the early 1970s, azathioprine and 6-mercaptopurine have been used as immunosuppressants to treat IBD by inhibiting the proliferation and activation of lymphocytes. Azathioprine is metabolized to 6-mercaptopurine and subsequently to 6-thioguanine nucleotides. They are effective for both active disease and maintaining remission in CD and UC. The metabolized thioguanine causes severe adverse effects including GI toxicity, hepatotoxicity, and pancreatitis.

- Because necrosis factor alpha (TNF- α) play an important role in the process of the inflammation in IBD, the new drugs have been recently developed to target the inflammatory immune factor such as TNF- α . The administration of humanized monoclonal antibodies is an entirely new and potentially highly successful concept for treating IBD. The first such product, infliximab, is available for treating refractory CD by inhibiting the functional activity of TNF- α .²⁰ Other available anti-TNF- α agents, adalimumab and certolizumab pegol, have been also approved to use in the United States. Although these anti-TNF- α antibody work well to suppress

inflammation, the severe side effects such as antibody resistance, fever, heart failure still remains.

1.3. Nitroxide radicals

- Cyclic nitroxides, also known as aminoxyls or nitroxyls, are stable free radicals. The methyl groups confer stability to the nitroxide radicals by preventing radical–radical dismutation and also limit access to reactive substances, which can quench the radical species. 4-hydroxyl-2,2,6,6-tetramethylpiperidine-1-oxyl (TEMPOL), six-membered piperidine nitroxide, is one of common used nitroxide radicals. Various states of TEMPOL are formed by the redox transformations between the oxidation states of nitroxide, hydroxylamine, and the oxoammonium cation (**Figure 1.2**).²¹ Because nitroxide radicals possess an impaired electron, they have been utilized as biophysical tools for electron paramagnetic resonance (EPR) spectroscopic studies such as spin label/oxyometry and spin strapping.²² However, possessing unique antioxidant properties nitroxide radicals have recently been used in novel therapies. Similar to Superoxide dismutase (SOD), nitroxide radicals act as a catalyst of superoxide anion to hydrogen peroxide (H_2O_2) and oxygen. Therefore, nitroxide compounds have been used for protection against oxidative damage in a number of cellular studies and clinical applications. TEMPOL and its hydroxylamine significantly protected Chinese hamster V79 lung fibroblasts from the damages induced by superoxide and H_2O_2 .²³ Similar protective effects of nitroxides were observed in cells exposed to oxidants indicating that nitroxides are effective in scavenging a wide variety of reactive intermediates.^{24,25}

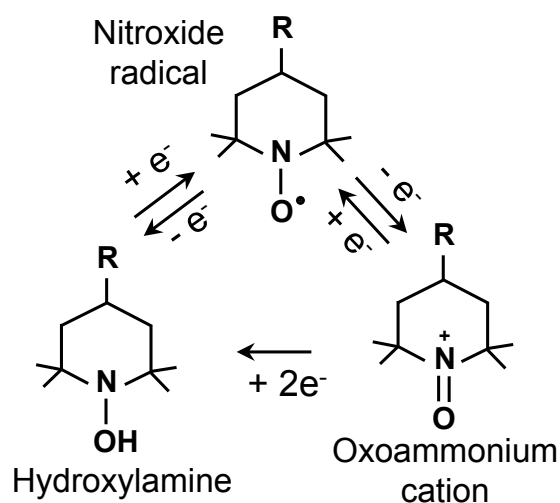


Figure 1.2: Nitroxide radical and the redox transformations between the oxidation states of nitroxide, hydroxylamine, and the oxoammonium cation.

- In addition, several clinical applications of nitroxide compounds have been discovered for radioprotection, functional imaging, and inflammation-cancer prevention. Whereas only 15% of the untreated C3H mice were alive at 30 days after irradiation with a single dose of 9 Gy, the nitroxide-treated mice showed significantly improved survival ranging from 35 to 100% depending on the nitroxide used.²⁶ In another experiment, TEMPOL-treated pigs significantly improved alopecia, a severe side effect of ionizing radiation, as compared to untreated pigs.²⁷ In a study of transient cerebral ischemia in rats, TEMPOL-treated group effectively prevented postischemic ROS formation and lipid peroxidation.²⁸ Furthermore, Cuzzocrea et al reported that administration of TEMPOL reduces the activation of NF- κ B *in vivo*,²⁹ suppressing inflammation in several mouse models such as pancreatitis, pleurisy, arthritis, colitis, uveoretinitis, and atherosclerosis.^{30,31,32,33,34} For the cancer therapy, the antioxidant activity of TEMPOL reduced oxidative DNA damage in Fanconi anemia fibroblasts and mice, delaying the tumor progression.³⁵ TEMPOL increased latency to tumorigenesis and doubled the lifespan of Atm-deficient mice, a mouse model of ataxia telangiectasia, which displays accelerated oxidative damage and stress.³⁶ TEMPOL

administered in either the drinking water or food to C3H mice significantly reduced the tumor incidence and improved the lifespan as compared to untreated-mice.³⁷ More studies on these nitroxide compounds now being conducted, more potential applications will be uncovered.

- Although these nitroxide radicals have a great potential as therapeutics, these compounds still face several problems under *in vivo* conditions. Because nitroxide radicals are low-molecular-weight (LMW) compounds, administration of these compounds results in the nonspecific dispersion in normal tissues, preferential renal clearance, rapid reduction of the nitroxide radical to the corresponding hydroxylamine, and unwanted adverse effects. Therefore, a novel approach is necessary to utilize these nitroxide compounds as an effective therapy.

1.4. Drug delivery system

1.4.1. Nanomedicine

- As mentioned above, administration of LMW compounds *in vivo* is not effective due to non-specific distribution, low stability, adverse effect. Recently, nanotechnology-based drug delivery systems have attracted a great attention of scientists from different fields. The term nanomedicine, the medical application of nanotechnology, was first used in the 2000.³⁸ Nanoparticles are defined as materials with the dimension between approximately 1 and 100 nm (**Figure 1.3**).³⁹ Nanoparticle-based drug delivery systems include nanocrystal, liposome, polymeric micelle, protein-based nanoparticle, dendrimer, carbon nanotube and polymer–drug conjugate.⁴⁰ These drug loading nanocarriers, which have prolonged blood circulation property, can minimize the nonspecific accumulation in normal tissues to preferentially accumulate in diseased tissues such as inflamed and cancer tissues by enhanced permeability and retention (EPR) effect, characterized by microvascular hyperpermeability to circulating macromolecules and impaired lymphatic drainage in tumor tissues.⁴¹ To effectively deliver drug to the targeted tumor

tissue, nanoparticles must have the ability to remain in the bloodstream for a considerable time without being eliminated.

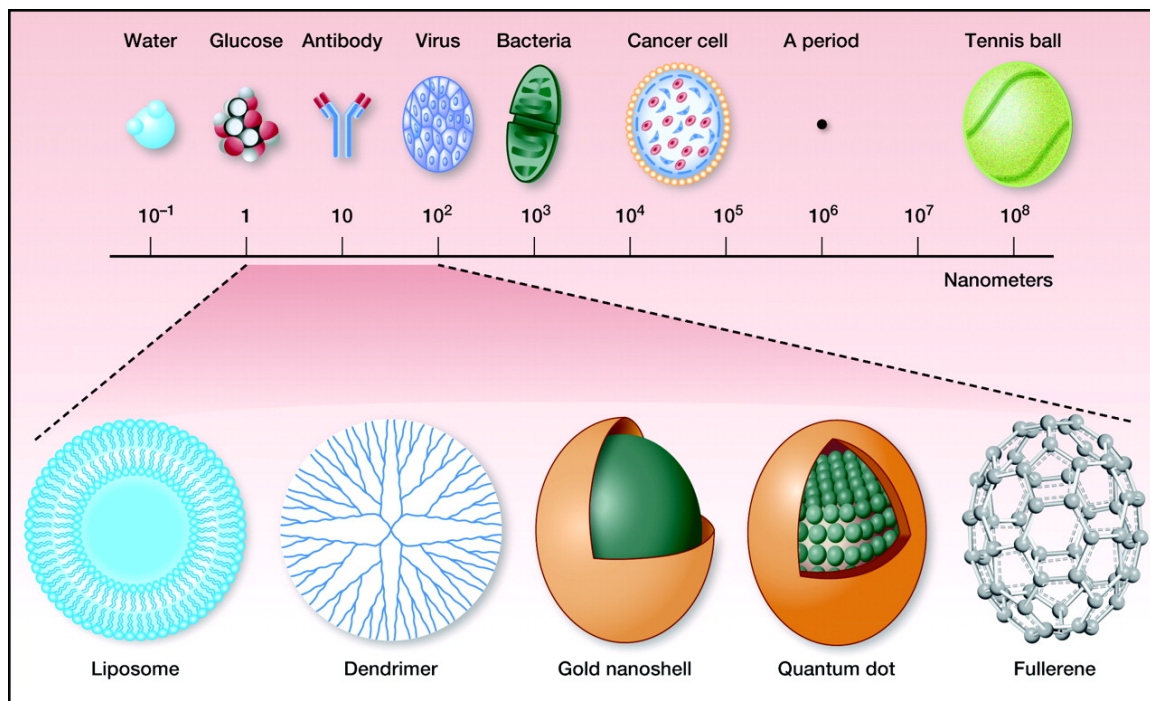


Figure 1.3: Definition of nanotechnology and examples of nanotechnology platforms used in drug development. (Ref. 39)

- The size and surface characteristics have a great effect on biodistribution of nanoparticles. The size of nanoparticles used in a drug delivery system should be large enough to prevent their rapid leakage into blood capillaries but small enough to escape capture by fixed macrophages that are lodged in the reticuloendothelial system.⁴² After administration, small particles (<20–30 nm) are eliminated by renal excretion.⁴³ Larger particles can be rapidly taken up by the mononuclear phagocytic system cells present in the liver, the spleen, and to a lesser extent, in the bone marrow. Nanoparticles of 150–300 nm are found mainly in the liver and the spleen,⁴⁴ whereas particles of 30–150 nm are located in bone marrow,⁴⁵ the heart, the kidney and the stomach.^{46,47} Modifying the surface chemistry of nanoparticles also plays an important role in organ distribution and half-life bloodstream circulation. The absorption of plasma proteins to the surface, which are

caused by surface charge or hydrophobicity, results in the higher susceptibility of nanoparticle to phagocytosis.⁴⁸ The most common method to improve the bloodstream circulation and prevent the plasma protein absorption is to block the surface using polymer such polyethylene glycol (PEG), polyvinyl alcohol (PVA), polysaccharides, ect... Among them, PEG appeared as an ideal candidate, and was extensively used to coat the surface of nanoparticles, since it has been shown to successfully prevent the uptake of mononuclear phagocytic system and lead to prolonged blood circulation time.^{49,50}

1.4.2. Gastrointestinal (GI) tract and oral drug delivery

- GI tract is a part of digestive system consisting of the stomach, small intestine, and large intestine (**Figure 1.1**). Intestinal epithelium is an efficient physical barrier that covers the surfaces of the GI tract, allowing selective absorption of nutrients, electrolytes and fluids, at the same time protecting the host from environmental pathogens. This epithelial cell layer comprises enterocytes, goblet cells, Paneth cells, and M cells, as shown in **Figure 1.4**.⁵¹ Enterocytes, the most abundant epithelial cells in the intestine, have the function to absorb nutrients. Goblet cells, the second most abundant cells interspersing among other cell types, secrete the mucus on the surface. Paneth cells can secrete certain antimicrobial proteins that selectively bind and kill the bacteria. M cells, which are specialized epithelial cells that reside predominantly in the Peyer's patches, can take up antigens and microorganisms from the intestinal lumen and then deliver them to the underlying immune system of mucosa.⁵² In addition, physical integrity of the intestinal epithelium can be attributed to the presence of tight junctions between contiguous epithelial cells, preventing paracellular uptake pathway of macromolecules in intestinal epithelium.⁵³

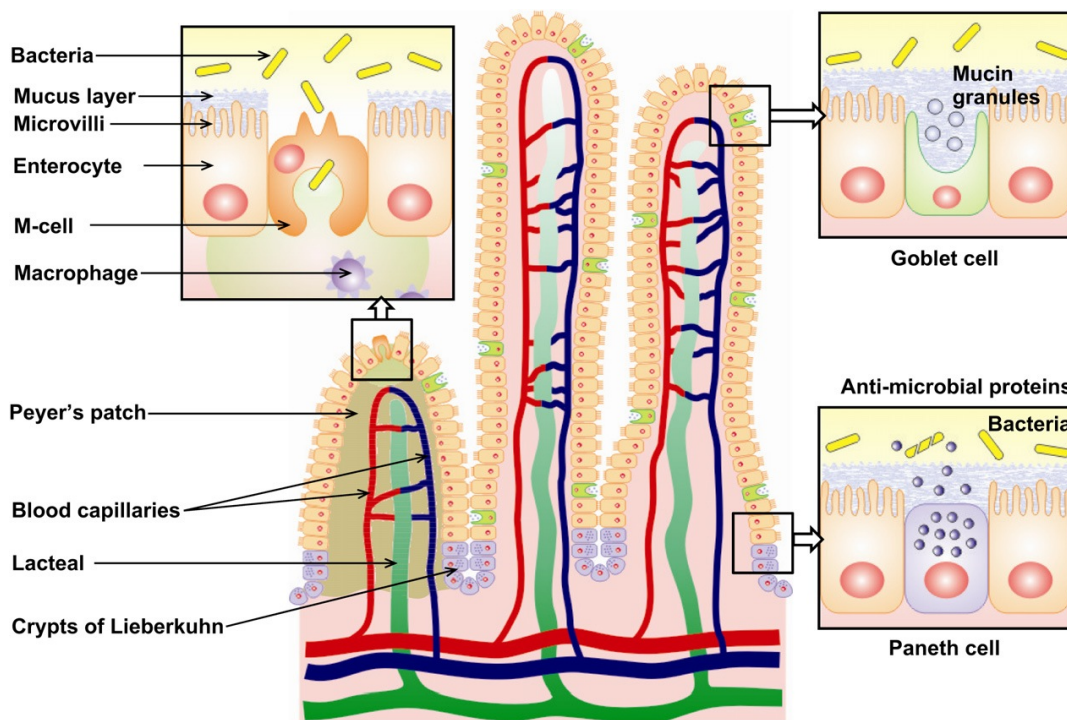


Figure 1.4: Schematic illustrations of the structure of the intestinal epithelium. (Ref. 51)

- Compare to other routes of drug administration such as intravenous, subcutaneous, and local injections, oral administration is the most widely used and readily accepted form of drug administration due to its safety as well as patient convenience and compliance. Despite these potential advantages, oral formulations face several common problems, particularly for peptides and proteins: poor stability in the gastric environment, low solubility and/or bioavailability and the mucus barrier can prevent drug penetration and subsequent absorption.⁵⁴ A number of drugs are susceptible to the variation of pH in the GI tract. The luminal pH in stomach is strong acidic in the stomach (pH 1–3), and rapidly changes to pH 6 in duodenum. The pH gradually increases in the small intestine from pH 6 to about pH 7.4 in the terminal ileum. The pH drops to 5.7 in the caecum, but again gradually increases, reaching pH 6.7 in the rectum.^{55,56} Oral administration of LMW drugs, particularly for protein drugs, is going to degradation not only by various pH but also a number of enzymes such as trypsin, elastase, carboxypeptidase existing in stomach and intestine.⁵⁷ On the other hand, mucus, a smooth and thick substance, covers the entire inner surface of the GI

tract from stomach to colon. In the rat GI tract, the thickness of mucus layer increases from stomach (about 200 μm) to colon (about 800 μm).⁵⁸ The mucus layer, a significant barrier, protects epithelial surfaces from the penetration of bacteria and foreign particles into mucosa. In the IBD patients, however, the overall thickness of the adherent mucus layer is reduced due to the reduction of goblet cells, and the opening tight junction of epithelium cells occurs, resulting the facile penetration of bacteria and foreign particles into mucosa.^{59,60} LMW drugs can be capsulated and protected from the harsh gastric environment by polymeric nanoparticles. The nanoparticle-based drug delivery systems may achieve mucoadhesion via hydrogen bonding, polymer entanglements with mucins, hydrophobic interaction, or combination of them.⁶¹ To improve oral delivery, polymeric nanoparticles can be applied by targeting M cells, which are more capable of transporting macromolecules as compared to other intestinal epithelial cells.^{62,63} In addition, transient opening of tight junctions could improve the permeation of drugs from the intestinal lumen to the systemic circulation.^{64,65} Therefore, if the anti-inflammatory drugs can be orally delivered to inflamed area of GI tract, it is anticipated to be an idea therapeutics for treatment of IBD patients.

1.5. Objective of this study

- Antioxidants are promising agents for treatment of UC patients because colonic mucosa of these patients overproduces ROS, which induce oxidative stress and intestinal damages. However, oral delivery of LWM antioxidant compounds faces some issues such as degradation in acidic environment of stomach, absorption into bloodstream via small intestine, resulting low accumulation in colon regions. Recently, several nanoparticles have been developed for delivery of bioactive agents such as siRNA and antioxidants to inflamed colon regions.^{66,67,68} Although these nanoparticles improve the efficiency to some extent, the accumulation of bioactive compounds in colon is still low due to the uncontrolled release of payload during delivery in GI tract, and the

toxicity of these nanocarriers must be concerned.

- The objective of this study is to develop an effective and safe nanotherapy for the treatment of colitis and colitis-associated colon cancer via oral administration. To overcome the current issues, we have developed a novel redox nanoparticles (RNP^O), in which nitroxide radicals TEMPO, as ROS scavenging moiety, are covalently installed to large molecular weight chains in order to avoid the possible internalization in healthy cells and mitochondria, which prevents adverse effect of nitroxide radicals in normal tissues. In addition, because ROS scavenging moiety is strongly connected in the nanoparticles, leakage of nitroxide radicals and toxicity of nanoparticle itself during drug delivery can be minimized. Redox nanoparticle RNP^O was prepared by self-assembly of methoxy-poly(ethylene glycol)-*b*-poly(4-[2,2,6,6-tetramethylpiperidine-1-oxyl]oxymethylstyrene) (MeO-PEG-*b*-PMOT), which is an amphiphilic block copolymer with stable nitroxide radicals in a hydrophobic segment as a side chain via an ether linkage (Figure 1.5).

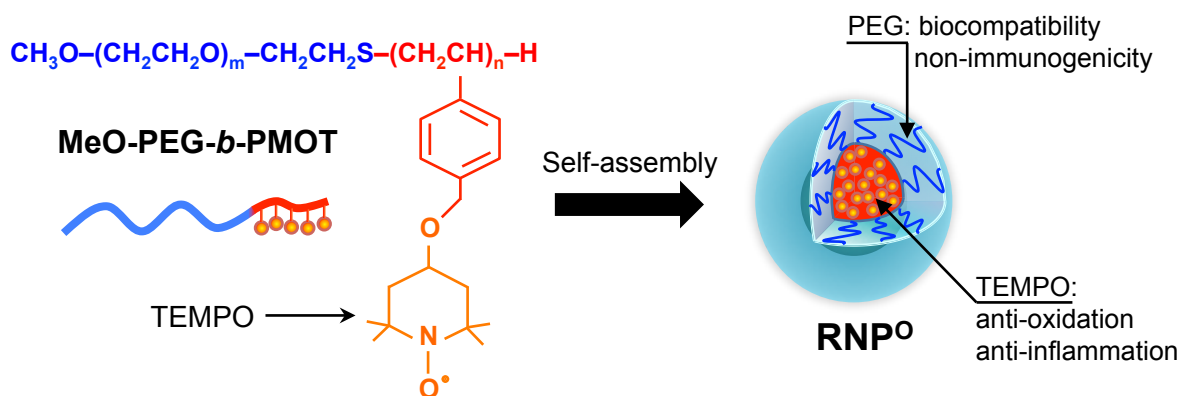


Figure 1.5: Schematic illustration of redox polymer MeO-PEG-*b*-PMOT and redox nanoparticle RNP^O using in this study.

This thesis includes six chapters.

- **Chapter 1** describes general introduction.
- **Chapter 2** describes the Synthesis of Redox polymers and Preparation of Redox nanoparticles.
- **Chapter 3** describes the specific Accumulation of orally administered redox nanoparticles in inflamed colon and Therapeutic effect of redox nanoparticle on colitis mice.
- **Chapter 4** describes the effect of redox nanoparticle on intestinal microflora.
- **Chapter 5** describes the therapeutic effect redox nanoparticles on colitis-associated colon cancer.
- **Chapter 6** describes the Summary and Conclusion.

1.6. References

1. Loftus EV Jr. *Gastroenterology* **2004**;126(6):1504–17.
2. Khor B, Gardet A, Xavier RJ. *Nature* **2011**;474(7351):307–17.
3. Abraham C, Cho JH. *N Engl J Med* **2009**;361(21):2066–78.
4. Hanauer SB. *Inflamm Bowel Dis* **2006**;12 Suppl 1:S3–9.
5. Pavlick KP, Laroux FS, Fuseler J, Wolf RE, Gray L, Hoffman J, et al. *Free Radic Biol Med* **2002**;33(3):311–22.
6. Simmonds NJ, Rampton DS. *Gut* **1993**;34:865–868.
7. Xavier RJ, Podolsky DK. *Nat Rev* **2007**;448:427–434.
8. Babbs CF. *Free Radic Biol Med* **1992**;13:169–182.
9. McCord JM. *Am J Med* **2000**;108:652–659.
10. Sasaki M, Klapproth J. *J Signal Transduct* **2012**;doi: 10.1155/2012/704953.
11. Bäckhed F, Ley RE, Sonnenburg JL, Peterson DA, Gordon JI. *Science* **2005**;307(5717):1915–20.
12. Elson CO, Cong Y, McCracken VJ, Dimmitt RA, Lorenz RG, Weaver CT. *Immunol Rev.* **2005**;206:260–76.
13. Loh G, Blaut M. *Gut Microbes* **2012**;3(6):544–55.

14. Feagins LA, Souza RF, Spechler SJ. *Nat Rev Gastroenterol Hepatol* **2009**;6(5):297–305.
15. Terzić J, Grivennikov S, Karin E, Karin M. *Gastroenterology* **2010**;138(6):2101–14.e5.
16. Meira LB, Bugni JM, Green SL, Lee CW, Pang B, Borenshtein D, et al. *J Clin Invest* **2008**;118(7):2516–25.
17. Mowat C, Cole A, Windsor A, Ahmad T, Arnott I, Driscoll R, et al. *Gut* **2011**;60(5):571–607.
18. Triantafyllidis JK, Merikas M, Georgopoulos F. *Drug Des Devel Ther* **2011**;5:185–210.
19. Karagozian R, Burakoff R. *Ther Clin Risk Manag* **2007**;3(5):893–903.
20. Anand B, Pithadia, Sunita Jain. *Pharmacological Reports* **2011**;63(3):629–42.
21. Soule BP, Hyodo F, Matsumoto K, Simone NL, Cook JA, Krishna MC, et al. *Free Radic Biol Med* **2007**;42(11):1632–50.
22. Fuchs J, Groth N, Herrling T, Zimmer G. *Free Radic Biol Med* **1997**;22(6):967–76.
23. Mitchell JB, Samuni A, Krishna MC, DeGraff WG, Ahn MS, Samuni U, et al. *Biochemistry* **1990**;29(11):2802–7.
24. Samuni A, Mitchell JB, DeGraff W, Krishna CM, Samuni U, Russo A. *Free Radic Res Commun* **1991**;12-13 (Pt 1):187–94.
25. Dhanasekaran A, Kotamraju S, Karunakaran C, Kalivendi SV, Thomas S, Joseph J, et al. *Free Radic Biol Med* **2005**;39:567–83.
26. Hahn SM, DeLuca AM, Coffin D, Krishna CM, Mitchell JB. *Int J Radiat Oncol Biol Phys* **1998**;42:839–42.
27. Goffman T, Cuscela D, Glass J, Hahn S, Krishna CM, Lupton G, Mitchell JB. *Int J Radiat Oncol Biol Phys* **1992**;22:803–6.
28. Kato N, Yanaka K, Hyodo K, Homma K, Nagase S, Nose T. *Brain Res* **2003**;979:188–93.
29. Cuzzocrea S, Pisano B, Dugo L, Ianaro A, Patel NS, Caputi AP, Thiemermann C. *Free Radic Res* **2004**;38(8):813–9.
30. Ledzinski Z, Wozniak M, Antosiewicz J, Lezoche E, Familiari M, Bertoli E, et al. *Int J Pancreatol* **1995**;18:153–60.
31. Cuzzocrea S, McDonald MC, Filipe HM, Costantino G, Mazzon E, Santagati S, et al. *Eur J Pharmacol* **2000**;390:209–22.

32. Cuzzocrea S, McDonald MC, Filipe HM, Mazzon E, Costantino G, Britti D, et al. *Arthritis Rheum* **2000**;43:320–8.
33. Cuzzocrea S, McDonald MC, Mazzon E, Dugo L, Lepore V, Fonti MT, Ciccolo A, et al. *Eur J Pharmacol* **2000**;406:127–37.
34. Zamir E, Zhang R, Samuni A, Kogan M, Pe'er J. *Free Radic Biol Med* **1999**;27:7–15.
35. Zhang QS, Eaton L, Snyder ER, Houghtaling S, Mitchell JB, Finegold M, et al. *Cancer Res* **2008**;68(5):1601–8.
36. Erker L, Schubert R, Yakushiji H, Barlow C, Larson D, Mitchell JB, et al. *Hum Mol Genet* **2005**;14(12):1699–708.
37. Mitchell JB, Xavier S, DeLuca AM, Sowers AL, Cook JA, Krishna MC, et al. *Free Radic Biol Med* **2003**;34(1):93–102.
38. Wagner V, Dullaart A, Bock AK, Zweck A. *Nat Biotechnol* **2006**;24(10):1211–7.
39. Zamboni WC, Torchilin V, Patri AK, Hrkach J, Stern S, Lee R, et al. *Clin Cancer Res* **2012**;18(12):3229–41.
40. Bamrungsap S, Zhao Z, Chen T, Wang L, Li C, Fu T, et al. *Nanomedicine (Lond)* **2012**;7(8):1253–71.
41. Maeda H. *J Control Release* **2012**;164(2):138–44.
42. Cho K, Wang X, Nie S, Chen ZG, Shin DM. *Clin Cancer Res* **2008**;14(5):1310–6.
43. Nakaoka R, Tabata Y, Yamaoka T, Ikada Y. *J Control Release* **1997**;46:253–61.
44. Moghimi SM. *Adv Drug Deliv Rev* **1995**;17:103–15.
45. Moghimi SM. *Adv Drug Deliv Rev* **1995**;17:61–73.
46. Banerjee T, Mitra S, Kumar SA, Kumar SR, Maitra A. *Int J Pharm* **2002**;243:93–105.
47. Gaumet M, Vargas A, Gurny R, Delie F. *Eur J Pharm Biopharm* **2008**;69(1):1–9.
48. Dobrovolskaia MA, McNeil SE. *Nat Nanotechnol.* **2007**;2(8):469–78.
49. Sheng Y, Liu C, Yuan Y, Tao X, Yang F, Shan X, et al. *Biomaterials* **2009**;30(12):2340–8.
50. Gref R, Minamitake Y, Peracchia MT, Trubetskoy V, Torchilin V, Langer R. *Science* **1994**;263(5153):1600–3.
51. Chen MC, Sonaje K, Chen KJ, Sung HW. *Biomaterials* **2011**;32(36):9826–38.
52. Kiyono H, Fukuyama S. *Nat Rev Immunol* **2004**;4(9):699–710.

53. Salama NN, Eddington ND, Fasano A. *Adv Drug Deliv Rev* **2006**;58(1):15–28.
54. Ensign LM, Cone R, Hanes J. *Adv Drug Deliv Rev* **2012**;64(6):557–70.
55. Fallingborg J. *Dan Med Bull* **1999**;46(3):183–96.
56. Evans DF, Pye G, Bramley R, Clark AG, Dyson TJ, Hardcastle JD. *Gut* **1988**;29(8):1035–41.
57. Bernkop-Schnürch A. *J Control Release* **1998**;52(1-2):1–16.
58. Atuma C, Strugala V, Allen A, Holm L. *Am J Physiol Gastrointest Liver Physiol* **2001**;280(5):G922–9.
59. Johansson ME, Sjövall H, Hansson GC. *Nat Rev Gastroenterol Hepatol* **2013**;10(6):352–61
60. Cerejido M, Contreras RG, Flores-Benítez D, Flores-Maldonado C, Larre I, Ruiz A, et al. *Arch Med Res* **2007**;38(5):465–78.
61. Lai SK, Wang YY, Hanes J. *Adv Drug Deliv Rev* **2009**;61(2):158–71.
62. Ma T, Wang L, Yang T, Ma G, Wang S. *Int J Pharm* **2014**;473(1-2):296–303.
63. Gupta PN, Khatri K, Goyal AK, Mishra N, Vyas SP. *J Drug Target* **2007**;15(10):701–13.
64. Sonaje K, Lin KJ, Tseng MT, Wey SP, Su FY, Chuang EY, et al. *Biomaterials* **2011**;32(33):8712–21.
65. Zhang J, Zhu X, Jin Y, Shan W, Huang Y. *Mol Pharm* **2014**;11(5):1520–32.
66. Wilson DS, Dalmaso G, Wang L, Sitaraman SV, Merlin D, Murthy N. *Nat Mater* **2010**;9(11):923–8.
67. Coco R, Plapied L, Pourcelle V, Jérôme C, Brayden DJ, Schneider YJ, et al. *Int J Pharm* **2013**;440(1):3–12.
68. Ulbrich W, Lamprecht A. *J R Soc Interface* **2010**;7 Suppl 1:S55–66.

Chapter 2

Synthesis of Redox polymers and Preparation of Redox nanoparticles

Astract

In this chapter, the synthesis of redox polymer methoxy-poly(ethylene glycol)-*b*-poly[p-4-(2,2,6,6-tetramethylpiperidine-1-oxyl)oxymethylstyrene] (MeO-PEG-*b*-PMOT) and preparation of redox nanoparticles (RNP^O) were described in detail. Firstly, methoxy-poly(ethylene glycol)-*b*-poly(chloromethylstyrene) (MeO-PEG-*b*-PCMS) block copolymer was synthesized using MeO-PEG-SH, possessing both silyl and methoxy terminal groups, as a telomer. Then, MeO-PEG-*b*-PMOT was synthesized by converting chloromethyl groups of MeO-PEG-*b*-PCMS to TEMPOs via a Williamson ether synthesis. Finally, RNP^O was prepared by dialysis method using a self-assembling block copolymer MeO-PEG-*b*-PMOT.

2.1. Introduction

- The recent progress of living polymerization systems now enables the synthesis of versatile types of block copolymer. Especially, several kinds of living radical polymerization techniques, such as atom transfer radical polymerization, reversible addition fragmentation chain transfer polymerization and nitroxide-mediated radical polymerization, have been established during last two decades and are being applied to widely different monomers such as hydrophilic monomers and non-conjugate monomers.^{1,2} Living polymerization systems allow both precise molecular weight control as well as the synthesis of a wide array of polymer architectures.^{3,4,5} Living polymerization methods allow for the creation of virtually limitless types of new materials from a basic set of monomers.⁶ There are seven generally accepted criteria for a living polymerization:⁷

- The polymerization proceeds to complete monomer conversion, and chain growth continues upon further monomer addition
- Number average molecular weight (M_n) of the polymer increases linearly as a function of conversion
- Number of active centers remains constant for the duration of the polymerization

- Molecular weight can be precisely controlled through stoichiometry
- Polymers display narrow molecular weight distributions, described quantitatively by the ratio of the weight average molecular weight to the number average molecular weight ($M_w/M_n \sim 1$)
- Block copolymers can be prepared by sequential monomer addition
- End-functionalized polymers can be synthesized

- Poly(ethylene glycol) (PEG), non-ionic hydrophilic polymer with stealth behavior, is the most commonly used polymer in the field of nanoparticle-based drug delivery.⁸ The concept of PEGylation was first introduced back in the late 1970s; however, it only reached widespread application in different carrier systems in the 1990s.^{9,10} Several structural factors have an influence on the biological and stabilizing effects of PEG have to be considered. The molar mass and the polydispersity of the polymer have been shown in many applications to be important for biocompatibility and stealth behavior. The molar mass of PEG used in different pharmaceutical and medical applications ranges from 400 Da to about 50 kDa. PEG with a molar mass of 20 kDa to 50 kDa is mostly used for the conjugation of low-molar-mass drugs such as small molecules, oligonucleotides, and siRNA. This results in fast renal clearance being avoided by increasing the size of the conjugates above the renal clearance threshold.^{11,12} PEGs with lower molar masses of 1 kDa to 5 kDa are often used for the conjugation of larger drugs, such as antibodies or nanoparticulate systems. In this way, opsonization and subsequent elimination by the reticuloendothelial system (RES) is avoided, enzymatic degradation is reduced, and cationic charges are hidden.^{13,14} The number of advantages of PEG have been reported. PEG reduces the tendency of particles to aggregate by steric stabilization, thereby producing formulations with increased stability during storage and application. PEG shows a high solubility in organic solvents and, therefore, end-group modifications are relatively easy. At the same time, PEG is soluble in water and has a low intrinsic toxicity that renders the polymer ideally suited for biological applications. When attached to hydrophobic drugs or carriers, the hydrophilicity of PEG increases

their solubility in aqueous media.^{15,16} PEG also prevents interactions with blood components as well as protein interactions such as enzymatic degradation or opsonization followed by uptake by the RES.^{17,18} PEGylated products show less immunogenicity, suppressing the recognition of body immune due to the steric hindrance.^{19,20} Although PEG possesses promising properties for the field of drug delivery, several drawbacks of PEG such as metabolized side products, changing pharmacokinetic behavior, degradation, etc... under the physiological environments should be carefully considered.

- In this chapter, in order to synthesize block copolymers with PEG, we used poly(chloromethylstyrene) (PCMS) as hydrophobic segment, possessing chloromethyl group, which can react with various nucleophilic groups. The polymerization of chloromethylstyrene (CMS) monomers can be carried out in the presence of free radical and cationic initiators by not anionic initiators due to the benzylic chlorine. Block copolymer possessing PCMS was synthesized by classical free-radical telomerization reaction using methoxy-poly(ethylene glycol)-sulfanyl (MeO-PEG-SH). The sulfanyl groups are known to have a very high chain transfer constant in free-radical polymerization reactions.^{21,22} Because the sulfanyl group of MeO-PEG-SH acts as a telogen without any side reaction, the design novel polymers will become feasible. Then, the nitroxide radical can be introduced in the hydrophobic segment (PCMS) reaction of hydroxyl groups of TEMPOL and chloromethyl groups in the basic conditions.^{23,24}

2.2. Materials and Methods

2.2.1. Materials

- MeO-PEG-SH (Mn = 5000), which possesses both sulfanyl and methoxy terminal groups, was purchased from NOF CORPORATION, Tokyo, Japan. 2,2'-Azobisisobutyronitrile (AIBN, Kanto Chemical Co., In., Tokyo, Japan) was purified by recrystallization in methanol (Wako Pure

Chemical Industries, Osaka, Japan). Chloromethylstyrene (CMS) was kindly provided by Seime Chemical Co., Ltd., Kanagawa, Japan. CMS was purified using a silica gel column to remove the inhibitor, followed a vaccum distillation. 4-hydroxyl-2,2,6,6-tetramethylpiperidine-1-oxyl (TEMPOL, Tokyo Chemical Industry Co., Ltd., Tokyo, Japan). Sodium hydride (NaH) , 2-propanol, N,N-dimethylformamide (DMF), toluene, diethyl ether were purchased from Kanto Chemical Co., Inc., Tokyo, Japan, and used without further purification.

2.2.2. Synthesis of MeO-PEG-*b*-PCMS

- The scheme of synthesis of MeO-PEG-*b*-PCMS block copolymer was shown in **Figure 2.1**. Briefly, 10 g of MeO-PEG-SH (Mn = 5,000; 2 mmol) was added into a flask containing 1 mmol of AIBN. The flask as degassed and filled with nitrogen gas, and the degassing-nitrogen-purge cycle was repeated three times. Then, 13.8 mL of purified CMS (100 mmol) and 100 mL of toluene were added to the flask under nitrogen flow. The flask was kept for 24 h at 60 °C in an oil bath for polymerization reaction. The yield of obtained MeO-PEG-*b*-PCMS copolymer was 82.2 % (13.3 g).

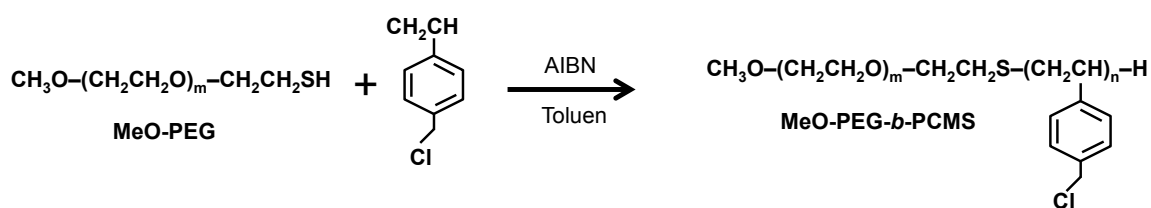


Figure 2.1: Scheme of synthesis of MeO-PEG-*b*-PCMS

2.2.3. Synthesis of redox polymer (MeO-PEG-*b*-PMOT)

- The scheme of synthesis of MeO-PEG-*b*-PMOT block copolymer was shown in **Figure 2.2**. Briefly, 10 g of obtained MeO-PEG-*b*-PCMS (Mw 7,800; 1.25 mmol) were added into a flask containing 200 mL of puried DMF. Then, 13 g of TEMPOL (62.5 mmol) and 3.5 g of NaH (125

mmol) were added into the flask. The reaction was kept at room temperature for 12 h under stirring. After reaction, the mixture was precipitated in cold 2-propanol (-20 °C), followed by centrifugation for 15 min at 5,000 rpm at 0 °C. The precipitation-centrifugation cycles was repeated three time, followed by freeze-drying with benzen. The yield of obtained MeO-PEG-*b*-PMOT copolymer was 87.5 % (11.5 g).

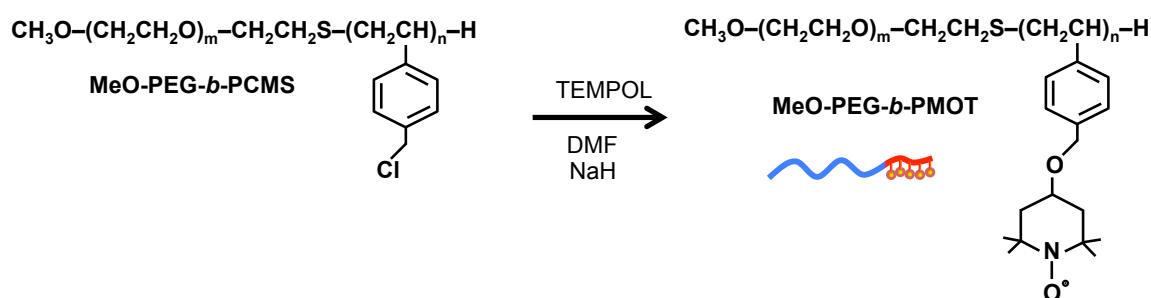


Figure 2.2: Scheme of synthesis of MeO-PEG-*b*-PMOT

2.2.4. Preparation of redox nanoparticles (RNP⁰)

- 1 g of obtained MeO-PEG-*b*-PMOT (Mw = 10,000) was dissolved in 30 mL of DMF. RNP⁰ was prepared by dialysis method (**Figure 2.3**). The dissolved polymer was transferred into a dialysis membrane (Spectra/Por, molecular-weight cutoff 3,500; Spectrum, USA) to dialyze for 24 h against water. The fresh water was changed after 2, 5, 8, and 24 h to obtain polymeric nanoparticles in water. The size of obtained RNP⁰ was evaluated using dynamic light scattering (DLS) measurement. The TEMPO introduction rate in the core of RNP⁰ was measured using electron spin resonance (ESR).

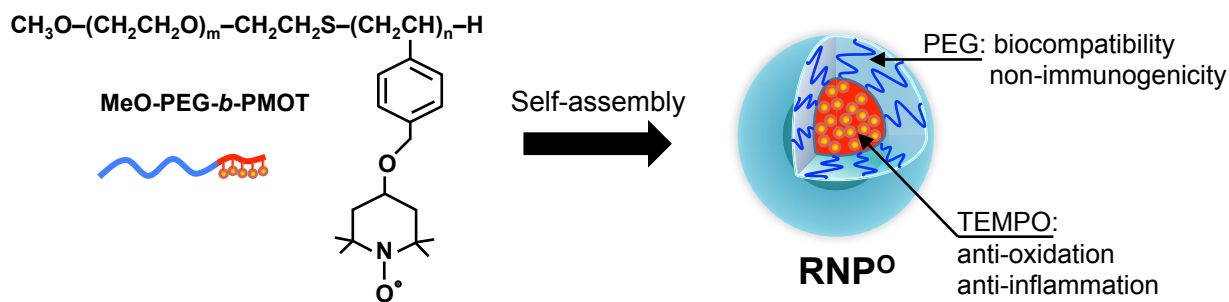


Figure 2.3: Preparation of RNP⁰ by self-assembling MeO-PEG-*b*-PMOT

2.3. Results

2.3.1. Synthesis of MeO-PEG-*b*-PCMS

- The MeO-PEG-*b*-PCMS copolymer was synthesized by the radical telomerization of CMS using MeO-PEG-SH as a telogen and AIBN as an initiator. The polymer molecular weight distribution of MeO-PEG-*b*-PCMS was evaluated by size exclusion chromatography (SEC, Tosoh HLC-8120GPC) using THF containing 2% triethylamine as solvent. As shown in Figure, the number-average molecular weight (M_n) and the weight-average molecular weight (M_w) values of MeO-PEG-*b*-PCMS were 6,300 and 7,800, respectively, by using standard PEG as calibration. The polymerization of CMS was determined by using ^1H NMR spectrum. Based on ^1H NMR, each MeO-PEG-*b*-PCMS possessed 16 unit of CMS (**Figure 2.4**).

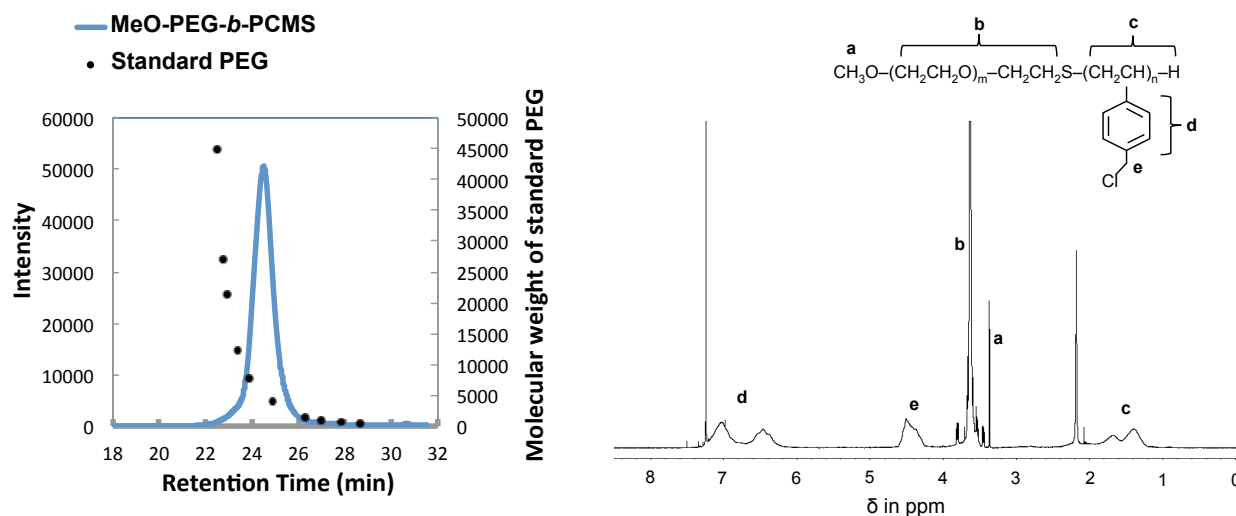


Figure 2.4: SEC diagram and ^1H NMR spectrum of MeO-PEG-*b*-PCMS. SEC diagram was obtained by using Tosoh HLC-8120GPC with THF containing 2% triethylamine as solvent, flow rate at 0.35 mL/min and standard PEGs as calibration. The ^1H NMR spectrum of MeO-PEG-*b*-PMOT was obtained using chloroform- d on a JEOL JNM-ECS 400 MHz.

2.3.2. Synthesis of redox polymer (MeO-PEG-*b*-PMOT)

- The MeO-PEG-*b*-PMOT redox polymer was synthesized by converting chloromethyl groups were converted to TEMPOs via a Williamson ether synthesis of benzyl chloride in the MeO-PEG-*b*-PCMS block copolymer with the alkoxide of TEMPOL. The polymer molecular weight distribution of MeO-PEG-*b*-PCMS was also evaluated by size exclusion chromatography (SEC, Tosoh HLC-8120GPC) using THF containing 2% triethylamine as solvent.

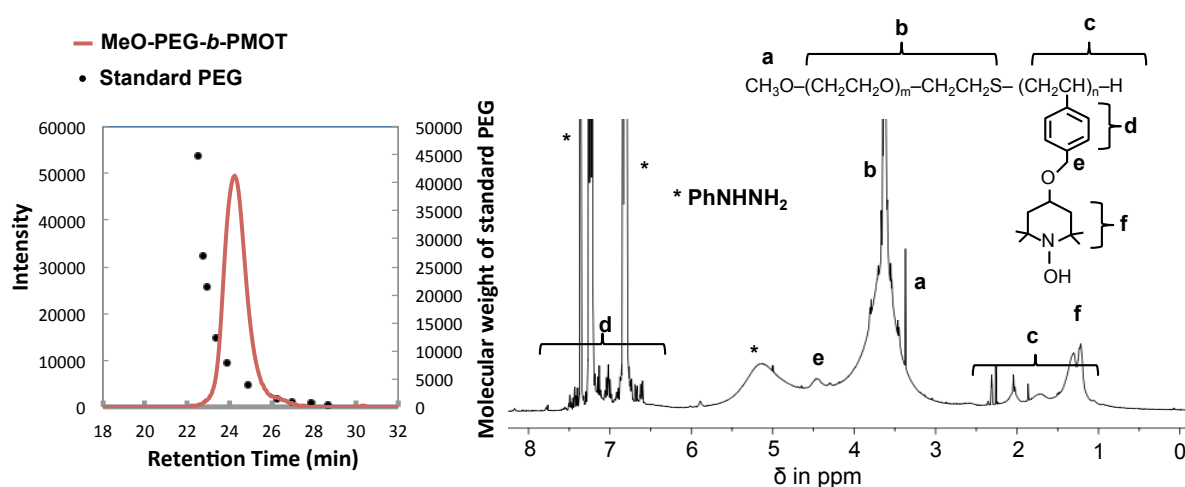


Figure 2.5: SEC diagram and ¹H NMR spectrum of MeO-PEG-*b*-PMOT. SEC diagram was obtained by using Tosoh HLC-8120GPC with THF containing 2% triethylamine as solvent, flow rate at 0.35 mL/min and standard PEGs as calibration. The ¹H NMR spectrum of MeO-PEG-*b*-PMOT was obtained using chloroform-*d* (in presence of phenylhydrazine) on a JEOL JNM-ECS 400 MHz.

- As shown in **Figure 2.5**, based on molecular weight calibration of standard PEGs, the *M_n* and *M_w* values of MeO-PEG-*b*-PMOT were 8,400 and 10,000, respectively. **Figure 2.5** also showed ¹H NMR of MeO-PEG-*b*-PMOT after reduction of TEMPO radicals by phenylhydrazine. As compared to ¹H NMR of MeO-PEG-*b*-PCMS, the new signals of ¹H NMR of MeO-PEG-*b*-PMOT at 1.18 and 1.26 ppm are attributed to the tetramethyl protons of the TEMPO

(**Figure 2.5**). The extent of TEMPO modification in MeO-PEG-*b*-PMOT was approximately 85% (1.2 μmol of nitroxide radical per 1 mg of MeO-PEG-*b*-PMOT) by using ESR measurements.

2.3.3. Preparation of redox nanoparticles (RNP⁰)

- Redox nanoparticles RNP⁰ was prepared by dialysis method. MeO-PEG-*b*-PMOT was dissolved in DMF and dialyzed against water. Using DLS measurement, the size and polydispersity index of RNP⁰ were ca. 40 nm and 0.1, respectively (**Figure 2.6**). The ESR signals of RNP⁰ were analyzed by ESR measurement. **Figure 2.6** showed the ESR spectra of low-molecular-weight (LMW) TEMPOL and RNP⁰. Basically, the ESR signal of LMW nitroxide radical TEMPOL has a sharp triplet due to an interaction between the ¹⁴N nuclei and the unpaired electron in the dilute solution. After the nitroxide radicals are introduced into the hydrophobic core of RNP⁰, the ESR spectrum of RNP⁰ becomes broader. The broadened ESR signals of RNP⁰ are attributed to the self-interaction and the restricted mobility of TEMPOs radicals in the core of RNP⁰. These results suggest that nitroxide radicals TEMPOs were successfully introduced into the core of RNP⁰.

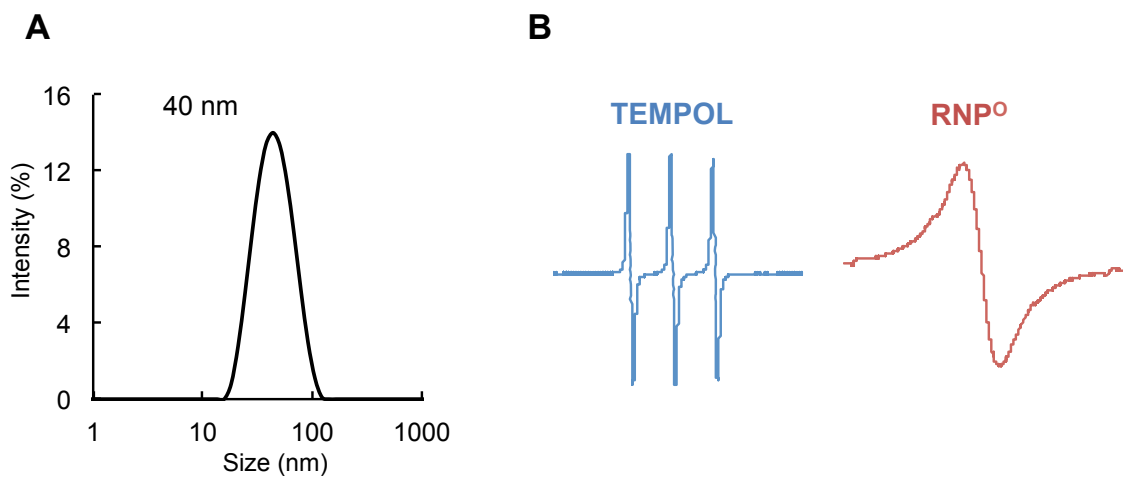


Figure 2.6: (A) Diameter of particles is determined by dynamic light scattering (DLS, Zetasizer Nano ZS, Worcestershire, UK). (B) ESR spectra of low-molecular-weight TEMPOL and RNP⁰. TEMPOL and RNP⁰ were dissolved in MilliQ water and the ESR signal intensities were measured by an X-band ESR spectrometer (JES-TE25X, JEOL, Tokyo, Japan) at room temperature.

2.4. Discussions and Conclusion

- To prepare amphiphilic block copolymer, poly(ethylene glycol) (PEG) and poly(chloromethylstyrene) (PCMS) were used in this study. PEG is most common used in the field of nanoparticle-based drug delivery systems, as described above. On the other hand, PCMS is known to be one of the important and the most widely studied functional polymers. Thousands of articles and patents have been presented about the synthesis, properties, and applications of these polymers. The PCMS or copolymers including PCMS units can react with various nucleophilic groups. The main nucleophilic substitution reactions of chloromethylstyrene include ether function, ester function, amine and ammonium salts, thioethers or thioesters, etc... Nitroxide radicals with different functional groups can be easily introduced in the PCMS or copolymer with PCMS. For examples, chloromethyl groups of PCMS were converted to TEMPOs via the amination of MeO-PEG-*b*-PCMS block copolymer with 4-amino-TEMPO.¹⁴ In this study, the chloromethyl groups were converted to TEMPOs via a Williamson ether synthesis of benzyl chloride in the MeO-PEG-*b*-PCMS block copolymer with the alkoxide of 4-hydroxy-TEMPO (TEMPOL). Based on the data of the SEC diagram, ¹H NMR spectra, and ESR assay, it is concluded that redox polymer MeO-PEG-*b*-PMOT was successfully synthesized. Amphiphilic block copolymer MeO-PEG-*b*-PMOT formed the redox nanoparticle RNP⁰ in the aqueous solution with the size of approximately 40 nm in diameter and remarkably narrow distribution. Because TEMPOs were covalently conjugated in a hydrophobic segment (PCMS) as a side chain via ether linkage, the problem about leakage of TEMPOs during delivery process will be solved. The ether linkage is stable against changing in pH, the prepared RNP⁰ is anticipated to be an ideal oral nanotherapeutics to deliver ROS scavenging nitroxide radicals in gastrointestinal tract.

2.5. References

1. Braunecker WA, Matyjaszewski K. *Prog Polym Sci* **2007**;32:93–146.
2. Goto A, Fukuda T. *Prog Polym Sci* **2004**;29:329–85
3. Domski GJ, Rose JM, Coates GW, Bolig AD, Brookhart M. *Prog Polym Sci* **2007**;32(1):30–92.
4. Mitani M, Saito J, Ishii S, Nakayama Y, Makio H, Matsukawa N, et al. *Chem Rec* **2004**;4(3):137–58.
5. Xu J, Jung K, Atme A, Shanmugam S, Boyer C. *J Am Chem Soc* **2014**;136(14):5508–19.
6. Webster OW. *Science* **1991**;251(4996):887–93.
7. Quirk RP, Lee B. *Polym Int* **1992**;27:359–67.
8. Otsuka H, Nagasaki Y, Kataoka K. *Adv Drug Deliv Rev* **2003**;55:403–19.
9. Monfardini C, Veronese FM. *Bioconjugate Chem* **1998**;9:418–50.
10. Wonganan P, Croyle MA. *Viruses* **2010**;2(2):468–502.
11. Baumann A, Tuerck D, Prabhu S, Dickmann L, Sims J. *Drug Discov Today* **2014**;19:1623–31.
12. Knauf MJ, Bell DP, Hirtzer P, Luo ZP, Young JD, Katre NV. *J Biol Chem* **1988**;263(29):15064–70.
13. Knop K, Hoogenboom R, Fischer D, Schubert US. *Angew Chem Int Ed Engl* **2010**;49(36):6288–308.
14. Jokerst JV, Lobovkina T, Zare RN, Gambhir SS. *Nanomedicine (Lond)* **2011**;6(4):715–28.
15. Joshi HN, Tejwani RW, Davidovich M, Sahasrabudhe VP, Jemal M, Bathala MS, et al. *Int J Pharm* **2004**;269(1):251–8.
16. Kadajji VG, Betageri GV. *Polymers* **2011**, 3(4), 1972–2009
17. Grayson SM, Godbey WT. *J Drug Targeting* **2008**;16:329–56.
18. Pannier AK, Wieland JA, Shea LD. *Acta Biomater* **2008** Jan;4(1):26–39.
19. Harris JM, Martin NE, Modi M. *Clin Pharmacokinet* **2001**;40(7):539–51.
20. Milla P, Dosio F, Cattel L. *Curr Drug Metab* **2012**;13(1):105–19.
21. Kerep P, Ritter H. *Macromol Rapid Commun* **2007**;28:759–66.
22. Lele BS, Leroux JC. *Macromolecules* **2002**;35:6714–23.
23. Yoshitomi T, Suzuki R, Mamiya T, et al. *Bioconjugate Chem* **2009**;20:1792–8.
24. Yoshitomi T, Miyamoto D, Nagasaki Y. *Biomacromolecules* **2009**;10:596–601.

Chapter 3

The specific accumulation of orally administered redox nanoparticle in inflamed colon and therapeutic effect on colitis mice

Abstract

Drugs used to treat patients with ulcerative colitis (UC) are not always effective because of non-specific distribution, metabolism in gastrointestinal tract, and side effects. A nitroxide radical-containing nanoparticle (RNP^O) has been developed to accumulate specifically in the colon to suppress inflammation and reduce the undesirable side effects of nitroxide radicals. RNP^O was synthesized by assembly of an amphiphilic block copolymer that contains stable nitroxide radicals in an ether-linked hydrophobic side chain. Biodistribution of RNP^O in mice was determined from radioisotope and electron spin resonance measurements. The effects of RNP^O were determined in mice with dextran sodium sulfate (DSS)-induced colitis and compared with those of low-molecular-weight (LMW) drugs (4-hydroxyl-2,2,6,6-tetramethylpiperidine-1-oxyl [TEMPOL] or mesalamine). RNP^O, with a diameter of 40 nm and a shell of poly(ethylene glycol), had a significantly greater level of accumulation in the colonic mucosa than LMW TEMPOL or polystyrene latex particles. RNP^O was not absorbed into the bloodstream through the intestinal wall, despite its long-term retention in the colon, which prevented its distribution to other parts of the body. Mice with DSS-induced colitis had significantly lower disease activity index and less inflammation following 7 days of oral administration of RNP^O, compared with DSS-induced colitis mice or mice given LMW TEMPOL or mesalamine. In conclusion, an orally administered RNP^O accumulates specifically in the colons of mice with colitis and is more effective in reducing inflammation than LMW TEMPOL or mesalamine. RNP^O might be developed for treatment of patients with UC.

3.1. Introduction

- Inflammatory bowel disease (IBD), including Crohn's disease (CD) and ulcerative colitis (UC), affects millions of patients worldwide.¹⁻⁴ Since the etiology and pathogenesis of IBD are not well understood, it is considered an intractable disease. The intestinal mucosa of patients with IBD

is characterized by reactive oxygen species (ROS) overproduction and an imbalance of important antioxidants, leading to oxidative damage. Self-sustaining cycles of oxidant production may amplify inflammation and mucosal injury.⁵⁻⁸ In several experimental models, antioxidant compounds and free radical scavengers have improved colitis.⁹⁻¹¹ However, these compounds are not completely effective due to a non-specific drug distribution, a low retention in the colon and side effects. If antioxidant compounds are specifically targeted to the diseased sites and effectively scavenge excessive generated ROS, they represent a safe and effective treatment for IBD.

- Nanoparticles such as liposome and polymeric micelles have gained worldwide attention as a new medical technology, because they change biodistribution of drugs to result in therapeutic effect of drugs significantly.^{12,13} In particular, the intratumoral microdistribution of nanoparticle has been studied for over two decades that nanoparticles can accumulate in sites of tumor due to the increased vascular permeability.¹⁴⁻¹⁷ Recently, we have developed an amphiphilic block copolymer, poly(ethylene glycol)-*b*-poly[p-4-(2,2,6,6-tetramethylpiperidine-1-oxyl)aminomethylstyrene] (PEG-*b*-PMNT), possessing stable nitroxide radicals in the hydrophobic segment as a side chain via an amine linkage, which forms core-shell-type micelles in the physiological environment with an average diameter of about 40 nm, and termed nitroxide radical-containing nanoparticle (RNP^N).¹⁸ Nitroxide radicals are confined in the core of this micelle, which shows high biocompatibility, including long-term blood circulation when administered intravenously and low toxicity. Therefore, RNP^N has been studied for therapy in oxidative stress injuries¹⁸⁻²² and bioimaging.^{23,24} For example, pH-sensitive RNP^N works effectively in acute renal injury¹⁸ and cerebral ischemia-reperfusion¹⁹ because it disintegrates in acidic conditions of diseased area by protonation of amino groups. However, pH-disintegrative character is not suitable for the treatment of UC via oral administration.

- In this chapter, I describe a novel nanotherapy for the treatment of UC via oral administration. In order to target the nanoparticle to the colon area, its accumulation in the colonic mucosa is optimized, preventing its uptake into the bloodstream. I designed a new redox polymer, methoxy-poly(ethylene glycol)-*b*-poly[p-4-(2,2,6,6-tetramethylpiperidine-1-oxyl)oxymethylstyrene] (MeO-PEG-*b*-PMOT), which is an amphiphilic block copolymer with stable nitroxide radicals in a hydrophobic segment as a side chain via an ether linkage and forms 40-nm-diameter core-shell-type micelles (RNP^O) by self-assembly in the aqueous environments regardless of pH (**Figure 3.1A**). Here, the specific accumulation of RNP^O in colon after oral administration was investigated by comparison to low-molecular-weight (LMW) compound, 4-hydroxyl-2,2,6,6-tetramethylpiperidine-1-oxyl (TEMPOL) and commercial available polystyrene latex particles with different sizes from 40 nm to 1 μ m. Also, I examine the therapeutic effect of RNP^O on dextran sodium sulfate (DSS)-induced colitis model in mice, compared to LMW TEMPOL and mesalamine, a commercial anti-ulcer drug. These results show that RNP^O significantly accumulates in colonic mucosa area, especially inflammatory sites, without absorption into bloodstream and has an extremely high therapeutic efficiency in mice with DSS-induced colitis (**Figure 3.1B**).

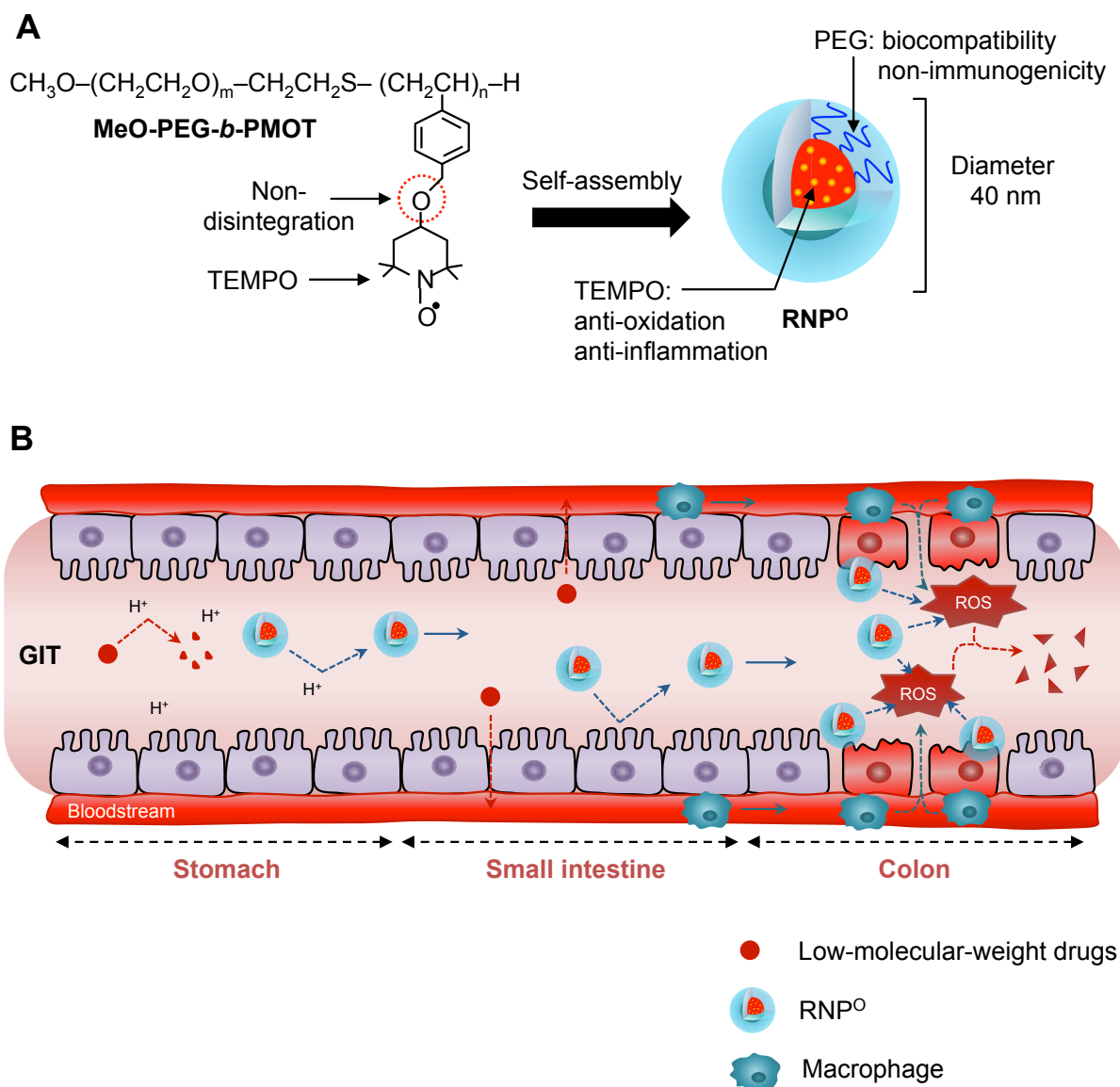


Figure 3.1. Schematic illustration of RNP^o and nanotherapy for DSS-induced UC in mice. **(A)** RNP^o is prepared by self-assembly of a poly(ethylene glycol)-*b*-poly(4-methylstyrene) block copolymer possessing nitroxide radical TEMPO moieties. **(B)** After oral administration, LMW drugs, such as TEMPOL, are degraded and absorbed into the bloodstream in stomach and small intestine before reaching the colon. In contrast, orally administered RNP^o is stable and withstands the harsh conditions of the gastrointestinal (GI) tract, and reach the colon to scavenge ROS, especially sites of inflammation.

3.2. Materials and Methods

3.2.1. Preparation of RNP^O

- RNP^O was prepared by a self-assembling MeO-PEG-*b*-PMOT block copolymer, as previously reported.¹⁸ Briefly, methoxy-poly(ethylene glycol)-*b*-poly(chloromethylstyrene) (MeO-PEG-*b*-PCMS) was synthesized by the radical telomerization of chloromethylstyrene (CMS) using methoxy-poly(ethylene glycol)-sulphanyl (MeO-PEG-SH; Mn = 5,000) as a telogen. The chloromethyl groups were converted to TEMPOs via a Williamson ether synthesis of benzyl chloride in the MeO-PEG-*b*-PCMS block copolymer with the alkoxide of TEMPOL, as previously reported. RNP^O was prepared from MeO-PEG-*b*-PMOT by dialysis method; Micelle without nitroxide radicals was similarly prepared from MeO-PEG-*b*-PCMS as a control and termed “micelle”.

3.2.2. Preparation of rhodamine-labeled RNP^O

- Rhodamine-labeled RNP^O was prepared via thiourethane bond between MeO-PEG-*b*-PMOT possessing reduced TEMPO moieties and rhodamine B isothiocyanate in DMF involved sodium hydride. Briefly, after 30 μmol (300 mg) of the obtained MeO-PEG-*b*-PMOT (Mn = 10,000) were weighed into a 100 mL flask, a CHCl₃ solution (2 mL) of phenylhydrazine (300 μmol, 33 mg) was added to the flask and stirred for 10 min at room temperature. The reacted polymer was recovered by precipitation into 10 mL of diethylether, followed by filtration to obtain reduced TEMPO possessing polymer. The obtained precipitate is recovered by freeze-drying with benzene. The yield of the obtained MeO-PEG-*b*-PMOT possessing reduced TEMPO moieties was 200 mg (66.6%). The obtained polymer (200 mg) was dissolved in anhydride DMF (1 mL) and added to sodium hydride (150 μmol, 5.4 mg) and rhodamine B isothiocyanate (90 μmol, 48 mg) in anhydride DMF solution (1 mL) and stirred for 10 h at room temperature. The yield of the obtained copolymer (MeO-PEG-*b*-PMOT-Rhodamine) was 205 mg. Rhodamine-labeled RNP^O was prepared from the obtained copolymer by the dialysis method.

3.2.3. Preparation of ¹²⁵I-labeled RNP^O

- ¹²⁵I-labeled RNP^O was prepared via reaction between RNP^O and Na[¹²⁵I] with present of

chloramine-T as a catalyst. RNP^O has polystyrene segment in its core, which acts as radioisotope (RI) labeling sites. Briefly, Na[¹²⁵I] solution (40 µL, 1480 kBq, Perkin-Elmer) and chloramine-T (600 mM, 20 µL) were mixed with RNP^O solution (60 mg/mL) at room temperature for 20 min. After reaction, ultracentrifugation (6,200 rpm, 40 min) was carried out 4 times and the obtained solution was passed through a gel filtration column (PD-10 column, GE Healthcare) to remove unreacted Na[¹²⁵I] and the starting reagents. Each 500 µL fraction was collected and its radioactivity was measured by a γ-counter (ARC-380, Aloka, Tokyo, Japan) to confirm ¹²⁵I-labeling of RNP^O and purification. The obtained ¹²⁵I-labeled RNP^O solutions were diluted with water to adjust the radioactivity to 1,179,836 cpm/mL, after which they were used for the *in vivo* body distribution studies.

3.2.4. Preparation of different sized polystyrene latex particles with nitroxide radicals

- Carboxylated polystyrene suspension (40 nm, 100 nm, 0.5 µm and 1 µm, 10% wt/vol, Magsphere Inc., USA) (1 mL) was poured into a 20 mL of glass tube and diluted with 5 mL of phosphate buffer solution (10 mM, pH 4.8). Then, 200 µL of an aqueous solution 1-ethyl-3-(3-dimethylaminopropyl) carbodiimide hydrochloride (EDC, 25 mg/mL) was added, followed by shaking for 20 min at 25 °C (shaking velocity = 1,000 rpm; shaking incubator SI-300, As One Cooperation, Japan). Activated carboxylated polystyrene was mixed with 150 mg of amino-TEMPO and this mixture was continuously vibrated for 4 hours. Then, pH was adjusted to pH 7 by NaOH 1N. This mixture was transferred into a preswollen membrane tube (Spectra/Por; molecular-weight cut off size: 3500) and then dialyzed for 24 hours against 2 L of water to remove unreacted amino-TEMPO. DLS and ESR measurement were carried out to determine the diameter and amount of reacted TEMPO of obtained nanoparticles.

3.2.5. Animals

- All experiments were carried out using 7-week-old male ICR mice (32–35 g) purchased from Charles River Japan, Inc. Mice were maintained in the experimental animal facilities at the University of Tsukuba. All experiments were performed according to the Guide for the Care and Use of Laboratory Animals at the University of Tsukuba.

3.2.6. Localization of RNP^O in the colon

- Localization of RNP^O in the colon was determined by fluorescent rhodamine-labeled RNP^O. Rhodamine-labeled RNP^O was prepared via thiourethane bond between MeO-PEG-*b*-PMOT possessing reduced TEMPO moieties and rhodamine B isothiocyanatein. Mice were killed 4 hours after oral administration of 1 mL of rhodamine-labeled RNP^O (5 mg/mL). Residues in the colon were gently removed with phosphate buffered saline (50 mM, pH 7.4), and 7- μ m thick colon sections were prepared. Localization of rhodamine-labeled RNP^O was recorded using a fluorescent microscope.

3.2.7. Accumulation of RNP^O in the colon

- Accumulation of RNP^O was determined by ESR assay. One mL of LMW TEMPOL, RNP^O and different sized polystyrene latex particles with an equivalent nitroxide concentration (1.33 mg; 7.5 μ M) were orally administered to mice. Mice were killed 1, 4, 12, 24, and 48 hours after oral administration. Whole colons were homogenized in 1 mL of phosphate buffered saline (50 mM, pH 7.4) containing potassium ferricyanide (50 mM). The ESR signal intensities in homogenized samples were measured by an X-band ESR spectrometer (JES-TE25X, JEOL, Tokyo, Japan) at room temperature. The amount of nitroxide radicals in the colon was determined by ESR measurements under the following conditions: frequency, 9.41 GHz; power, 10.00 mW; center field, 333.3; sweep width, 5 mT; sweep time, 0.5 min; modulation, 0.1 mT; time constant, 0.1 s.

3.2.8. Biodistribution of RNP^O

- ¹²⁵I-labeled RNP^O was prepared via reaction between RNP^O and Na[¹²⁵I] with present of chloramine-T as a catalyst (see Supplementary Materials and Methods). Mice were fasted for 1 day before the experiment and 0.5 mL of ¹²⁵I-labeled RNP^O (20 mg/mL) was orally administered. Then, mice were sacrificed at 0.25, 0.5, 1, 2, 4, 8, 12, and 24 hours after oral administration. The major digestive organs (small intestine, cecum, and colon) and blood were isolated, and their

radioactivities were measured by a γ -counter (ARC-380, Aloka, Japan). The percentage of radioactivity in each organ was determined based on the initial total radioactivity.

3.2.9. Induction of colitis by DSS and drug administration

- Colitis in mice was induced by 3% (wt/vol) DSS (5,000 daltons; Wako Pure Chemicals) supplemented in the drinking water for 7 days. The experiment was designed to six groups: normal control group, DSS-injured group, LMW TEMPOL-treated group, micelle-treated group, RNP^O-treated group and mesalamine-treated group. The equivalent doses of drugs (0.2 mM/kg) were orally administered daily during the 7 days of DSS treatment. The concentrations of LMW TEMPOL, micelle and RNP^O were adjusted in distilled water, and the solutions were filtered with a 0.25- μ m cellulose acetate filter. Mesalamine was suspended in 0.5% (wt/vol) carboxymethyl cellulose.

3.2.10. Evaluation of colitis severity by disease activity index (DAI) and colon length

- During 7 days of treatment, body weight change, visible stool consistency, and fecal bleeding were assessed daily. DAI is the summation of the stool consistency index (0–3), fecal bleeding index (0–3), and weight loss index (0–4). After 7 days of treatment, mice were sacrificed after anesthesia with sodium pentobarbital (40 mg/kg), and the entire colon (from cecum to rectum) was collected. Colon length was measured and gently washed with physiological saline. Then, 1 cm of the distal section was used for histological assessment. The remaining section was used to measure MPO activity, interleukin (IL)-1 β and superoxide.

3.2.11. Histological assessment

- After washing, 1 cm of the distal colon was fixed in 4% (vol/vol) buffered formalin for 1 day and 70% (vol/vol) alcohol for 2 days prior to paraffin embedding. Then, 7- μ m thick sections of

the distal colon were prepared and stained with hematoxylin and eosin. Histology of the colon was evaluated using a microscope.

3.2.12. Myeloperoxidase (MPO) activity

- Colon tissue samples were collected immediately after mice were sacrificed and were homogenized in cold 50 mM phosphate buffer (pH 6) supplemented with 0.5% (wt/vol) hexadecyltrimethylammonium bromide (Sigma-Aldrich). Supernatants were collected by centrifugation for 10 min at 10,000 rpm at 4 °C and kept at –80 °C until the assay. The enzymatic reaction was carried out in a 96-well plate by adding 190 µL of 50 mM phosphate buffer (pH 6), 5 µL of 10 mg/mL *o*-dianisidine hydrochloride, 5 µL of 20 mM H₂O₂, and 10 µL of the supernatant sample. After 30 min at room temperature, the absorbance at 460 nm was measured. The protein concentration of the supernatant sample was measured using a BCA kit (Thermo Scientific Pierce Protein Research Products). MPO activity was determined by comparison to a standard MPO curve (Sigma-Aldrich M6908).

3.2.13. Interleukin IL-1 β measurement

- Colon tissue samples were collected immediately after mice sacrifice and were homogenized in cold phosphate buffer saline. After centrifugation for 10 min at 10,000 rpm 4 °C, supernatants were collected and measured concentration of IL-1 β by using an enzyme-linked immunosorbent assay (ELISA) kit for mice (Thermo Scientific Pierce Protein Research Products), according to the manufacturer's instructions.

3.2.14. Measurement of colon superoxide production in vivo

- To determine superoxide production, colon supernatant (100 µL) was added to a 96-well black plate (NUNC) containing 3.3 mM dihydroethidium (DHE; Wako Pure Chemicals), followed

by incubation at 37 °C for 20 min. The fluorescence intensity of each well was measured using an excitation wavelength of 530 nm and an emission wavelength of 620 nm. DHE alone was read to calculate a zero-point. Superoxide values, from which the zero-point value was subtracted, were expressed as intensity per mg of protein. The superoxide value of the control group was standardized to 100%.

3.2.15. Intravital observation by in vivo live imaging

- Aqueous solution of DSS (3% wt/vol) was administered by free access for 7 days to induce colitis in mice. One mL of RNP^O (10 mg/mL) was orally administered daily. After 7 days of treatment, mice were anesthetized with urethane (15 g/kg, Sigma-Aldrich) and an arc-shaped incision was made in the peritoneum to expose the colon. Then, approximately 1 cm length incision was made to observe the colonic mucosa and the remained contents in the colon were removed gently by physiological saline. Mice were set on the stage of microscope and in vivo live imaging was acquired after 2 hours with a microscope. Dead cells in colonic mucosa were identified by staining of propidium iodide in physiological buffer (50 µg/mL; Wako Pure Chemicals) under an excitation wavelength of 488 nm and an emission wavelength of 515 nm.

3.2.16. Survival rate experiment

- The survival rate of mice was determined by replacing drinking water with a 3% (wt/vol) solution of DSS for 15 days. Starting on day 5, drugs were oral administered daily until day 15, and the number of surviving mice was counted until day 15.

3.2.17. Statistical analysis

- All values are expressed as mean ± standard error of mean (SEM). Differences between groups were examined for statistical significance using the one-way and two-way ANOVA,

TEMPOL. Because nitroxide radicals were introduced into the particles, their accumulation could be quantitatively monitored by electron spin resonance (ESR) measurements. When LMW TEMPOL was orally administered to mice, almost no ESR signal was observed in the colon, as shown in **Figure 3.3A**. In contrast, polystyrene latex particles showed a higher accumulation in the colon compared to LMW TEMPOL. From these results, the size-dependent accumulation in colon was observed. Polystyrene latex particles with 40 nm and 100 nm in size accumulated higher than large-sized particles (0.5 μm and 1 μm), which is consistent with previous reports.^{25,26} Interestingly, when RNP^O was administrated orally to mice, considerable high accumulation of RNP^O in colon was observed, as compared to polystyrene latex particles, even though the same size (40 nm). The area under the concentration-time curve (AUC), an important parameter in biopharmaceuticals and pharmacokinetics, of RNP^O was 1223.3, which was significantly higher than 27.8 of LMW TEMPOL. The AUC of polystyrene latex particles with sizes 40 nm, 100 nm, 0.5 μm and 1 μm were 249.5, 204.7, 83.7 and 32.9, respectively. High colloidal stability of RNP^O due to the PEG tethered chains on the surface might be effective to accumulate in colonic mucosa as compared to polystyrene latex particles. The extremely high accumulation of RNP^O in colonic mucosa can be anticipated for high performance efficiency as a colitis therapy.

- Next, the specific accumulation of RNP^O in the injured colon was investigated. Aqueous solution of DSS (3% wt/vol) was administered by free access to induce colitis in mice. RNP^O was orally administered at day 5 and quantified the amount of RNP^O in the colon by ESR measurements 4 hours after administration. Interestingly, the amount of accumulated RNP^O in the colon of DSS-injured mice was 50% higher than that in the normal colon under the same administration conditions ($1.57 \pm 0.18 \mu\text{g/cm}$ of colon length for DSS-treated mice and $1.01 \pm 0.13 \mu\text{g/cm}$ of colon length for normal mice) (**Figure 3.3B**). This result suggested that RNP^O accumulates to a greater extent in inflammatory sites, such as in UC.

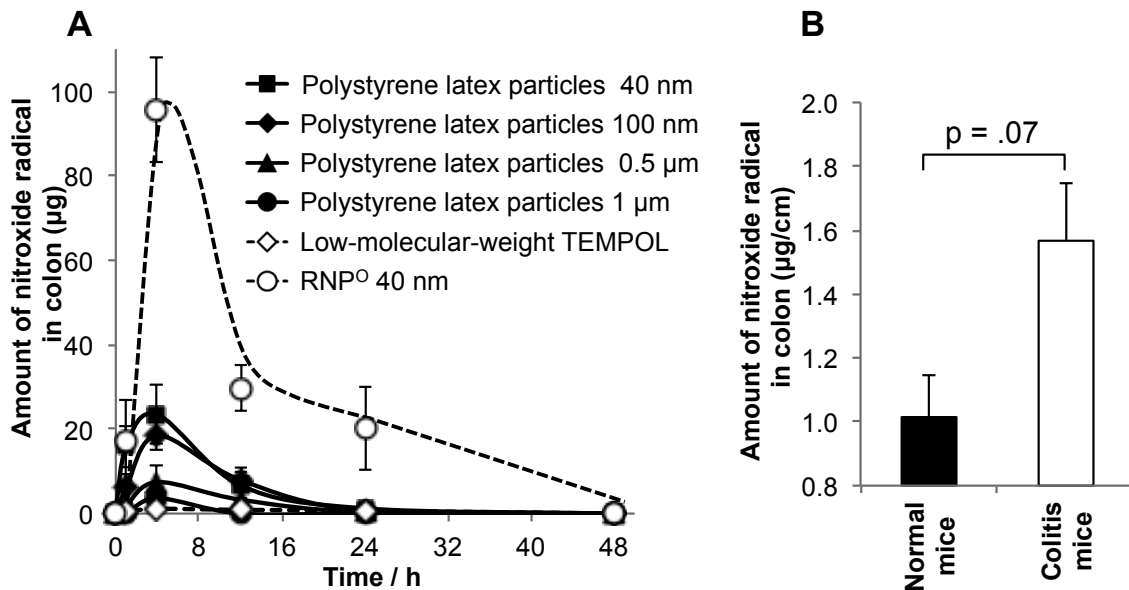


Figure 3.3: Specific accumulation of RNP^O in colon. (A) Accumulation of LMW TEMPOL, RNP^O and polystyrene latex particles in the colon. Amount of nitroxide radical was measured by ESR. (B) Specific accumulation of RNP^O in the inflamed colon. The amount of nitroxide radicals in the normal colon and the inflamed colon was determined by ESR measurement 4 hours after administration of RNP^O. The data are expressed as mean \pm SEM, $n = 3$.

3.3.2. Distribution and non-absorption into bloodstream of RNP^O after oral administration

- As previously mentioned, I confirmed the specific accumulation of RNP^O in the DSS-injured colon. It is also important to estimate the non-specific distribution in whole body. Therefore, to precisely evaluate non-specific distribution, I used radioisotope ¹²⁵I-labeled RNP^O, which moved from the small intestine, to the cecum, and to the colon over time after oral administration (Figure 3.4A). Specifically, in the first hour after administration, 3.2% of the initial dose of RNP^O had reached the colon. It accumulated to a maximum of 14.5% of the initial dose 4 hours after administration. Twenty-four hours after administration, there was 0.5% of the initial dose of RNP^O remaining in the colon. Importantly, no the uptake of RNP^O into the bloodstream was observed (Figure 3.4A). This is in sharp contrast to LMW compounds, such as TEMPOL.

This difference in bloodstream uptake via the gastrointestinal (GI) tract was further confirmed by ESR measurements. LMW TEMPOL was absorbed into the bloodstream through the GI tract in normal mice and even more in DSS-treated mice (**Figure 3.4B**). However, when RNP^O was administered orally, there was no observable ESR signal in the blood, which was consistent with the results from the experiments of ¹²⁵I-labeled RNP^O. In this chapter, oral nanotherapy with RNP^O prevented uptake into the bloodstream, suggesting a lack of systemic side effects.

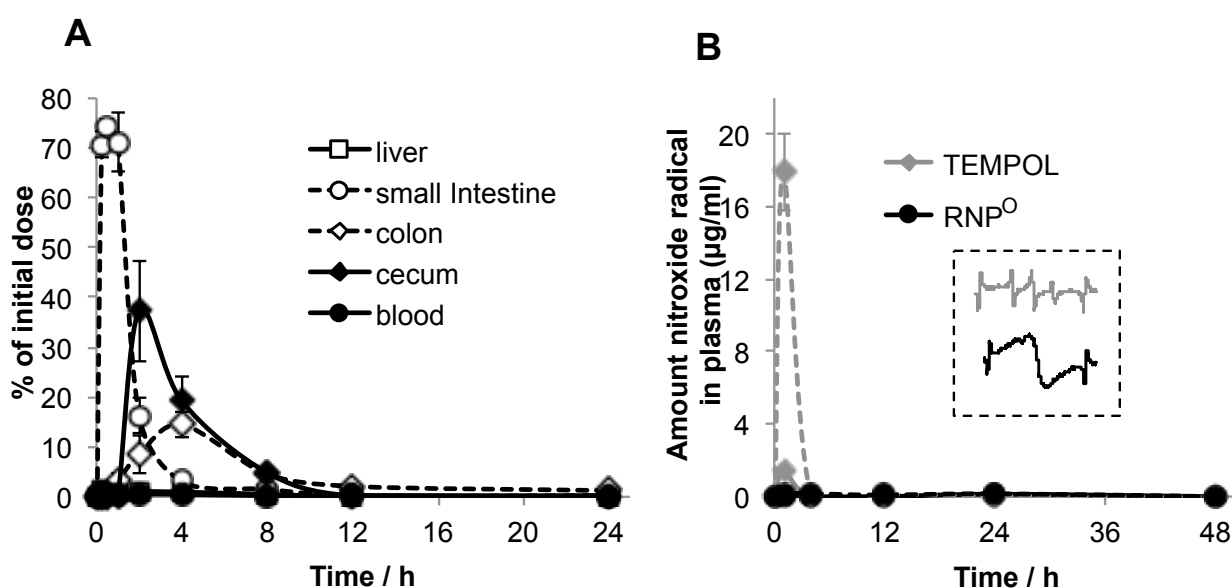


Figure 3.4. Biodistribution of RNP^O in GI tract and bloodstream. **(A)** The biodistribution of RNP^O was determined using ¹²⁵I-labeled RNP^O. The percentages of radioactivity in each organ and in the blood were determined by comparison to the initial total radioactivity. The data are expressed as mean ± SEM, *n* = 5. **(B)** Absorption of LMW TEMPOL and RNP^O into the bloodstream of normal mice (*solid line*) and colitis mice (*dashed line*). After administration of LMW TEMPOL and RNP^O, the amount of nitroxide radicals in the plasma was determined by ESR measurement. The data are expressed as mean ± SEM, *n* = 3. (*Inset*) The ESR spectra of LMW TEMPOL (*grey spectrum*) and RNP^O (*black spectrum*) in the colon homogenate after 4 h oral administration.

3.3.3. Stability of RNP^O in GI tract

Next, the stability of orally administered RNP^O in the GI tract was evaluated using ESR spectra of RNP^O in the colon. The ESR signals of LMW TEMPOL in the colon showed a sharp triplet due to an interaction between the ¹⁴N nuclei and the unpaired electron, as previously reported¹⁸ (**Figure 3.4B**, *inset, grey spectrum*). In contrast, the ESR signals of RNP^O in the colon were broad (**Figure 3.4B**, *inset, black spectrum*), suggesting that RNP^O remains as core-shell type micelle even in the GI tract. The stability of self-assembled RNP^O with several tens of nanometers in GI tract could prevent the uptake into the bloodstream through the intestinal wall. After reaching colon, RNP^O is accumulated in inflamed and mucosal area, followed by effectively scavenging ROS. It is noted that RNP^N, which contains amino group as side chains in the hydrophobic segment, is absorbed into the bloodstream when administered orally (data not shown). It is likely that the disintegration of RNP^N in the stomach facilitates its uptake into the bloodstream through the intestinal wall, which was not observed in RNP^O.

3.3.4. Therapeutic effect of RNP^O on DSS-induced colitis in mice

- Since orally administered RNP^O accumulated in the colonic mucosa of DSS-injured mice and was not absorbed into the bloodstream, it is anticipated to be an ideal nanomedicine for UC treatment. Therefore, its therapeutic and suppressive effects on DSS-induced colitis model in mice was investigated. RNP^O was orally administered daily to DSS-injured mice for 7 days. Additional DSS-injured mice were treated with LMW TEMPOL, commercially anti-ulcer mesalamine and micelle without nitroxide radicals as controls. After 7 days of treatment, the severity of colitis was assessed on the basis of DAI²⁷, colon length, and histological analysis. Mice treated with DSS had a significant increase in DAI and shortening of the colon compared to control mice (**Figure 3.5A and B**). The treatments with LMW TEMPOL or mesalamine showed efficiency to decrease DAI as compared to DSS-treated mice, though this efficiency was not significant. On the contrary,

RNP^O-treated mice showed much lower DAI and preserved colon length compared to DSS-treated mice ($P < 0.01$) and other LMW drugs-treated mice. It should be noted that no effect was observed when polymeric micelle without nitroxide radicals was administered instead of RNP^O.

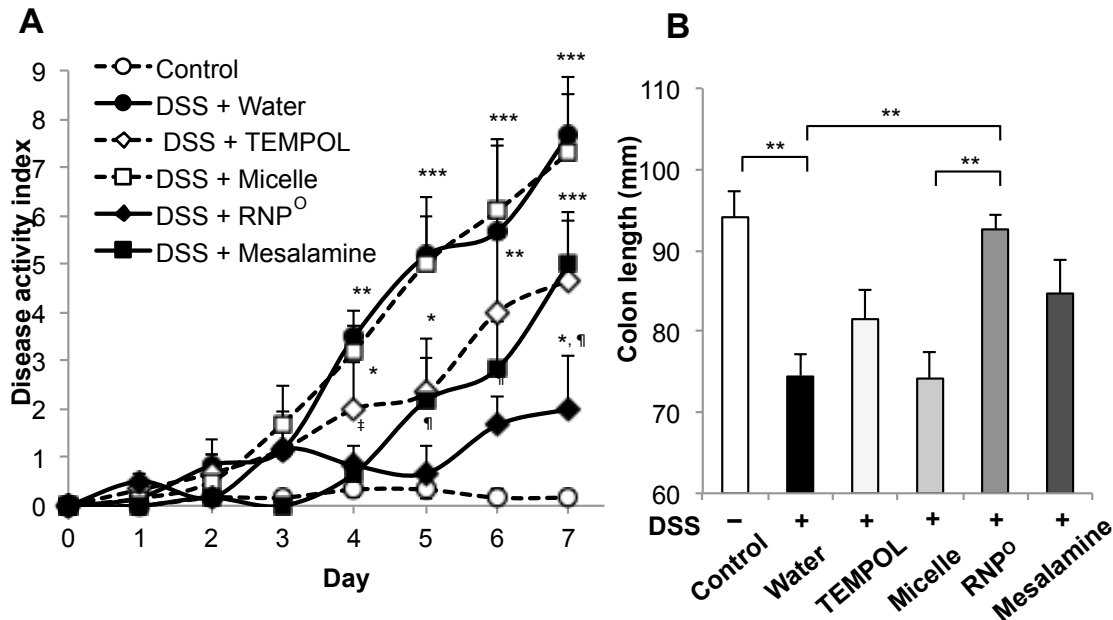


Figure 3.5. Therapeutic effect of RNP^O on DSS-induced colitis in mice. (A) Changes in disease activity index. The data are expressed as mean \pm SEM, * $P < 0.05$, ** $P < 0.01$ and *** $P < 0.001$ vs. control group; † $P < 0.05$ and †† $P < 0.001$ vs. DSS groups, $n = 6-7$, two-way ANOVA, followed by Bonferroni post-hoc test. (B) Preservation of colon length. After 7 days of treatment, the colon was collected and measured. The data are expressed as mean \pm SEM, ** $P < .01$, $n = 6-7$.

- Additionally, histological analyses showed that mucosal structures of DSS- and micelle-treated mice were significantly damaged, viz., destruction of crypts and high levels of neutrophil invasion were observed in these mice. LMW TEMPOL- or mesalamine-treated mice showed moderately damaged mucosal structures. Contrary of those treatments, RNP^O-treated mice showed almost similar to that of control mice (**Figure 3.6**), indicating the significant therapeutic effect of RNP^O on DSS-induced colitis in mice.

- Then ability of RNP^O to suppress systemic inflammation in DSS-induced colitis was

analyzed. Hematological analyses were performed to reveal the massive infiltration of leukocytes. Blood from RNP^O-treated mice had a significant lower level of white blood cells compared to DSS- and micelle-treated mice ($P < 0.05$), indicating lower levels of neutrophil invasion in RNP^O-treated mice (**Figure 3.7A**).

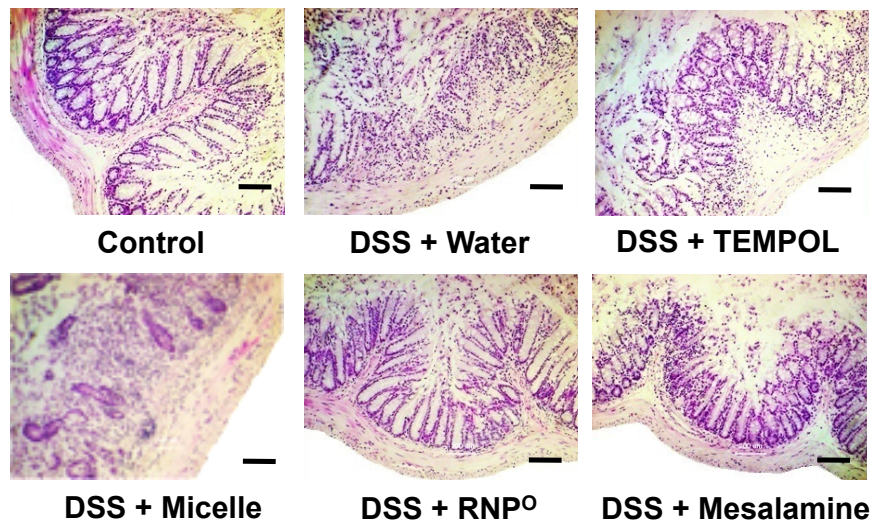


Figure 3.6: Oral administration of RNP^O protects mucosal architecture from DSS-induced injury. Sections of the distal colon were stained by H&E. *Scale bars*, 200 μm .

LMW TEMPOL and mesalamine showed the effect to suppress white blood cells in DSS-treated mice; however, the significance was not observed. Furthermore, results of the hematological analysis indicated higher levels of red blood cells and hemoglobin in the blood of RNP^O-treated mice (**Figure 3.7B** and **C**). This suggests that the intestinal wall was protected from hemorrhage in RNP^O-treated mice. I further investigated the desquamation of impaired epithelial cells and cell death in colonic mucosa by intravital observation using *in vivo* microscopic live imaging and propidium iodide staining.²⁸ The results showed that a great number of desquamated cells and cell death existed in colonic mucosa of DSS-treated mice (**Figure 3.7D**). In contrast, in colonic mucosa of RNP^O-treated mice, the desquamation and cell death was remarkably suppressed. On the basis of these results, it was confirmed that colonic injury is protected by the oral administration of RNP^O.

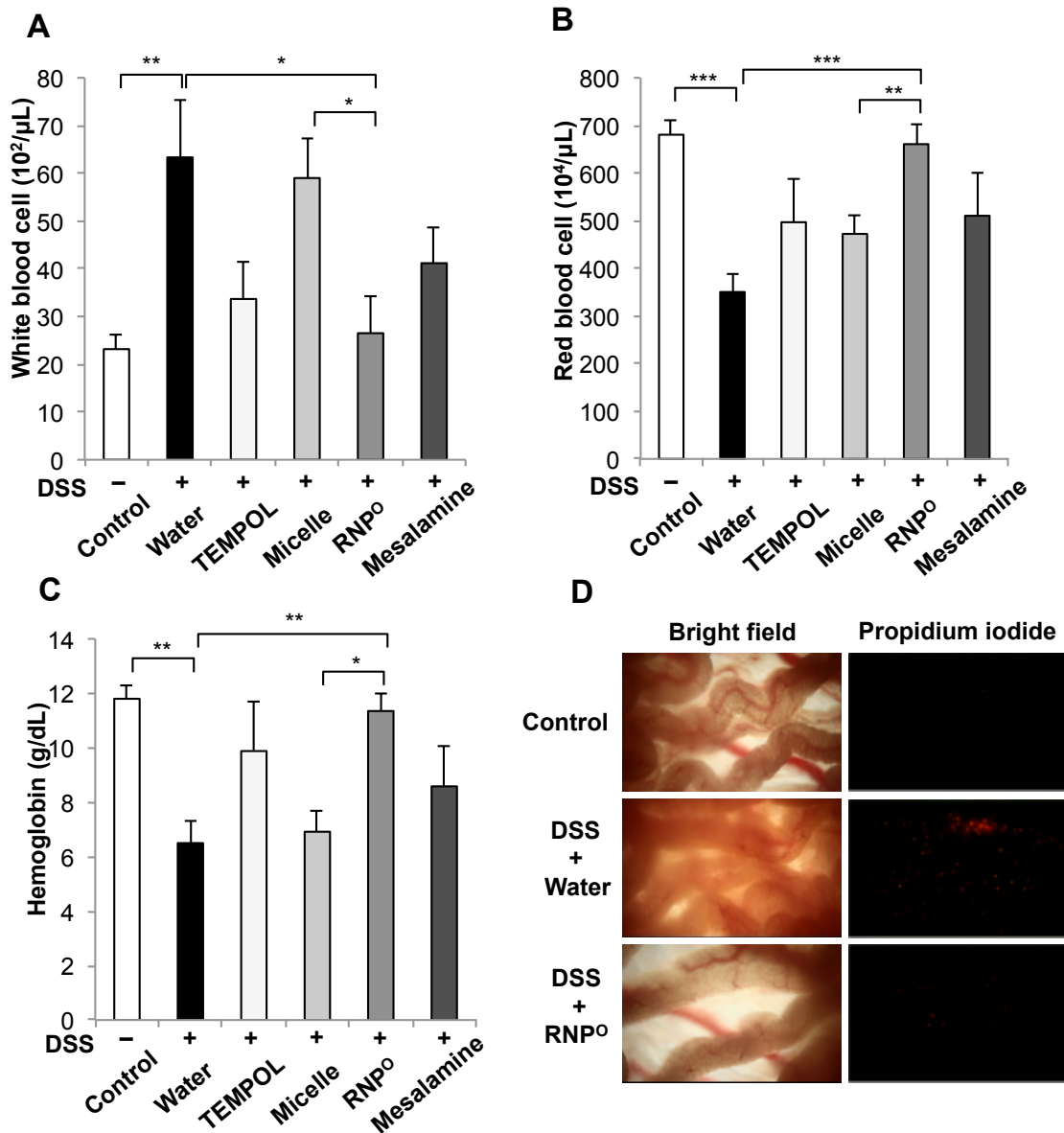


Figure 3.7. Hematological analyses in the peripheral blood and intravital observation of colon. (A–C) After 7 days of treatment, hematological analyses were performed by automatic hematology analyzer (Celltac α , MEK-6358; Nihon Kohden Co., Tokyo, Japan). Blood samples were analyzed for white blood cells (A), red blood cells (B), and hemoglobin (C). The data are expressed as mean \pm SEM, * P < 0.05, ** P < 0.01, *** P < 0.001, n = 6. (D) The desquamation of impaired epithelial cells and cell death in colonic mucosa were determined by in vivo microscopic live imaging and propidium iodide staining.

3.3.5. RNP^O suppresses pro-inflammatory mediators and enhances survival rate in mice

- In addition, after 7 days of treatment, pro-inflammatory mediators in the colonic mucosa, including MPO activity, IL-1 β and superoxide, were determined. These pro-inflammatory mediators are well-known markers of inflammation and play an important role in UC. LMW TEMPOL and mesalamine did not effectively suppress these pro-inflammatory mediators induced by DSS (**Figure 3.8A–C**). On the other hand, RNP^O-treated mice showed a significant suppression of pro-inflammatory mediators in colonic tissue ($P < 0.01$). It should be noted that no therapeutic effect was observed for polymeric micelle without nitroxide groups, indicating that effective delivery of nitroxide groups in colonic mucosa area is one of the most important factors for UC treatment. Because LMW drugs tend to be absorbed into the bloodstream via mesentery, sufficient dose of drugs might not reach to target area to result in low therapeutic efficacy. Side effects in whole body should also be considered such kind of LMW drugs. Finally, I investigated the effect of orally administered RNP^O on the survival rate of mice with colitis induced by 5-day administration of DSS. After 15 days of treatment, orally administered LMW TEMPOL and mesalamine slightly increased the survival rate (33.3% and 50%, respectively) compared with DSS- and micelle-treated mice (16.7%) (**Figure 3.8D**). On the other hand, RNP^O treatment significantly increased the survival rate of DSS-treated mice to 83.3%. This indicates that RNP^O has not only suppressive but also therapeutic effects on mice with DSS-induced colitis.

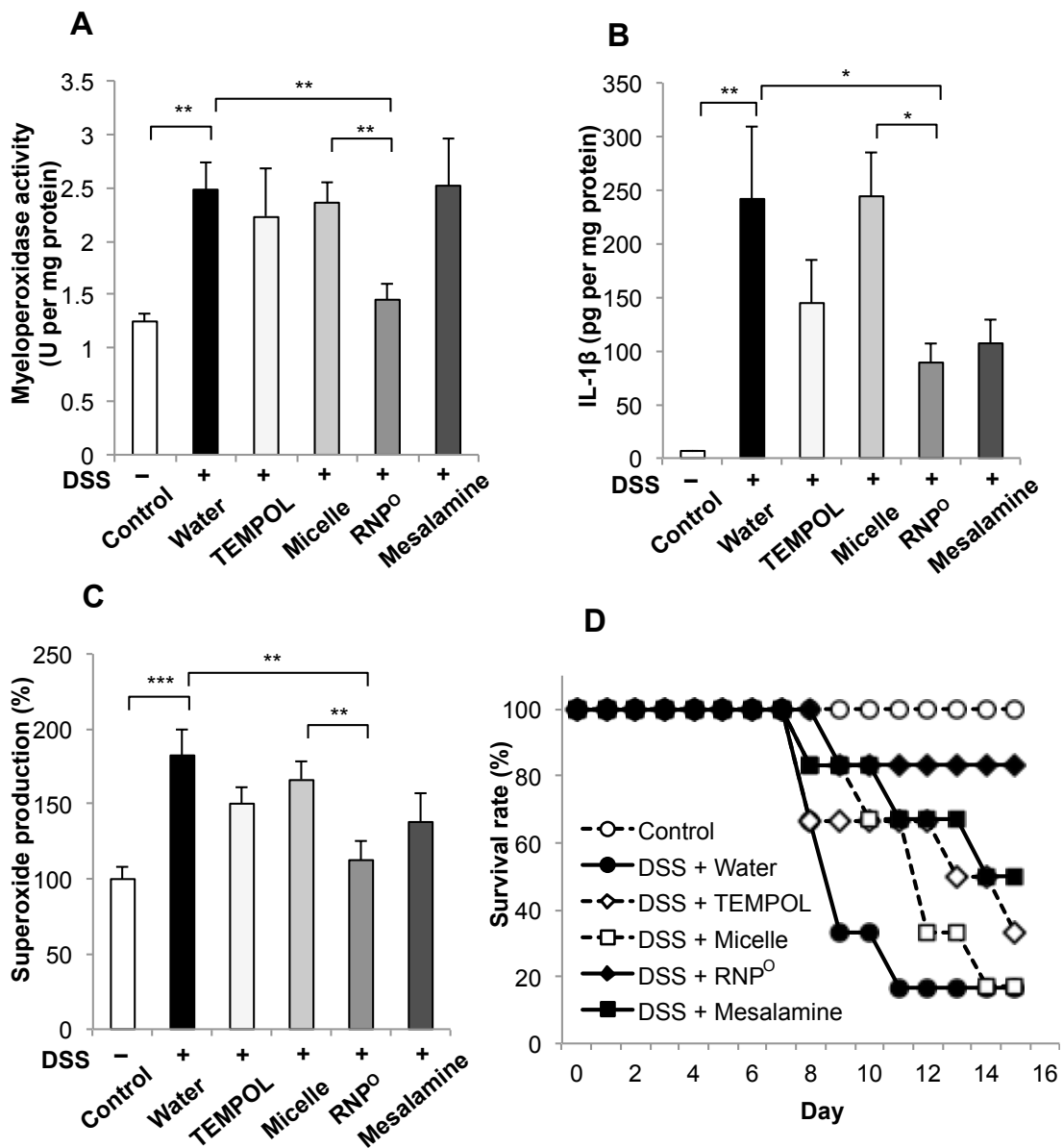


Figure 3.8. RNP^O reduced pro-inflammatory mediators and increased survival rate in colitis mice.

(A) MPO activity was determined by a colorimetric assay using *o*-dianisidine hydrochloride and H₂O₂ as substrates. (B) Measurement of IL-1 β in colon homogenate was performed with an ELISA

kit for mice. (C) Generation of superoxide in colon homogenates was measured by dihydroethidium (DHE) fluorescence. The data are expressed as mean \pm SEM, * P < .05, ** P < .01, *** P < .001, n = 6. (D) The survival rate of mice was determined after 15 days of 3% (wt/vol) DSS

treatment, n = 6.

3.4. Discussion and Conclusions

- Despite significant advances in treatments, IBD remains a major clinical problem, because no drug is entirely effective. For many years, there were only 2 treatment options for IBD: corticosteroids and mesalamine.^{29,30} Although they are effective in treating IBD in some extent, their severe side effects have raised significant concerns among both physicians and patients, and limited their use. In addition, anti-TNF- α antibody is employed to suppress inflammation of UC, which works well though it is cost-oriented therapy with multiple side effects.³¹ Recently, many promising LMW medications, such as antioxidants, have been found beneficial in experimental models of UC.^{9-11,32} Unfortunately, results of clinical trials investigating these promising drugs have been largely negative. The drawbacks of current LMW drugs are poor stability in stomach, low solubility and side effects on whole body when they enter the bloodstream. In this chapter, I have developed a novel nitroxide radical-containing nanoparticle RNP^O that accumulates specifically in colon area to suppress the inflammation in DSS-induced colitis mice. For UC treatment via oral administration, this nanoparticle showed excellent properties, including high accumulation in inflamed tissues of colon and non-absorption into the bloodstream.

- Here, it was found that the accumulation in colon area depends on the sizes and PEGylated character of particles. Both LMW drugs, submicron- and micron-sized polystyrene latex particles showed poor accumulation in colon, whereas higher accumulation of particles with approximately several tens of nanometers was observed. Optimal size of several tens of nanometers allowed easier diffusion in the mucosa compared to larger sized particles.^{25,26,33} In addition, 40-nm-diameter RNP^O with PEG shell showed significantly high accumulation and long retention in colon area compared to polystyrene latex particles with similar size of 40 nm. PEGylated character of RNP^O might protect nitroxide radicals in the hydrophobic core from harsh conditions of GI tract after oral administration, resulting in the significant accumulation in colon area.³⁴ Furthermore, PEG chains

of RNP^O may achieve mucoadhesion due to their ability to inter-diffuse among the mucus network and polymer entanglement with mucin, which is composed of glycoprotein.³⁵ Therefore, PEGylated character of RNP^O showed much significant effect on its accumulation in colonic mucosa. Eventually, I observed the accumulation of RNP^O in colon is almost 50 times higher than that of LMW TEMPOL. To deliver sufficient dose of anti-inflammatory drugs for UC treatment, high dose of drugs is required, however it leads to undesirable side effects, because almost all LMW drugs tend to metabolize in upper GI tract or absorb into bloodstream.^{36,37} In case of RNP^O, no absorption into bloodstream was observed via oral administration route, which improves accumulation in colon region and prevents side effects to whole body. Another interesting phenomenon in this chapter is the higher accumulation of nanoparticles in inflammatory colon than healthy colon. Mucus layer in colon area is significantly thicker than that in small intestine, which is considered as a significant barrier to nanoparticle penetration.³⁸ In colon of patients with UC, the overall thickness of the adherent mucus layer is reduced due to the reduction of goblet cells,^{38,39} resulting in the facile penetration of nanoparticles in inflammatory tissues. In addition, the opening tight junction of epithelium cells in UC is another explanation for higher accumulation of nanoparticles.⁴⁰ It should be noted that no absorption of RNP^O into bloodstream was observed even in colitis mice.

- After investigating the distribution of RNP^O in GI tract, DSS-induced colitis model mice was used to compare suppressive effect of RNP^O with LMW TEMPOL and mesalamine, a commercial medication for UC treatment. These results showed that LMW TEMPOL and mesalamine did not clearly show their effects, whereas RNP^O effectively reduced the severity of colitis by suppression of DAI and damage of colonic architecture. It is noted that micelle without nitroxide radicals did not show any therapeutic effect at all on colitis mice, indicating that ROS scavenging character of nitroxide radicals plays critical role in the effect of RNP^O on colitis mice. Further investigations, it is confirmed that RNP^O did not simulate the whole body immune system

as well as effectively suppressed pro-inflammatory mediators such as MPO, IL-1 β and superoxide. The therapeutic efficiency of RNP^O was further confirmed by survival data, which showed higher survival rate of RNP^O-treated mice compared to LMW TEMPOL- or mesalamine-treated mice.

- In conclusion, I have developed a novel nitroxide radical-containing nanoparticle, RNP^O, which possesses anti-oxidative nitroxide radicals in the core for treatment of DSS-induced colitis mice. RNP^O significantly accumulated not only in the mucosa but also higher in inflammatory sites of the colon, resulting in a high therapeutic effect, which was not observed in LMW drugs. In addition, RNP^O may lack the undesirable side effects of LMW TEMPOL, since it is not absorbed into the bloodstream. Based on obtained results in this study, the therapeutic efficiency of nitroxide radicals could be successfully enhanced by using nanoparticles to suppress inflammation in the colon area and reduce undesirable side effects. Therefore, I believe that RNP^O may become an important therapeutic agent for the treatment of UC.

3.5. References

1. Khor B, Gardet A, Xavier RJ. *Nat Rev* **2011**;474:307–17.
2. Podolsky DK. *N Engl J Med* **2002**;347:417–29.
3. Abraham C, Cho HJ. *N Engl J Med* **2009**;361:2066–78.
4. Edward VL. *Gastroenterology* **2004**;126:1504–17.
5. Simmonds NJ, Rampton DS. *Gut* **1993**;34:865–8.
6. Xavier RJ, Podolsky DK. *Nat Rev* **2007**;448:427–34.
7. Babbs CF. *Free Radic Biol Med* **1992**;13:169–82.
8. McCord JM. *Am J Med* **2000**;108:652–9.
9. Jin Y, Kotakadi VS, Ying L, et al. *Carcinogenesis* **2008**;29:2351–9.
10. Ju J, Hao X, Lee MJ, et al. *Cancer Prev Re* **2009**;2:143–52.
11. Aggarwal BB, Harikumar KB. *Int J Biochem Cell Biol* **2009**;41:40–59.

12. Kim B, Rutka J, Chan W. *N Engl J Med* **2010**;36:2434–43.
13. Otsuka H, Nagasaki Y, Kataoka K. *Adv Drug Deliv Rev* **2003**;55:403–19.
14. Maeda H, Fang J, Inutsuka T, et al. *Int Immunopharmacol* **2003**;3:319–28.
15. Weis SM, Cheres DA. *Nat Med* **2011**;17:1359–70.
16. Davis ME, Chen ZG, Shin DM. *Nat Rev Drug Dis* **2008**;7:771–82.
17. Cabral H, Matsumoto Y, Mizuno K, et al. *Nat Nanotech* **2011**;6:815–23.
18. Yoshitomi T, Hirayama A, Nagasaki Y. *Biomaterials* **2011**;32:8021–8.
19. Marushima A, Suzuki K, Nagasaki Y, et al. *Neurosurgery* **2011**;68:1418–26.
20. Chonpathompikunlert P, Yoshitomi T, Han J, et al. *Ther Deliv* **2011**;2:585–97.
21. Chonpathompikunlert P, Yoshitomi T, Han J, et al. *Biomaterials* **2011**;32:8605–12.
22. Yoshitomi T, Nagasaki Y. *Nanomedicine (London)* **2011**;6:509–18.
23. Yoshitomi T, Suzuki R, Mamiya T, et al. *Bioconjugate Chem* **2009**;20:1792–8.
24. Yoshitomi T, Miyamoto D, Nagasaki Y. *Biomacromolecules* **2009**;10:596–601.
25. Lamprecht A, Schafer U, Lehr CM. *Pharm Res* **2001**;18:788–93.
26. Francis MF, Cristea M, Winnik FM. *Pure Appl Chem* **2004**;76:1321–35.
27. Cooper HS, Murthy SN, Shah RS, et al. *Lab Invest* **1993**;69:238–49.
28. Bryson GJ, Harmon BV, Collins RJ. *Immunol Cell Biol* **1994**;72:35–41.
29. Friend DR, Sellin J. *Adv Drug Deliv Rev* **2005**;57:215–6.
30. Stephen BH. *Gastroenterology* **2004**;126:1582–92.
31. Singh K, Chaturvedi R, Barry DP, et al. *J Biol Chem* **2011**;286:3839–50.
32. Helieh S, Theresa S, Craig J, et al. *J Nutr Biochem* **2005**;16:297–304.
33. Jiang W, Kim B, Rutka J, et al. *Nat Nanotech* **2008**;3:145–50.
34. Tobio M, Sanchez A, Vila A, et al. *Colloids Surf B* **2000**;18:315–23.
35. Lai SK, Wang YY, Hanes J. *Adv Drug Deliv Rev* **2009**;61:158–71.
36. Friend, D.R. *Adv Drug Deliv Rev* **2005**;57:247–65.

37. Laroui H, Dalmasso G, Thu Nguyen HT, et al. *Gastroenterology* **2010**;138:843–53.
38. Ensign LM, Cone R, Hanes J. *Adv Drug Deliv Rev* **2012**;64:557–70.
39. Pullan RD, Thomas G, Rhodes M, et al. *Gut* **1994**;35:353–9.
40. Cerejido M, Contreras RG, Flores-Benítez D, et al. *Arch Med Res* **2007**;38:465–78.

Chapter 4

Effect of redox nanoparticle on intestinal microflora

Abstract

Patients with ulcerative colitis (UC) exhibit overproduction of reactive oxygen species (ROS) and imbalance of colonic microflora. In chapter 3, a novel redox nanoparticle (RNP^O), which effectively scavenged ROS in the inflamed mucosa of mice with dextran sodium sulfate (DSS)-induced colitis after oral administration, was developed. The objective of this chapter was to examine whether the orally administered RNP^O changed the colonic microflora in healthy mice and those with colitis. RNP^O was synthesized by self-assembly of an amphiphilic block copolymer that contains stable nitroxide radicals in hydrophobic side chain via ether linkage. Colitis was induced in mice by supplementing DSS in drinking water for 7 d, and RNP^O was orally administered daily during DSS treatment. The alterations of fecal microflora during treatment of DSS and RNP^O were investigated using microbiological assays. It was investigated that RNP^O did not result in significant changes to the fecal microflora in healthy mice. Although total aerobic and anaerobic bacteria were not significantly different between experimental groups, a remarkable increase in commensal bacteria (*Escherichia coli* and *Staphylococcus* sp.) was observed in mice with DSS-induced colitis. Interestingly, orally administered RNP^O remarkably reduced the number of these commensal bacteria increasing in mice with colitis. On the basis of the obtained results, it is confirmed that the oral administration of RNP^O did not change any composition of bacteria in feces, which strongly suggests protective effect of RNP^O on healthy environment in intestinal microflora. RNP^O may become an effective and safe medication for treatment of UC.

4.1. Introduction

- Inflammatory bowel disease (IBD), including Crohn's disease and ulcerative colitis (UC), affects millions of patients worldwide.^{1,2} Although the exact etiologies of IBD remain uncertain, the intestinal mucosa of IBD patients is reported to be characterized by overproduction of reactive oxygen species (ROS) and imbalances of important antioxidants, leading to oxidative damage and

destruction of the mucosal barrier.^{3,4} In addition, intestinal microflora has attracted considerable attention because it contributes to the intestinal function of improving healthy gastrointestinal (GI) tract and plays a potential role in the pathogenesis of UC.^{5,6} An imbalance in the constitution of intestinal microflora could lead to the dysregulation of host immunoreactivity towards intestinal bacteria, resulting in GI disorders and IBD.

- It has been reported that intestinal microflora play important role in regulating host inflammatory response and in maintaining the immunological homeostasis.^{7,8} The distal ileum and the colon are the areas with the highest bacterial numbers and are the main sites of inflammation in IBD. The number of bacteria in large intestine can reach upward of $10^{13} - 10^{14}$ bacteria, with more than 500 different bacterial species living together in a state of balance.^{9,10} In addition, the GI surface has regular contacts with food components and chemical substances, which may positively or negatively affect the balance of intestinal microflora. For instance, oral administration of dextran sodium sulfate (DSS), a well-known polysaccharide used to induce colitis in a murine model, is toxic to the colonic epithelium and alters the constitution of intestinal microflora,¹¹ leading to the activation of inflammatory responses and inflammation.

- In chapter 3, a novel redox nanoparticle (RNP^O) with ROS scavenging potential of stable nitroxide radicals has been developed. RNP^O is a core-shell-type polymeric micelle that is 40 nm in diameter and prepared by self-assembly of methoxy-poly(ethylene glycol)-*b*-poly[4-(2,2,6,6-tetramethylpiperidine-1-oxyl)oxymethylstyrene] (MeO-PEG-*b*-PMOT), which is an amphiphilic block copolymer that contains stable nitroxide radicals in a hydrophobic segment as a side chain via ether linkage (**Figure 4.1A**). It was investigated that the orally administered RNP^O specifically accumulated in the colonic mucosa and effectively scavenged ROS in the inflamed colon of mice with DSS-induced colitis.¹² However, the impact of RNP^O on the colonic microflora remains unknown. In this chapter, I examined whether orally administered

RNP⁰ would induce the alteration of fecal bacteria in healthy control mice and mice with DSS-induced colitis to elucidate action of RNP⁰ in the GI tract.

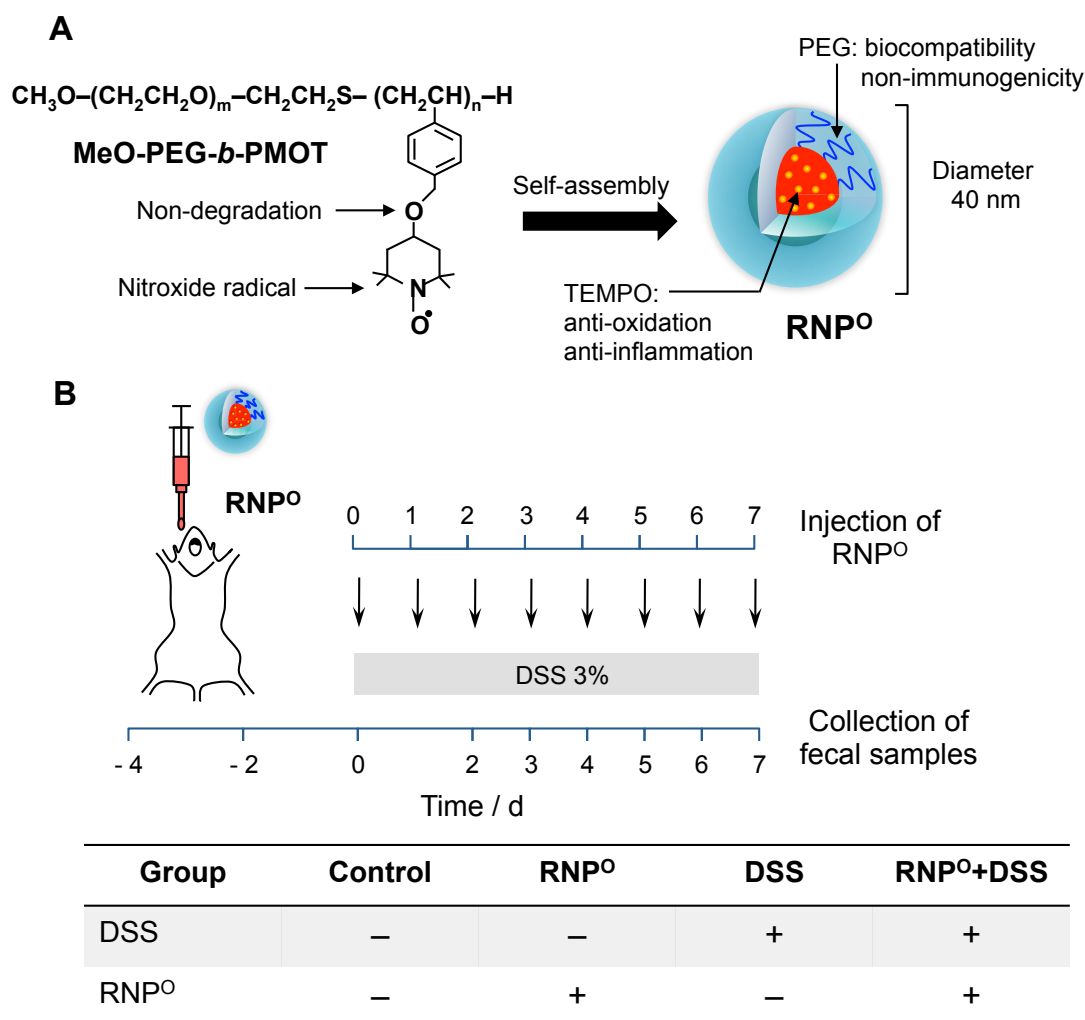


Figure 4.1. Schematic illustration of the redox nanoparticle RNP⁰ and the experimental design. (A) RNP⁰ was prepared using a self-assembling amphiphilic block copolymer (MeO-PEG-*b*-PMOT) composed a hydrophilic PEG segment and a hydrophobic poly(4-methylstyrene) segment possessing 2,2,6,6-tetramethylpiperidine-1-oxyl (TEMPO) moieties via ether linkage. (B) Murine colitis was induced by supplementation of 3% (wt/vol) DSS in the drinking water for 7 d and RNP⁰ (166.7 mg/kg) was orally administered daily during the 7 d of DSS treatment. The animals were divided into 4 groups, n = 5 mice per group.

4.2. Materials and Methods

4.2.1. Preparation of redox polymer and RNP^O

- RNP^O was prepared by self-assembling of the MeO-PEG-*b*-PMOT block copolymer, as previously reported.^{13, 14} Briefly, poly(ethylene glycol)-*b*-poly(chloromethylstyrene) (MeO-PEG-*b*-PCMS) was synthesized by radical telomerization of chloromethylstyrene (CMS; AGC Seimi Chemical, Ibaraki, Japan) using methoxy-poly(ethylene glycol)-sulfanyl (MeO-PEG-SH; Mn = 5,000; NOF Co., Inc., Tokyo, Japan) as a telogen. Nitroxide radical moieties were introduced as a side chain of the PCMS segment via Williamson ether synthesis of benzyl chloride in the MeO-PEG-*b*-PCMS block copolymer with the alkoxide of 4-hydroxyl-2,2,6,6-tetramethylpiperidine-1-oxyl (TEMPO; Tokyo Chemical Industry, Tokyo, Japan). MeO-PEG-*b*-PMOT was dissolved in N,N-dimethylformamide (Wako Pure Chemicals, Osaka, Japan) followed by transfer into a membrane tube (Spectra/Por, molecular weight cut-off size: 3,500 Da, Spectrum Laboratories Inc., Savannah, GA, USA) and then dialyzed for 24 h against 2 L of distilled water, which was changed after 2, 4, 8, 12, and 20 h to obtain the polymeric nanoparticle RNP^O. The average size of RNP^O (42.1 ± 1.7 nm, polydispersity index = 0.18) was measured using dynamic light scattering (Zetasizer Nano ZS, Worcestershire, UK). The amount of nitroxide radicals inside the nanoparticle (1.2 μmol of nitroxide radical per 1 mg of MeO-PEG-*b*-PMOT) was measured using electron spin resonance spectroscopy (JES-TE25X, JEOL, Tokyo, Japan).

4.2.2. Animals

- All experiments were performed using 7-week-old male ICR mice (32–35 g) purchased from Charles River Japan, Inc. (Yokohama, Japan). Mice were maintained in the experimental animal facilities at the University of Tsukuba. The animals were housed in the Laboratory Animals Resource Center of the University of Tsukuba on a 12 h-light-dark cycle with controlled humidity and temperature. Mice were given *ad libitum* access to food and water according to the Guide for the Care and Use of Laboratory Animals Resource Center of the University of Tsukuba.

4.2.3. Murine model of DSS-induced colitis and experimental groups

- Murine colitis was induced by supplementation of 3% (wt/vol) DSS (5,000 Da; Wako Pure Chemicals, Osaka, Japan) in the drinking water for 7 d. The experiment was designed to include 4 groups: healthy control mice (Control group), RNP^O administered-healthy mice (RNP^O group), DSS-induced colitis mice (DSS group), and RNP^O administered-colitis mice (RNP^O+DSS group) (**Figure 4.1B**). The dose of RNP^O was 166.7 mg/kg/d, which contained 0.2 mmol of nitroxide radicals. The concentration RNP^O was adjusted in distilled water, and the solutions were filtered with a 0.25- μ m cellulose acetate filter (Advantec, Toyo Roshi Ltd., Tokyo, Japan) before oral administration.

4.2.4. Microbiological assay and medium

- Mouse fecal samples were collected at predetermined time points, as shown in **Figure 4.1B**. The fecal specimen (50–100 mg) was immediately transferred into 1 mL of cold sterile brain-heart infusion medium (BHI; Becton Dickinson, Sparks, MD, USA) containing 0.5% cysteine (Sigma, St. Louis, MO, USA), followed by mixing for 1 min at a low temperature (4–10 °C). Ten-fold serial dilutions (10^{-1} – 10^{-7}) were performed in BHI medium and 100 μ L of the appropriate dilutions were spread onto agar plates to calculate colony forming units (CFU)/g feces. BHI agar was used to count the number of aerobic bacteria. Gifu anaerobic medium (GAM) agar was used to count the number of anaerobic bacteria, which were incubated in anaerobic condition (AnaeroPack, Mitsubishi Gas Chemical, Tokyo, Japan). Bromothymol blue (BTB) lactose agar were used for detection and quantification of *Escherichia coli* (*E. coli*). Mannitol salt agar (MSA) was used for detection and quantification of *Staphylococcus* sp. The colonies were counted and expressed as colony numbers after 24 h of incubation at 37 °C. All GAM, BTB, and MSA media were purchased from Nissui Pharmaceutical Co. Ltd. (Tokyo, Japan). *E. coli* and *Staphylococcus* sp. were identified using the BBL Crystal Enteric/Nonfermenter Identification Kit (Becton Dickinson) and MicroScan WalkAway-96 system with a Pos Combo 3.1J panel (Siemens Medical Solutions

Diagnostics, Tokyo, Japan), respectively.

4.2.5. Statistical analysis

- The data are expressed as mean \pm standard deviation (SD). Differences between groups were examined for statistical significance using 1-way analysis of variance (ANOVA), followed by Tukey's honestly significant difference (HSD) post-hoc comparison (Statistical Package for the Social Sciences [SPSS] software, IBM Corp., Endicott, NY, USA). A probability value of less than 0.05 was considered significant for all statistical analyses.

4.3. Results

4.3.1. Effect of RNP^O on DSS-induced colitis mice

- Colitis in mice was induced by oral administration of DSS because the DSS model of colitis has numerous clinical and pathological similarities to human IBD, particularly UC.¹⁵ The symptoms of DSS-induced colitis may include watery diarrhea, bloody feces, and body weight loss. As shown in **Figure 4.2A**, the severity of colitis in the mice steadily increased during 7 d of DSS treatment, and the symptoms of watery diarrhea, bloody feces, and loss of body weight were evident in these mice. The therapeutic effect of RNP^O was confirmed again by the daily oral administration, which significantly reduced the symptoms of mice with DSS-induced colitis (**Figure 4.2B** and **C**). Changes in the fecal characteristics after oral administration of DSS, such as color and consistency, were clearly observed in the mice with colitis compared to that of control mice. In contrast, treatment with RNP^O did not result in any significant changes in the fecal characteristics of the mice with colitis relative to control mice (**Figure 4.2B**). In addition, a significant loss of body weight was observed in the DSS-treated mice after 7 d. However, the body weight of mice treated with RNP^O+DSS was similar to that of the control mice (**Figure 4.2C**), confirming the therapeutic effect of orally administered RNP^O on the mice with DSS-induced

colitis.

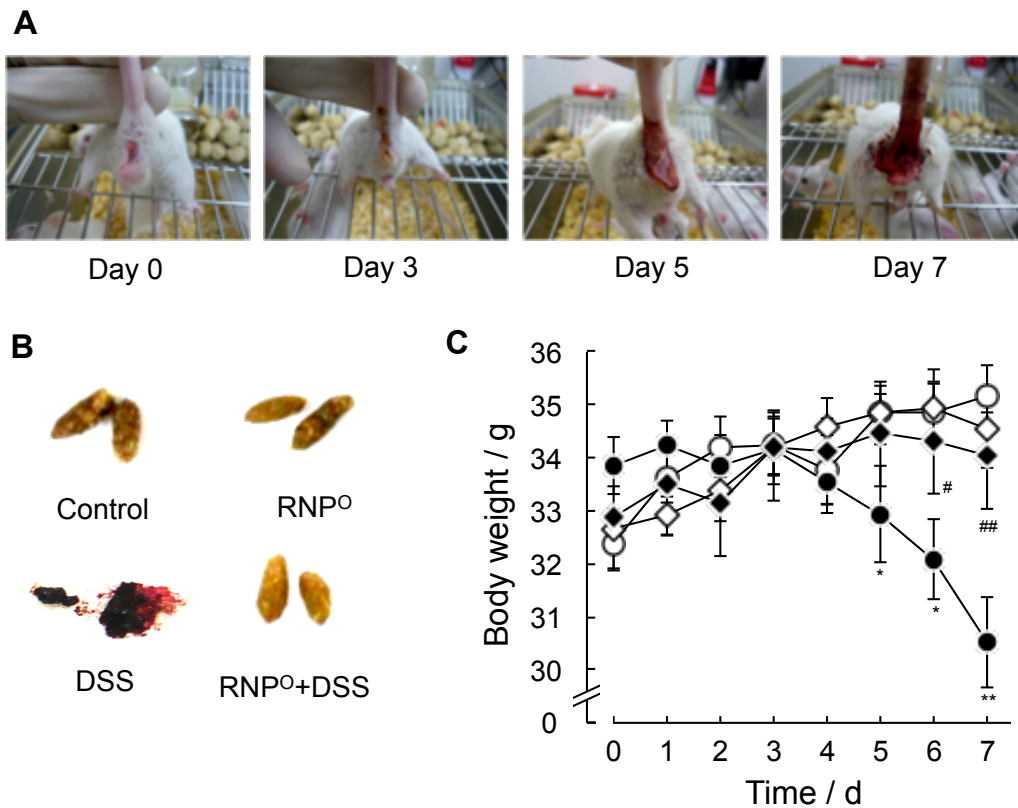


Figure 4.2. Effect of orally administered RNP⁰ on DSS-induced colitis in mice. **(A)** Severe symptoms of the mice with colitis at 0, 3, 5, and 7 d after DSS treatment (3% wt/vol). **(B)** Fecal characteristics of the 4 groups after 7 d of DSS and RNP⁰ treatment. **(C)** Body weight changes during 7 d of DSS and RNP⁰ treatment (Control: *white circle*; RNP⁰: *white diamond*; DSS: *black circle*; RNP⁰+DSS: *black diamond*). The data are expressed as mean \pm standard deviation, * $P < 0.05$ and ** $P < 0.01$ versus the control group, # $P < 0.05$ and ## $P < 0.01$ versus the colitis group, $n = 5$ mice per group.

4.3.2. Effect of RNP⁰ on microflora in normal and DSS-induced colitis mice

- The effect of RNP⁰ on population of intestinal microflora was then evaluated. Van der Waaij et al. reported that the composition of microflora in the lumen of intestinal mucosa is similar

to that of feces.¹⁶ Since I wanted to confirm the time-dependent variation of bacteria population in intestinal mucosa during treatment of DSS and RNP^O, the fecal specimens were analyzed. The fecal microflora population was evaluated using the spread plate method in specific microbiological media as described by Xia et al. and Verrecke et al.^{17,18} The numbers of anaerobic and aerobic bacteria were determined using GAM and BHI media, respectively. As shown in **Figure 4.3A** and **B**, no remarkable differences in the total numbers of anaerobic and aerobic bacteria between experimental groups were observed during the DSS and RNP^O treatments.

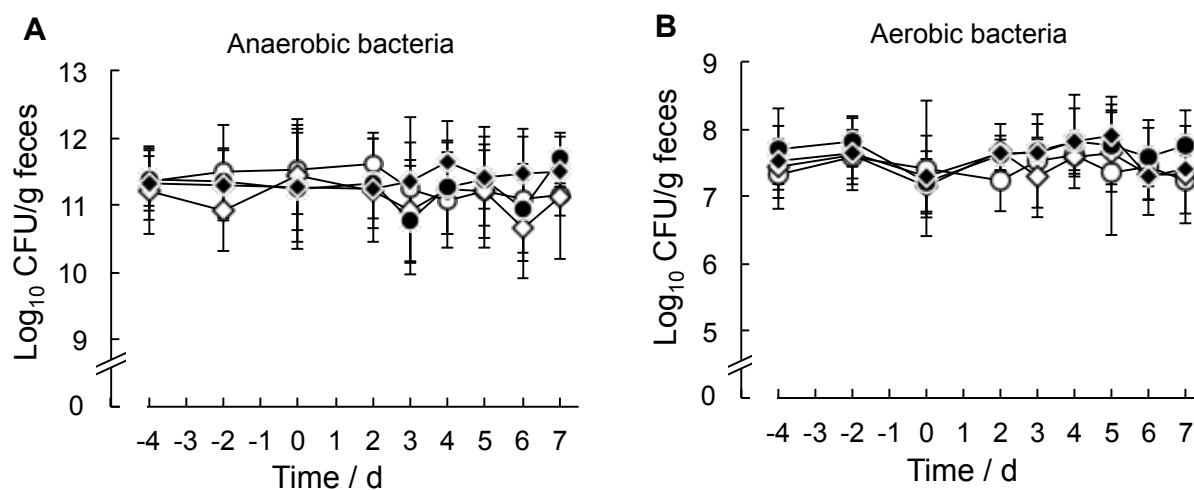


Figure 4.3. Alteration of anaerobic and aerobic bacteria during treatment with DSS and RNP^O. (A) The number of anaerobic bacteria was counted in GAM medium and (B) the number of aerobic bacteria was counted in BHI medium (Control: *white circle*; RNP^O: *white diamond*; DSS: *black circle*; RNP^O+DSS: *black diamond*). The data are expressed as mean \pm standard deviation, n = 5 mice per group.

- To further investigate the alterations of the fecal microflora composition in the mice with colitis after oral administration of RNP^O, commensal bacteria such as *E. coli* and *Staphylococcus* sp. were focused on. The *E. coli* produces brown-yellow colonies in the yellow zone on BTB medium (**Figure 4.4A**). Using a bacterial identification kit, these colonies were identified as *E. coli* (data not shown). Under normal conditions, the average number of *E. coli* was 10⁴–10⁶ CFU/g of tissue

and it was not changed by orally administered RNP^O. However, the number of *E. coli* significantly increases in DSS-treated mice, corresponding to the presence and severity of inflammation in colitis mice. Interestingly, the number of *E. coli* in mice treated with RNP^O+DSS was significantly reduced compared to DSS-treated mice (**Figure 4.4B**).

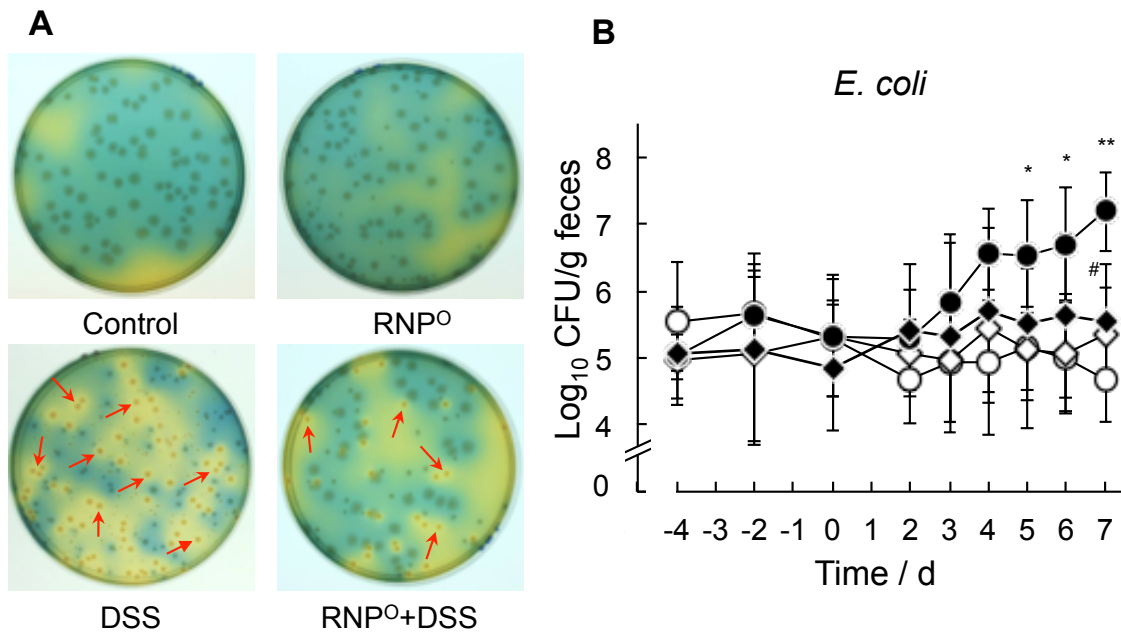


Figure 4.4. Alteration of *E. coli* during treatment with DSS and RNP^O. **(A)** The *E. coli* colonies in BTB medium after 7 d of DSS and RNP^O treatment (brown-yellow colonies with yellow zones; red arrow). **(B)** Alteration of *E. coli* number during treatment with DSS and RNP^O (Control: white circle; RNP^O: white diamond; DSS: black circle; RNP^O+DSS: black diamond). The data are expressed as mean \pm standard deviation, * $P < 0.05$ and ** $P < 0.01$ versus the control group, # $P < 0.05$ versus the colitis group, $n = 5$ mice per group.

- Similarly, changes in number of *Staphylococcus* sp. were also observed on MSA medium during treatment with RNP^O and DSS. As shown in **Figure 4.5A**, the small brown-yellow colonies in the yellow zones in MSA medium caused by mannitol fermentation were identified as mannitol-positive *Staphylococcus* sp., which increased significantly in the fecal samples of the

mice with DSS-induced colitis. In contrast, treatment with RNP^O remarkably reduced the number of *Staphylococcus* sp. in the fecal samples of the mice with DSS-induced colitis (**Figure 4.5B**). Importantly, the numbers of *Staphylococcus* sp. in mice treated with RNP^O alone were also similar to those of the control mice (10^4 – 10^6 CFU/g feces), indicating that oral administration of RNP^O did not affect the growth of these commensal bacteria.

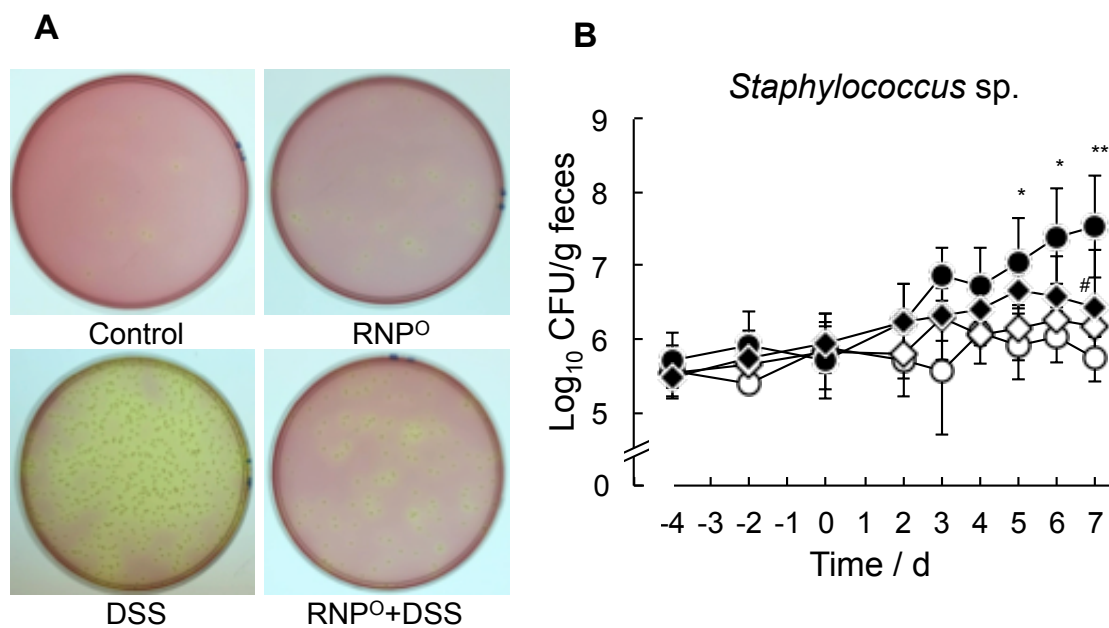


Figure 4.5. Alteration of *Staphylococcus* sp. during treatment with DSS and RNP^O. **(A)** The *Staphylococcus* sp. colonies in MSA medium after 7 d of DSS and RNP^O treatment (yellow-brown colonies with yellow zones). **(B)** Alteration of *Staphylococcus* sp. number during treatment with DSS and RNP^O (Control: white circle; RNP^O: white diamond; DSS: black circle; RNP^O+DSS: black diamond). The data are expressed as mean \pm standard deviation, * $P < 0.05$ and ** $P < 0.01$ versus the control group, # $P < 0.05$ versus the colitis group, $n = 5$ mice per group.

4.4. Discussion and Conclusions

- UC is a chronic, relapsed and inflammatory disease because its pathogenic mechanism is still unclear. Current medications such as aminosalicylates and glucocorticoids used to treat UC

patients are not always effective because of their non-specific distribution, absorption into the bloodstream and undesired side effects.^{19,20} In addition, these commercial drugs have been reported to affect the intestinal microflora after oral administration. For example, oral mesalamine and sulfasalazine, mainstays of treatment for UC patients, significantly decreased the total concentration of mucosa-associated bacteria.^{21,22} For the last decade, IBD was treated with chimeric anti-tumor necrosis factor alpha monoclonal antibodies, which suppressed inflammation in the GI tract to some extent. However, these costly therapies have been reported to have several adverse effects associated with systemic administration.²³ Therefore, development of an effective and safe medication for treatment of IBD is becoming very important.

- In chapter 3, a novel oral nanotherapy using redox nanoparticle RNP^O was developed for treatment of UC. It was revealed that orally administered RNP^O significantly accumulates in colon area, and the ROS scavenging capacity of RNP^O is the key factor responsible for the therapeutic effect in mice with DSS-induced colitis by reducing the oxidative stress and inflammatory responses. In addition, orally administered RNP^O was not absorbed into the bloodstream of normal and even mice with DSS-induced colitis, indicating that RNP^O did not affect on intestinal permeability of nanoparticle.¹² However, the effect of RNP^O on the colonic microflora, which plays a potential role in UC pathogenesis, remains unknown. Thus, in this chapter, I investigated the effect of orally administered RNP^O on the fecal microflora in healthy control mice and those with DSS-induced colitis.

- The results in this chapter showed that oral administration of RNP^O did not show the significant changes in microflora in healthy mice, indicating the innocuousness of this oral nanoparticle therapeutics against healthy colonic microflora. RNP^O possesses the shell of PEG, which is an excellent biocompatible polymer,²⁴ improving the stability of nanoparticle in GI tract, and reducing the immune responses and toxicity to microflora in colon. Actually, RNP^O did not

affect at all to the microflora in normal mice. It was also found that the number of commensal bacteria such as *E. coli* and *Staphylococcus* sp. remarkably increased in the fecal samples of DSS-induced colitis mice.

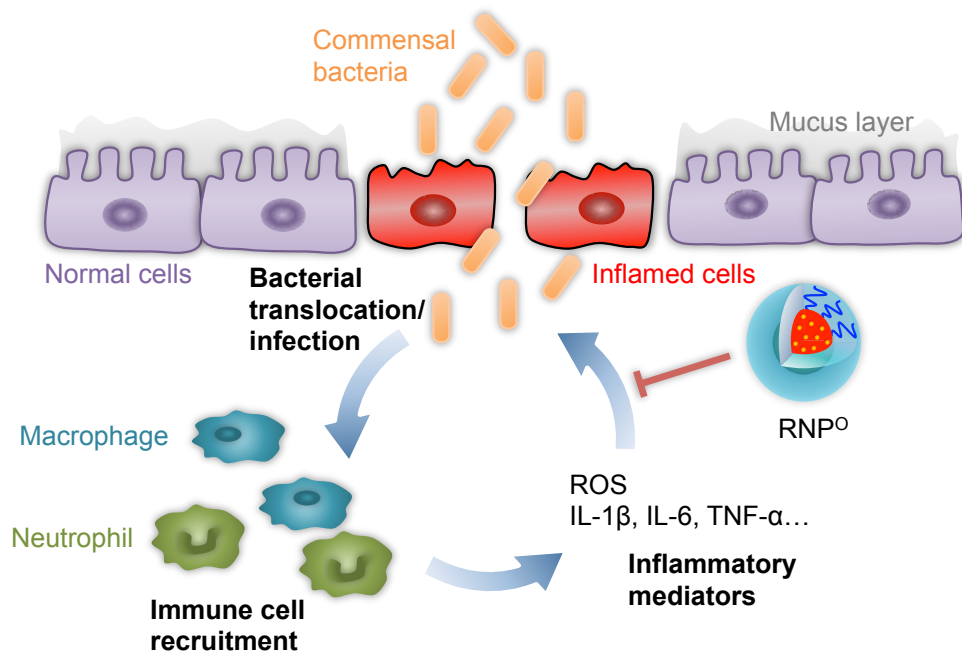


Figure 4.6. The hypothesis of RNP^o-mediated suppression of the infection by commensal bacteria in the colonic mucosa via ROS scavenging. In the inflamed colonic mucosa induced by DSS, immune cells such as macrophages and neutrophils are recruited and activated to release ROS and pro-inflammatory cytokines, leading to colonic tissue damages. A defect of the mucosal barrier induces translocation and infection by commensal bacteria and repeatedly activates the immune cells as a “vicious cycle”, which amplifies the inflammation and mucosal injury. Accumulation of RNP^o in the colon scavenges the overproduced ROS and inhibits pro-inflammatory cytokines, which protects the colonic mucosa from damage, resulting in inhibition of bacterial infection and inflammatory responses.

- The association between the abundance of *E. coli* and *Staphylococcus* sp. and the severity of colitis suggests that these bacteria have a pro-inflammatory action by activating the immune

responses and imbalance of microflora.²⁵⁻²⁸ The balance of intestinal microflora plays a pivotal role to maintain the immunological homeostasis to the healthy host; however, the disruption of the normally stable microflora might be predicted to result in the pathological conditions of IBD.^{29,30} Interestingly, RNP^O treatment restored the balance of intestinal microflora in both normal and colitis mice, indicating the safety of RNP^O for clinical trials.

- In the healthy colonic mucosa, epithelial cells are covered by a thick layer of mucus, which enables colonization by commensal and beneficial bacteria and provides a barrier to pathogenic bacteria.³¹ However, the thin mucus layer and crypt loss were observed in the inflamed colons of DSS-treated mice.^{32,33} In DSS-induced intestinal inflammation, interstitial macrophages and leukocytes produce ROS and epithelial cells produce antimicrobial proteins to prevent the translocation and infection of bacteria into the tissue.³⁴⁻³⁶ A low level of luminal colonic ROS innately protects epithelial cells from bacterial antigens, contributes to intracellular signaling pathways, and promotes the production of pro-inflammatory cytokines. However, in the case of severe intestinal inflammation, a high level of ROS induces epithelial tissue damage and increased permeability, leading to the translocation and infection by commensal bacteria.^{37,38} In chapter 3, oral administration of RNP^O effectively scavenged the overproduced ROS, reduced the production of pro-inflammatory mediators in the mice with DSS-induced colitis, and did not stimulate the immune system. The results of this chapter showed that orally administered RNP^O significantly reduced the number of increased commensal bacteria in DSS-treated mice, indicating that the anti-inflammatory effect of RNP^O might reduce translation and infection by commensal bacteria in the colonic mucosa. Based on the results in this chapter, it is assumed that although RNP^O did not directly affect the colonic microflora, RNP^O scavenged the overproduced ROS and inhibited pro-inflammatory mediators to protect the colonic mucosa, thus preventing the increase in commensal bacteria in the inflamed mucosa (**Figure 4.6**). Taken together, these results demonstrated the protective effect of RNP^O on the colonic mucosa due to ROS scavenging,

suppression of inflammatory responses, and inhibition of commensal bacterial translocation/infection.

- In conclusion, the oral nanotherapeutic RNP^O, which possesses a biocompatible PEG shell and anti-oxidative nitroxide radicals in the core, did not affect the balance of microflora in healthy large intestines and inhibited the increase in commensal bacteria in the colonic mucosa of mice with DSS-induced colitis by scavenging ROS and suppressing inflammation. The results in this chapter contribute to the clarification of the therapeutic and safe effects of RNP^O for the treatment of UC via oral administration. Based on these results, RNP^O is a promising therapeutic medication for UC treatment.

4.5. References

1. Podolsky DK. *N Engl J Med* **2002**;347:417–29.
2. Edward VL. *Gastroenterology* **2004**;126:1504–17.
3. Simmonds NJ, Rampton DS. *Gut* **1993**;34:865–8.
4. Babbs CF. *Free Radic Biol Med* **1992**;13:169–81.
5. Gionchetti P, Rizzello F, Lammers KM, Morselli C, Sollazzi L, Davies S, et al. *World J Gastroenterol* **2006**;12:3306–13.
6. Khor B, Gardet A, Xavier RJ. *Nat Rev* **2011**;44:307–17.
7. Sartor RB. *Res Immunol* **1997**;148:567–76.
8. Strauch UG, Obermeier F, Grunwald N, Gürster S, Dunger N, Schultz M, et al. *Gut* **2005**;54:1546–52.
9. Gibson GR, Roberfroid M. *J Nutr* **1995**;125:1401–12.
10. Sasaki M, Klapproth J. *J Signal Transduct* **2012**;doi: 10.1155/2012/704953.
11. Araki Y, Andoh A, Tsujikawa T, Fujiyama Y, Bamba T. *Eur J Gastroenterol Hepatol* **2011**;13:

107–12.

12. Vong LB, Tomita T, Yoshitomi T, Matsui H, Nagasaki Y. *Gastroenterology* **2012**;143:1027–36.e3.

13. Yoshitomi T, Miyamoto D, Nagasaki Y. *Biomacromolecules* **2009**;10:596–601.

14. Yoshitomi T, Nagasaki Y. *Nanomedicine* **2011**;6:509–18.

15. Solomon L, Mansor S, Mallon P, Donnelly E, Hoper M, Loughrey M, et al. *Comp Clin Pathol* **2010**;19:235–39.

16. Van der Waaij LA, Harmsen HJ, Madjipour M, Kroese FG, Zwiers M, van Dullemen HM et al. *Inflamm Bowel Dis* **2005**;10:865–71.

17. Xia Y, Chen HQ, Zhang M, Jiang YQ, Hang XM, Qin HL. *J Gastroenterol Hepatol* **2011**;26:405–11.

18. Vereecke L, Sze M, Mc Guire C, Rogiers B, Chu Y, Schmidt-Supprian M, et al. *J Exp Med* **2010**;207:1513–23.

19. Friend DR, Sellin J. *Adv Drug Deliv Rev* **2005**;57:215–16.

20. Hanauer SB. *Gastroenterology* **2004**;126:1582–92.

21. Swidsinski A, Loening-Baucke V, Bengmark S, Lochs H, Dörffel Y. *Inflamm Bowel Dis* **2007**;1:51–6.

22. West B, Lendrum R, Hill MJ, Walker G. *Gut* **1974**;15:960–5.

23. Singh K, Chaturvedi R, Barry DP, Coburn LA, Asim M, Lewis ND, et al. *J Biol Chem* **2011**;286:3839–50.

24. Otsuka H, Nagasaki Y, Kataoka K. *Adv Drug Deliv Rev* **2003**;55:403–19.

25. Resta-Lenert S, Barrett KE. *Gut* **2003**;52:988–97.

26. Kotlowski R, Bernstein CN, Sepehri S, Krause DO. *Gut* **2007**;56:669–75.

27. Lu J, Wang A, Ansari S, Hershberg RM, McKay DM. *Gastroenterology* **2003**;125:1785–95.
28. Vesterlund S, Karp M, Salminen S, Ouwehand AC. *Microbiology* **2006**;152:1819–26.
29. Takaishi H, Matsuki T, Nakazawa A, Takada T, Kado S, Asahara T et al. *Int J Med Microbiol* **2008**;298:463–72.
30. Abraham C, Medzhitov R. *Gastroenterology* **2011**;140:1729–37.
31. Hans W, Schölmerich J, Gross V, Falk W. *Eur J Gastroenterol Hepatol* **2000**;12:267–73.
32. Johansson ME, Gustafsson JK, Sjöberg KE, Petersson J, Holm L, Sjövall H, et al. *PLoS One* **2010**;5:e12238.
33. Zhou FX, Chen L, Liu XW, Ouyang CH, Wu XP, Wang XH, et al. *World J Gastroenterol* **2012**;18:2344–56.
34. Ganz T, Weiss J. *Semin Hematol* **1997**;34:343–54.
35. Pavlick KP, Laroux FS, Fuseler J, Wolf RE, Gray L, Hoffman J, et al. *Free Radic Biol Med* **2002**;33:311–22.
36. Roessner A, Kuester D, Malfertheiner P, Schneider-Stock R. *Pathol Res Pract* **2008**;204:511–24.
37. Keshavarzian A, Fusunyan RD, Jacyno M, Winship D, MacDermott RP, Sanderson IR. *Am J Gastroenterol* **1999**;94:04–12.
38. Brownlee IA, Knight J, Dettmar PW, Pearson JP. *Free Radic Biol Med* **2007**;43:800–8.

Chapter 5

Therapeutic effect redox nanoparticle on colitis-associated colon cancer

Abstract

Oral chemotherapy is the preferred treatment for colon cancer. However, this strategy faces many challenges, including instability in the gastrointestinal (GI) tract, insufficient bioavailability, low tumor targeting, and severe adverse effects. In this chapter, I investigated the effect of redox nanoparticle (RNP^O) as an ideal oral therapeutics for colitis-associated colon cancer treatment. RNP^O possesses nitroxide radicals in the core, which act as reactive oxygen species (ROS) scavengers. Orally administered RNP^O highly accumulated in colonic mucosa, and specifically internalized in cancer tissues, but less in normal tissues. Despite of long-term oral administration of RNP^O, no noticeable toxicities were observed in major organs of mice. Because RNP^O effectively scavenged ROS, it significantly suppressed tumor growth after accumulation at tumor sites. Combination of RNP^O with the conventional chemotherapy, irinotecan, led to remarkably improved therapeutic efficacy and effectively suppressed its adverse effects on GI tract. Therefore, RNP^O is promising oral nanotherapeutics for cancer therapies.

5.1. Introduction

- Inflammatory bowel disease (IBD), which includes chronic gastrointestinal (GI) disorders such as Crohn's disease (CD) and ulcerative colitis (UC), affects millions of patients worldwide.¹⁻⁴ After 30 years of living with these diseases, 18–20% of UC and 8% of CD patients develop colitis-associated colon cancer (CAC), the third most common malignancy and one of the major causes of cancer-related death.^{5,6} In IBD patients, the increasing of reactive oxygen species (ROS) causes oxidative stress and oxidative cellular damage promoting carcinogenesis.^{7,8} It has been reported that antioxidants such as N-acetylcysteine and resveratrol inhibited CAC development.^{9,10} While oral administration of drugs are preferred by patient due to its convenience and compliance, these low-molecular-weight (LMW) compounds are not always effective due to nonspecific drug distribution, low retention in the GI tract, and absorption in the bloodstream, causing undesired

adverse effects in the entire body. On the other hand, chemotherapy using 5-fluorouracil (5-FU) or irinotecan (Iri) has been used alone or in combination with other drugs as the first-line therapeutic agents for colorectal cancer.^{11,12} However, these anticancer drugs are insufficient bioavailability and low tumor targeting. Furthermore, patients treated with these chemotherapeutic agents suffer from severe adverse effects such as mucositis and diarrhea, which limits the dose intensification and compromises efficacy.¹³

- Nanotechnology has enabled significant advances in the areas of cancer diagnosis and therapy.¹⁴⁻¹⁶ Though a number of nanoparticle-drug combinations are assessed in preclinical or clinical applications, most of delivery systems are intravenously injectable formulations and are incapable of oral administration.^{17,18} On the other hand, it has been reported that nanocomposites such as silver nanoparticle for therapeutics itself exhibits the undesired toxicity on the GI tract after repeated oral administration.^{19,20} Oral nanotherapy using a redox nanoparticle (RNP^O) has been developed for suppressing inflammation in mice with colitis,²¹ and indomethacin-induced small intestinal inflammation.²² RNP^O was prepared by self-assembly of methoxy-poly(ethylene glycol)-*b*-poly(4-[2,2,6,6-tetramethylpiperidine-1-oxyl]oxymethylstyrene) [MeO-PEG-*b*-PMOT], which is an amphiphilic block copolymer with stable nitroxide radicals in a hydrophobic segment as a side chain via an ether linkage (**Figure 5.1A**). The size of RNP^O is approximately 40 nm in diameter, with a remarkably narrow distribution (**Figure 5.1B**) and extremely high colloidal stability owing to the PEG shell layer. As shown in **Figure 5.1C**, RNP^O is stable and maintains micelle form under physiological conditions without aggregation. This stable character improves accumulation tendency of RNP^O to colonic mucosa, but not commercially available polystyrene particles. Furthermore, these 40 nm particles prevent the uptake into bloodstream via mesentery. Along with these characteristics, it has been confirmed that RNP^O effectively scavenges ROS to result in significant suppression of inflammation in mice with colitis.²¹ Suppression of inflammation in the tumor microenvironments is reported to work as suppressor of tumor

progression and resistance against chemotherapy.²³ Notably, RNP^O did not cause any disturbance to the population of intestinal bacteria.²⁴ Based on these characteristics of RNP^O, I proposed that it would be a suitable oral therapeutics for cancer. Thus, it is interesting to apply RNP^O as a novel oral therapeutics for treatment of colon cancer.

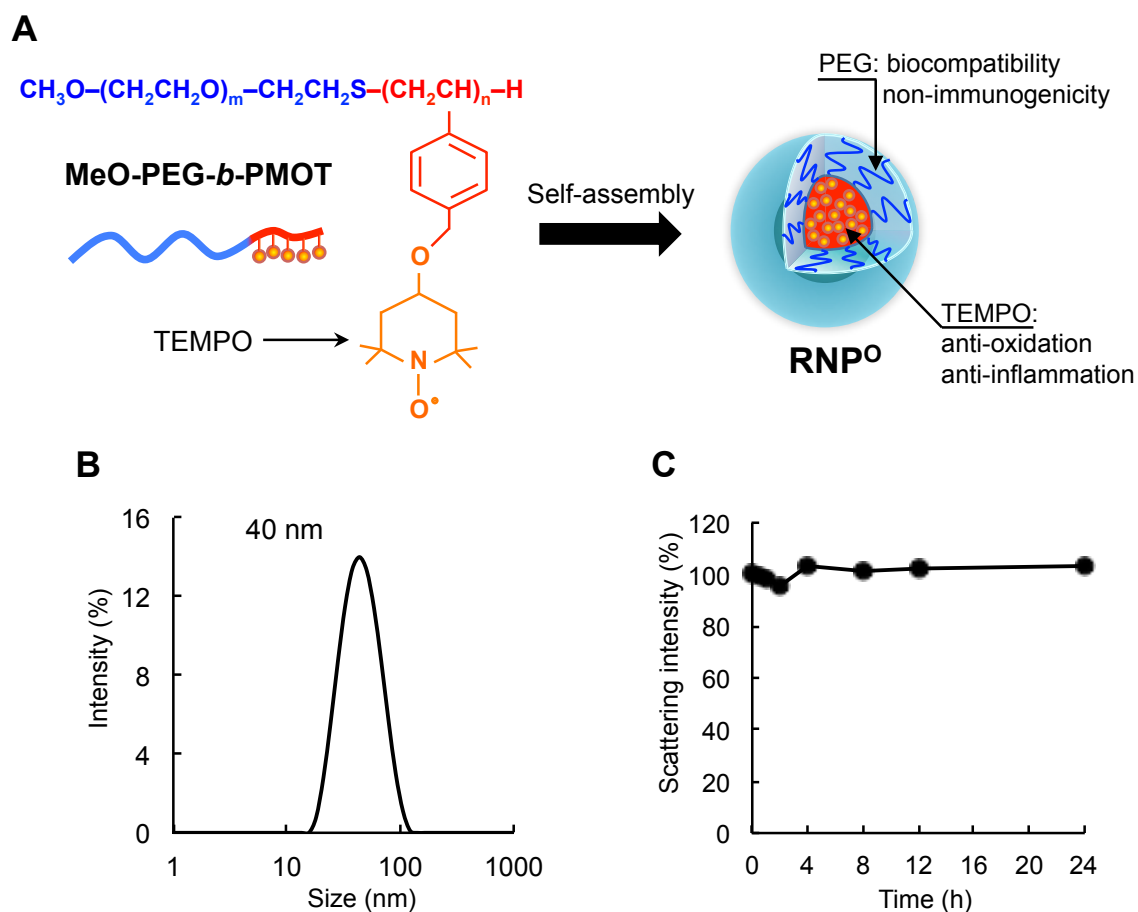


Figure 5.1. Schematic illustration of RNP^O and its characteristics. (A) RNP^O was prepared by self-assembly of a poly(ethylene glycol)-*b*-poly(4-methylstyrene) block copolymer possessing nitroxide radical TEMPO moieties. (B) The size of RNP^O and C, the stability of RNP^O under physiological conditions (PBS pH 7.4, 10% FBS) were measured by dynamic light scattering using a Zetasizer Nano ZS (Malvern Instruments, Ltd., Malvern, UK).

- In this chapter, azoxymethane (AOM) and dextran sodium sulfate (DSS) were used to

chemically induce CAC in mice, and the efficacy of oral RNP^O as a nanomedicine and combination therapy was investigated. No blood absorption and non-toxicity of RNP^O were observed despite of long-term oral administration, which improves accumulation in colon region and prevents undesired adverse effects to entire body. Orally administered RNP^O tends to internalize in colon cancer cells, but not normal colon cells, indicating the extremely low adverse effects of this oral nanotherapeutics. Oral administration of RNP^O effectively suppressed inflammation in the colon region, resulting in both high protective and therapeutic effects against CAC development. It is interesting to note that when RNP^O was combined with conventional chemotherapy, the therapeutic effect on CAC was significantly enhanced, retaining low adverse effects of the chemotherapy on the GI tract.

5.2. Materials and Methods

5.2.1. Preparation of RNP^O

- RNP^O was prepared by a self-assembling MeO-PEG-*b*-PMOT block copolymer, as previously reported.^{21,25} Briefly, methoxy-poly(ethylene glycol)-*b*-poly(chloromethylstyrene) (MeO-PEG-*b*-PCMS) was synthesized by the radical telomerization of chloromethylstyrene (CMS; Seimi Chemical Co., Ltd., Kanagawa, Japan) using methoxy-poly(ethylene glycol)-sulphonyl (MeO-PEG-SH; NOF Corporation Co., Ltd., Tokyo, Japan; Mn = 5,000) as a telogen (the degree of polymerization of CMS = 16 units). The chloromethyl groups were converted to TEMPOs via a Williamson ether synthesis of benzyl chloride in the MeO-PEG-*b*-PCMS block copolymer with the alkoxide of 4-hydroxy-2,2,6,6-tetramethylpiperidine-1-oxyl (TEMPOL; Tokyo Chemical Industry Co., Ltd., Tokyo, Japan), as previously reported (the extent of TEMPO modification = 85%). RNP^O was prepared from MeO-PEG-*b*-PMOT using a dialysis method.

5.2.2. Cell lines and cultures

- The mouse colorectal carcinoma cell line C-26 (RCB2657) was obtained from Riken BioResource Center (Riken Tsukuba Institute, Ibaraki, Japan). C-26 cells were grown in Dulbecco's modified eagle medium (DMEM; Sigma-Aldrich, St. Louis, MO) containing 10% fetal bovine serum (Sigma-Aldrich, St. Louis, MO), and 1% antibiotics (penicillin/streptomycin/neomycin; Invitrogen, Carlsbad, CA) in a humidified atmosphere of 5% CO₂ at 37 °C.

5.2.3. Cellular uptake of RNP^O in vitro

- The experiment was carried out using rhodamine-labeled RNP^O (Rho-RNP^O) to analyze the cellular uptake of these nanoparticles by fluorescent confocal microscope. Rho-RNP^O was prepared via a thiourethane bond between MeO-PEG-*b*-PMOT possessing reduced TEMPO moieties and rhodamine B isothiocyanate (Sigma-Aldrich, St. Louis, MO) in dimethylformamide-involved sodium hydride, as previously reported (21). C-26 colon cancer cells were seeded in 12-well plates at a certain density (5×10^4 cells per well). After 2 d of culturing, the DMEM was replaced with fresh media, and the Rho-RNP^O solution (100 µg/mL) was added. At a predetermined time intervals, the cells were washed 3 times with fresh media. Hoechst 33342 (Invitrogen) and LysoTracker (Green DND-26, Invitrogen) were added for 15 min at 37 °C before imaging in order to stain nuclei and lysosomes, respectively. Photos of cellular uptake were taken and analyzed using a fluorescent confocal microscope system (Zeiss LSM 700, Carl Zeiss Microscopy GmbH, Jena, Germany) under oil immersion at 63× magnification.

5.2.4. Animal

- All experiments were carried out using 7 to 8-week-old male ICR mice (32–35 g) purchased from Charles River Japan, Inc. (Yokohama, Japan). Mice were maintained in the

experimental animal facilities at the University of Tsukuba under controlled temperature (23 ± 1 °C), humidity ($50 \pm 5\%$) and lighting (12 h light-dark cycles). The animals were given free access to food and water. All experiments were performed in accordance with the Regulation for Animal Experiments in the University of Tsukuba and the Fundamental Guideline for Proper Conduct of Animal Experiments and Related Activities in Academic Research Institutions under the jurisdiction of the Ministry of Education, Culture, Sports, Science, and Technology.

5.2.5. Cellular internalization of RNP^O in vivo

- Cellular isolation procedure was based on a previous report with modifications.²⁶ Colon tissues were collected from normal mice and mice with AOM/DSS-induced CAC at 5 h after oral administration of RNP^O (300 mg/kg); then, gently removed feces with PBS, followed by a mechanical fragmentation. Colonic tissues were treated with collagenase (10 mg/mL; Wako Pure Chemical Industries, Osaka, Japan) for 30 min at 37 °C with slow agitation, followed by a centrifugation at 10,000 rpm at 4 °C for 5 min. Cell pellets were gently resuspended in acetic acid (0.1 M, pH 3). Samples were centrifuged to separate extracellular RNP^O and intracellular internalized RNP^O. Supernatants and cell pellets were oxidized by potassium ferricyanide (10 mM; Kanto Chemical Co., Inc, Tokyo, Japan) for electron spin resonance (ESR) measurement under conditions described in the Supplementary Materials.

5.2.6. Induction of colitis and CAC by AOM and DSS

- Colitis was induced in mice by 3% (wt/vol) DSS (5,000 daltons; Wako Pure Chemical Industries, Osaka, Japan) supplemented in the drinking water for 7 d. For the CAC model, mice were injected intraperitoneally with 10 mg/kg body weight of AOM (Sigma-Aldrich, St. Louis, MO) followed by 2 cycles of 7-d of 3% DSS in the drinking water for 70 d.

5.2.7. Endoscopic imaging and tumor scoring

- To continuously observe the tumor development in CAC mice, a video endoscopy system (TESALA AVS, Olympus, Tokyo, Japan) for mouse was used according to the manufacturer's instructions. The experimental endoscope setup consisted of a probe (2.7 mm outer diameter) with a rod lens containing a light-emitting diode light source, a camera unit connected to a laptop monitor, and an air supply to facilitate regulated inflation of the mouse colon. After setting up the endoscope system, the mice were anesthetized by inhalation of isoflurane (Intervet, Inc., Tokyo, Japan). The endoscopic procedure was viewed on a color monitor and real time video was recorded via firewire connected to a laptop with Light Capture software (I-O Data device, Inc., Kanazawa, Japan).

- A previously described tumor scoring system was used to evaluate tumor development in mouse colons.²⁷ Tumors observed during endoscopies were counted to obtain the overall number of tumors. The sizes of all tumors in a given mouse were also scored to yield the tumor score. Tumor size was graded as follows: grade 1 (very small but detectable tumor), grade 2 (tumor covering up to 1/8 of the colonic circumference), grade 3 (tumor covering up to 1/4 of the colonic circumference), grade 4 (tumor covering up to 1/2 of the colonic circumference), and grade 5 (tumor covering more than 1/2 of the colonic circumference). The endoscope analysis was performed weekly or every 2 weeks starting after the second cycle of DSS administration until the end of the experiment.

5.2.8. Iri-induced intestinal mucositis in mice

- Intestinal mucositis was induced in mice by daily intraperitoneal injection of Iri (50 mg/kg) for 4 d.²⁸ To confirm the effect of RNP^O, mice were given RNP^O (300 mg/kg) by oral gavage daily during Iri treatment. Diarrhea assessment was performed after the treatment. The severity of diarrhea was scored as previously described.²⁹ [0 (normal–normal stools or absent), 1 (slight–wet and soft stools), 2 (moderate–wet and unformed stools), 3 (severe–watery stools)]. At day 5, mice

were sacrificed, and blood and intestinal samples were collected for hematological and histological assessments, respectively.

5.2.9. Statistical analysis

- All values are expressed as mean \pm standard error of the mean (SEM). Differences between groups were examined for statistical significance using 1-way analysis of variance, followed by Bonferroni or Turkey's post hoc test (SPSS software; IBM Corp, Armonk, NY). A value of $P < 0.05$ was considered significant for all statistical analyses.

5.3. Results

5.3.1. Accumulation of free drinking RNP^O in the GI tract and its non-toxicity

- The accumulation of nanoparticles in the colon region is one of the most important features of an effective nanomedicine for colon diseases including cancer. RNP^O was given to mice in free drinking water for a week and ESR assays were used to assess the distribution of RNP^O in the GI tract. ESR assays were performed for the blood and the main GI tract organs (stomach, small intestine, cecum, and colon) at a predetermined time. As shown in **Figure 5.2A**, RNP^O accumulation in the GI tract gradually increased over the administration time, particularly in the small intestine, cecum and colon regions, indicating high accumulation and long retention of RNP^O in these areas. Conversely, no RNP^O uptake in the bloodstreams of mice was observed, even for long-term administration. Lack of bloodstream uptake prevented potential adverse effects of the nitroxide radicals to the entire of body.

- To investigate the toxicity of RNP^O in the GI tract, healthy mice were treated long-term with orally administered RNP^O; hematology was analyzed and histology was assessed for tissues from the GI tract as well as other organs. There were no remarkable differences in the

hematological analysis of RNP⁰-treated mice as compared to healthy mice (**Figure 5.2B**). Additionally, there were no noticeable toxicities in tissues from the GI tract and other organs, even in mice treated with a high concentration of RNP⁰ (5 mg/mL) for a month (**Figure 5.2C**). These results indicate that, during long-term oral administration, RNP⁰ highly accumulates in the GI tract without any observed toxicity to healthy organs.

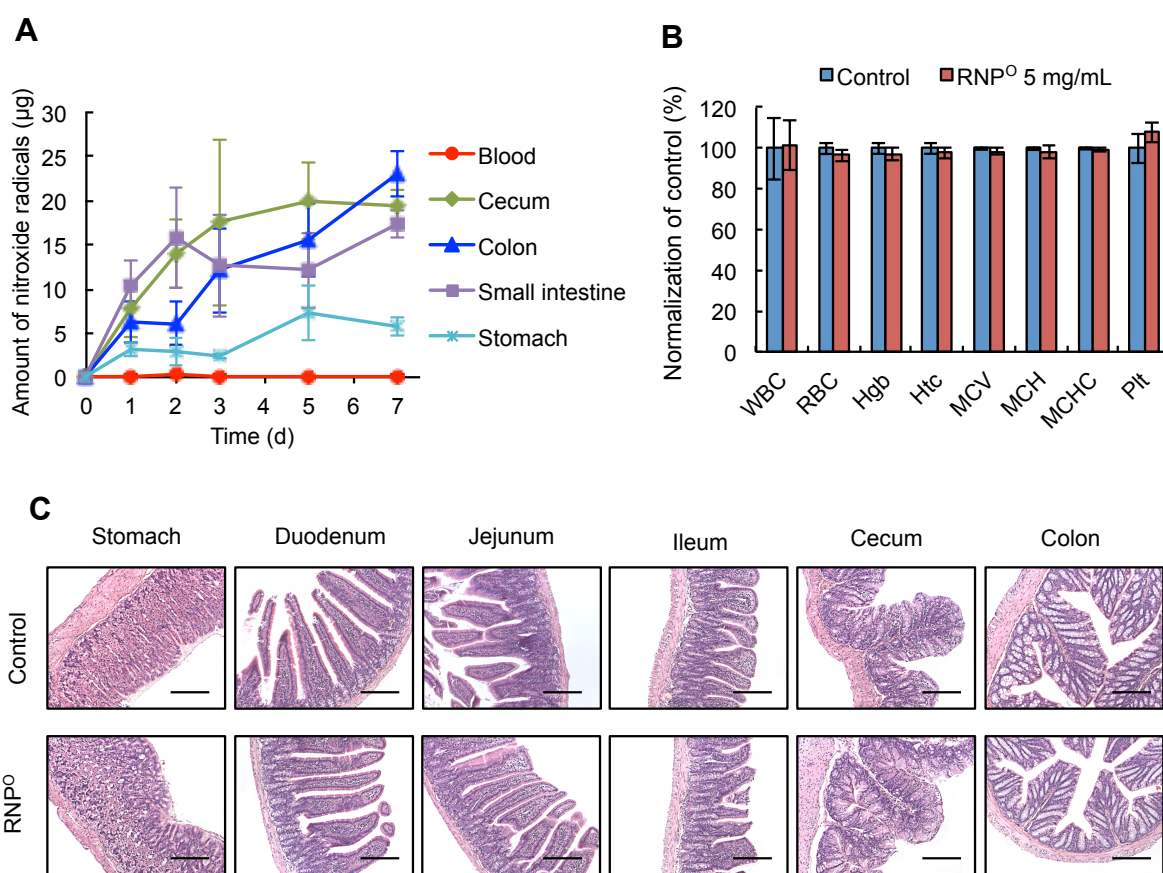


Figure 5.2. Accumulation of free drinking RNP⁰ in the gastrointestinal (GI) tract and its non-toxicity. **(A)** Accumulation of free drinking RNP⁰ in the GI tract and blood. **(B)** Hematological analyses were performed using an automatic hematology analyzer (Celltac α , MEK-6358; Nihon Kohden Co, Tokyo, Japan). White blood cell (WBC), red blood cell (RBC), hemoglobin (Hgb), hematocrit (Htc), mean corpuscular volume (MCV), mean corpuscular hemoglobin (MCH), mean corpuscular hemoglobin concentration (MCHC), and platelets (Plt) were measured. **(C)** Histological assessments of GI tissues in mice given RNP⁰ (5 mg/mL) for a month. The data are expressed as mean \pm SEM, $n = 5$ mice. The images are representative of $n = 3$. Scale bar = 100 μ m.

5.3.2. Specific cellular internalization of RNP^O in cancer tissues

- Specific cellular internalization of RNP^O in colon tissues was analyzed *in vivo* using mice with AOM/DSS-induced CAC and compared to healthy mice. After oral gavage of RNP^O, colon tissues were collected from these mice and isolated cells were oxidized for ESR assays. It is interesting to note that the total ESR intensity of RNP^O is significantly higher in cancer tissues compared to normal tissues (**Figure 5.3A**). Alternatively, RNP^O remarkably surrounded mucosa of tumor sites due to the defective structure of mucus layer in these sites,³⁰ resulting in the facile penetration of the nanoparticles to mucosa. Additionally, clear ESR signals were detected inside cancer cells, but not inside normal cells (**Figure 5.3A**), indicating that RNP^O did not internalize in healthy cells. This result demonstrates that RNP^O tends to accumulate in cancer cells, where large amounts of ROS and pro-inflammatory cytokines are produced. The ESR spectra of RNP^O also give the information about its morphology. Basically, the ESR signal of LMW nitroxide radical TEMPOL has a sharp triplet due to an interaction between the ¹⁴N nuclei and the unpaired electron in the dilute solution. After the nitroxide radicals are introduced into the hydrophobic core of RNP^O, the ESR spectrum of RNP^O becomes broader. The broad ESR signals of RNP^O were observed outside of both normal cells and cancer cells (**Figure 5.3B and C**), indicating that RNP^O remains in a core-shell-type micelle form when it exists outside of cells. Notably, no ESR signals were detected inside normal cells (**Figure 5.3D**), which is in sharp contrast to the signals observed in cancer cells (**Figure 5.3E**). Interestingly, a triplet peak on ESR spectrum was observed inside cancer cells (**Figure 5.3E**), indicating exposure of the nitroxide radicals after disintegration of RNP^O inside cancer cells.

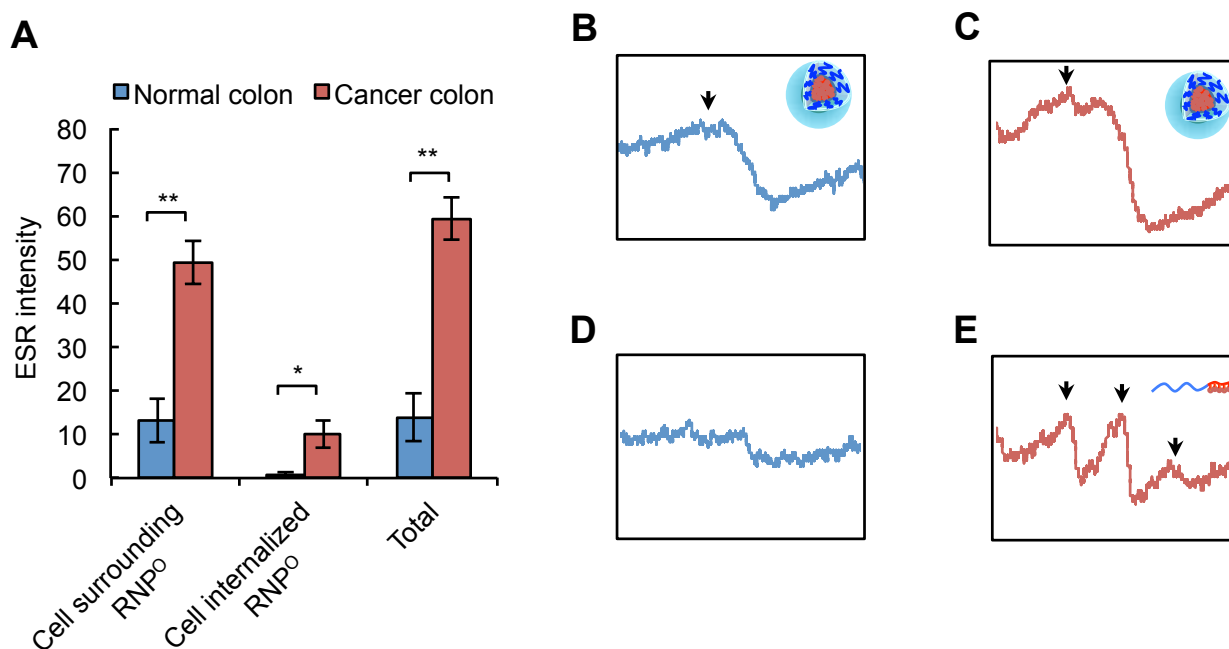


Figure 5.3. Cellular uptake of RNP^O *in vivo* (A) Cellular uptake of RNP^O in normal and cancer tissues *in vivo*. The data are expressed as mean \pm SEM, * $P < 0.05$ and ** $P < 0.01$, $n = 3$ mice. (B – E) ESR spectra of cellular surface surrounding RNP^O and cellular internalized RNP^O in normal cells and cancer cells, respectively.

- In order to investigate the intracellular internalization mechanism of RNP^O in cancer cells, the uptake of RNP^O in C-26 colon cancer cells *in vitro* was carried out. Here, RNP^O was labeled using Rhodamine, making its red under a fluorescent microscope. Nuclei were blue and lysosomes were green when stained with Hoechst 33342 and LysoTracker Green DND-26, respectively. The merged image in **Figure 5.4** shows yellow and red fluorescence in the cytoplasm, suggesting uptake of RNP^O into C-26 cells via both endocytosis pathway and simply diffusion due to the leaky cellular membranes of damaged cancer cells. Higher accumulation in colonic mucosa, specific internalization in cancer cells, and low uptake in normal cells are the most important characteristics of RNP^O, which are anticipated for high therapeutic efficiency with extremely low adverse effects.

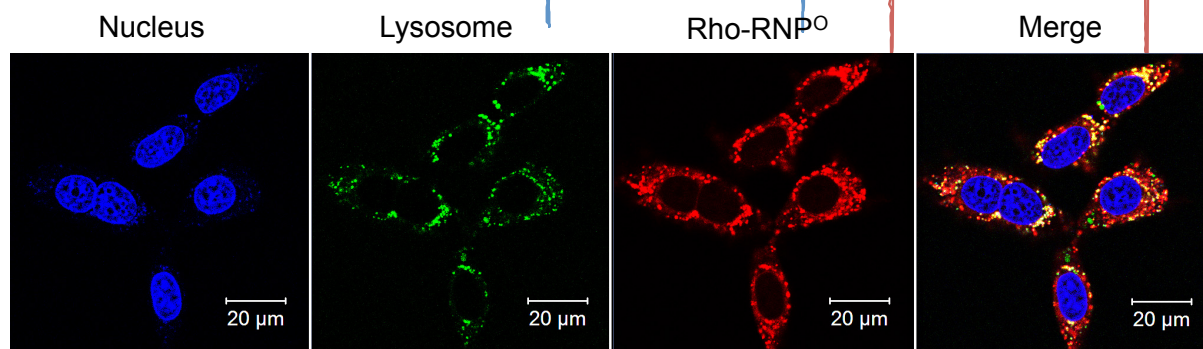


Figure 5.4. Cellular uptake of RNP⁰ *in vitro*. Cellular uptake of RNP⁰ in C-26 colon cancer cells after 1 h incubation with Rho-RNP⁰. Rho-RNP⁰ (red), lysosomes (green, stained by LysoTracker Green DND-26), and nuclei (blue, stained by Hoechst 33342) were imaged. *Scale bar* = 20 μ m.

5.3.3. RNP⁰ prevents AOM/DSS-induced CAC by suppressing inflammation

- Since RNP⁰ preferentially accumulates at the site of colon tumor, it will be interested in the efficacy of RNP⁰ in the CAC model mice. In this model, colon cancer is driven by the combination of a carcinogenic agent (AOM) and an inflammatory agent (DSS). In chapter 3, I confirmed that orally administered RNP⁰ strongly scavenges ROS in DSS-induced colitis mice and almost completely cures.²¹ Separately, it was reported that intravenously administered RNP⁰ suppresses an activation of nuclear factor kappa B (NF- κ B) in cancer cells of mice with subcutaneously transplanted tumors.³¹ If oral administration of RNP⁰ works similarly in CAC mice without any adverse effects to the entire body, it will be an ideal cancer chemotherapeutics. **Figure 5.4** shows a protective effect of orally administered RNP⁰ to the CAC mice. Here, RNP⁰ (200 mg/kg) was administered daily by oral gavage for 1 week for the first and fourth weeks, which are the same terms of DSS treatment (**Figure 5.4A**). In contrast to the CAC mice, which experience a significantly reduction in body weight during DSS treatment, no body weight loss was observed during RNP⁰ administration (**Figure 5.4B**). As anticipated, a disease activity index significantly decreased (**Figure 5.4C**) in RNP⁰-treated mice. The pro-inflammatory cytokine interferon-gamma (IFN- γ) was also significantly reduced in RNP⁰-treated mice (**Figure 5.4D**), suggesting that oral

administration of RNP⁰ effectively suppressed inflammation in the colon, even in CAC mice.

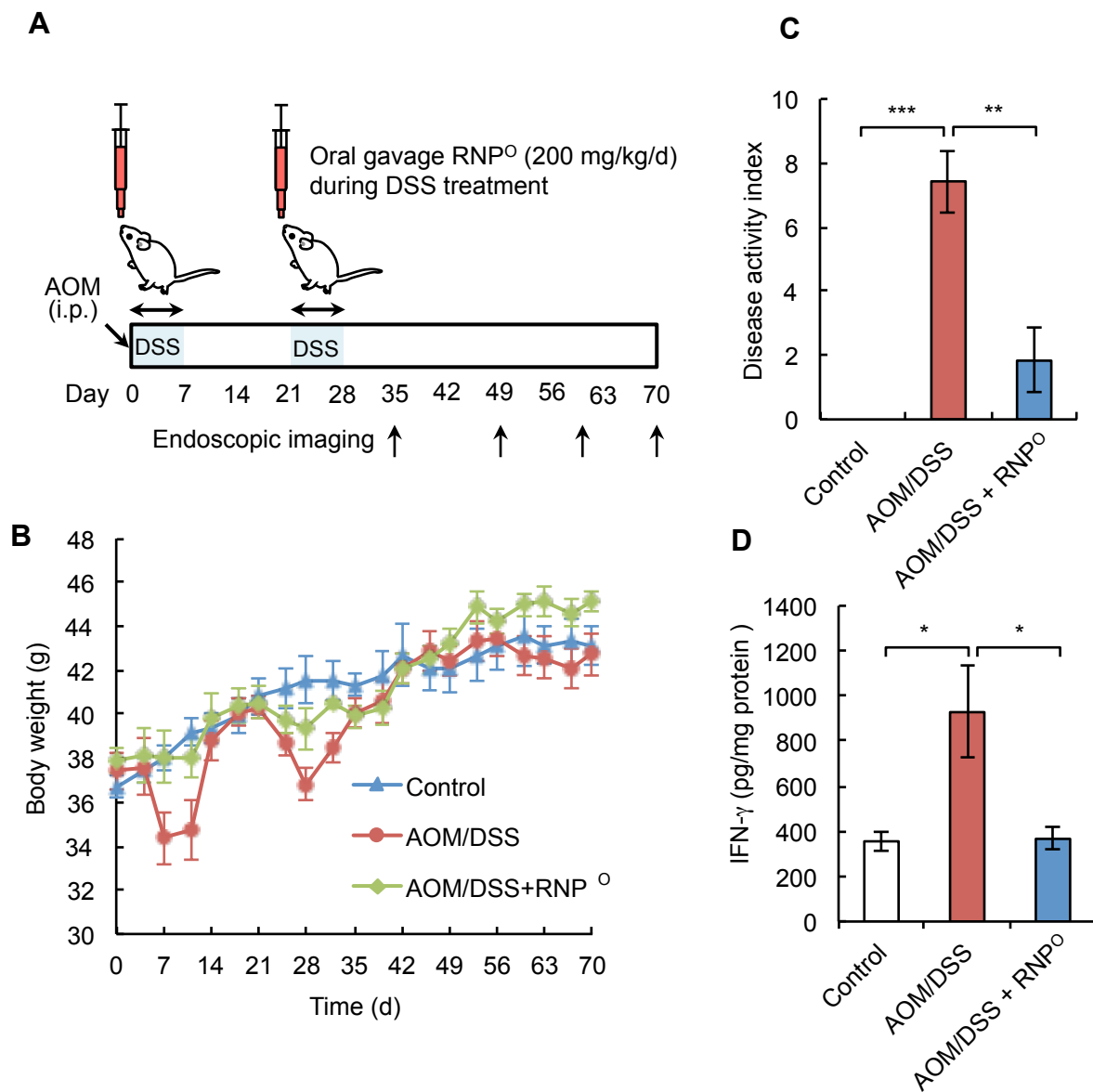


Figure 5.5. RNP⁰ suppressed the inflammation in AOM/DSS-induced CAC in mice. (A) Scheme of AOM/DSS-induced CAC and RNP⁰ administration. (B) Body weight change during 70 d of treatment. (C) Disease activity index of colitis on day 7 of DSS treatment. (D) The production of pro-inflammatory cytokine IFN- γ . The data are expressed as mean \pm SEM, * P < 0.05, ** P < 0.01 and *** P < 0.001, n = 6 mice.

During 70 d of treatment, an endoscope system was used to confirm colon tumor development in mouse and evaluated the tumor score, which significantly increased in mice treated with AOM/DSS. In contrast to the AOM/DSS-treated mice, mice given RNP^O did not show the increase in tumor scores (**Figure 5.6A and B**). Furthermore, histologically, the colons of AOM/DSS-treated mice possessed high levels of adenoma-carcinoma, which were not observed in mice treated with RNP^O (**Figure 5.6C**). This result indicates that oral gavage of RNP^O during DSS administration effectively suppressed inflammation, completely preventing colon tumor development.

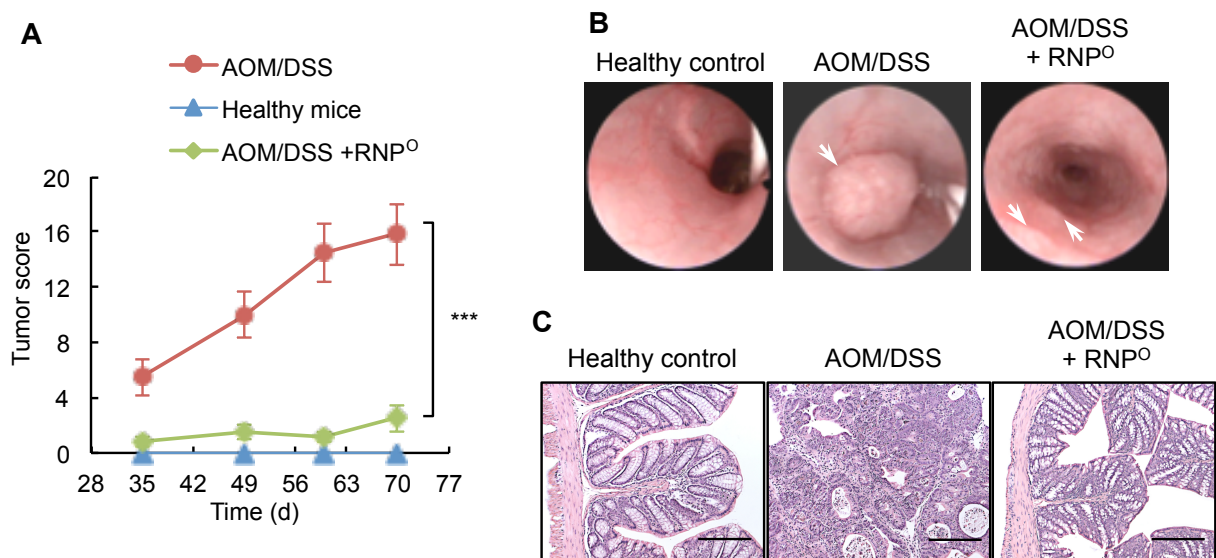


Figure 5.6: Protective effect of orally administered RNP^O on AOM/DSS-induced CAC in mice. **(A)** Tumor development profile. The data are expressed as mean \pm SEM, *** $P < 0.001$, $n = 6$ mice. **(B)** Endoscopic imaging of mice after 70 d of treatment. White arrows indicate tumors. **(C)** Histology of colon by H&E staining. Sections was stained by H&E, and assessed histologically. Representative sections are shown for $n = 3$ mice. Scale bars = 100 μ m.

5.3.4. Therapeutic effect of free drinking RNP^O against AOM/DSS-induced CAC

- Simultaneous administration of RNP^O and the inflammation agent DSS led to complete suppression of inflammation and colon tumor progression. The next challenge was to test the ability of RNP^O to works after DSS treatment. Here, drinking water was supplemented with different concentrations of RNP^O in drinking water (1 mg/mL, 2.5 mg/mL, or 5 mg/mL) starting

after the DSS administration and continuing until the end of the experiment, as shown in **Figure 5.7A**.

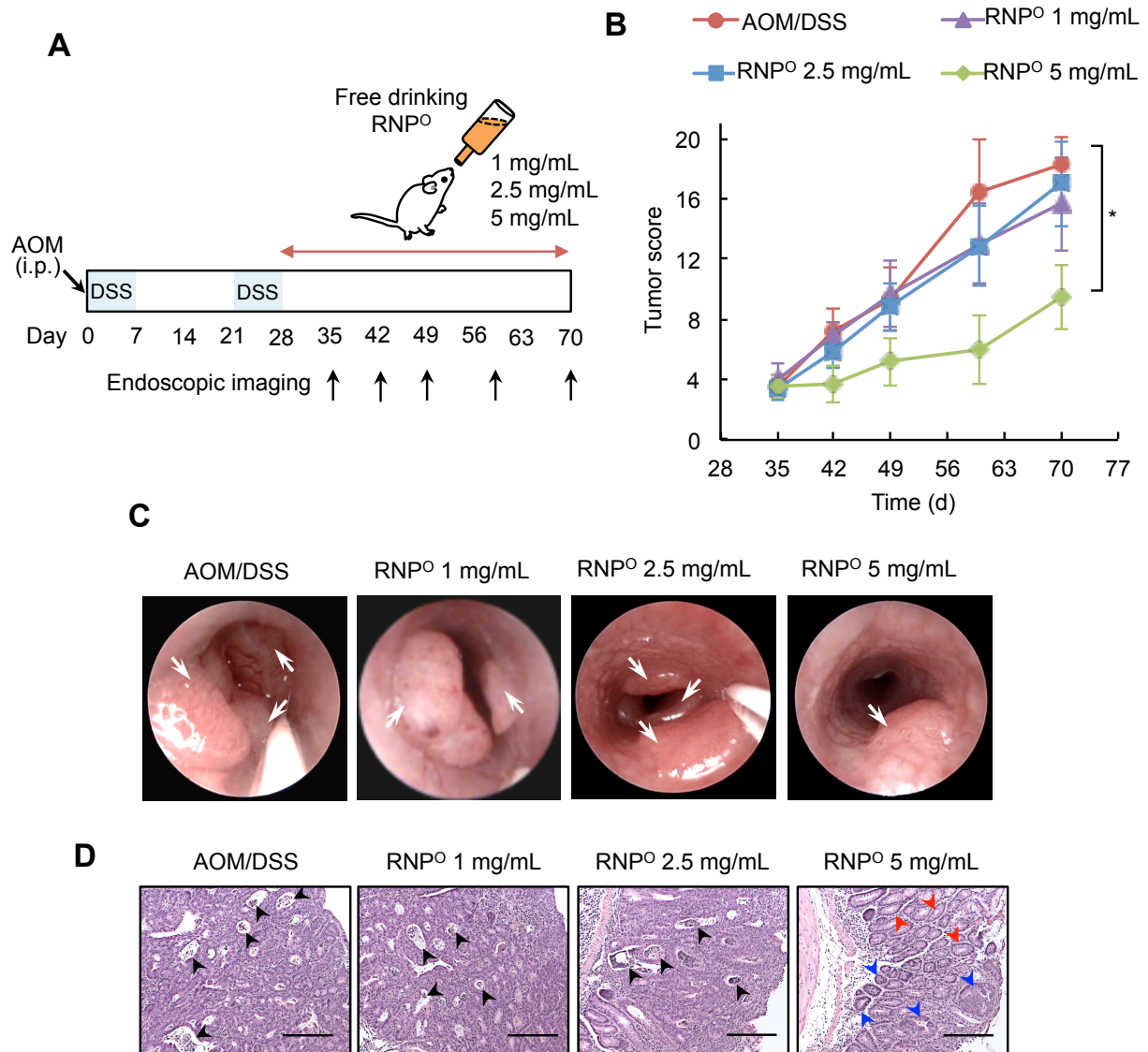


Figure 5.7. Therapeutic effect of free drinking RNP^O on AOM/DSS-induced CAC in mice. **(A)** Scheme of AOM/DSS-induced CAC and RNP^O administration. **(B)** The therapeutic effect of RNP^O against CAC development was evaluated by analysis of tumor scores. The data are expressed as mean ± SEM, **P* < 0.05, *n* = 6 mice. **(C)** Endoscopic imaging of mice after 70 d of treatment. White arrows indicate tumor. **(D)** histology of colon by H&E staining. Black arrows indicate the necrotic cells surrounded by carcinoma, blue arrows indicate adenoma, and red arrows indicate normal crypts. Representative sections are shown for *n* = 3 mice. Scale bars = 100 μm.

- **Figure 5.7B** and **C** shows a profile of tumor progression during this treatment. As shown in the figure, no significant differences in tumor score were observed in mice treated with 1 mg/mL or 2.5 mg/mL RNP^O compared to AOM/DSS-treated mice. In contrast, mice given 5 mg/mL RNP^O had significantly reduced tumor scores compared to AOM/DSS-treated mice (**Figure 5.7 B** and **C**). Histological assessments (**Figure 5.7D**) revealed carcinoma tissues in mice treated with 1 mg/mL or 2.5 mg/mL RNP^O; however, only adenomas, but not carcinomas, were observed in mice given 5 mg/mL RNP^O (**Figure 5.7D**). These results indicate that free drinking RNP^O also works effectively to retard tumor growth, even after tumor generation in CAC mice.

5.3.5. RNP^O improves the anticancer efficacy of Iri and reduces its adverse effects

- On the basis of above investigation, it is confirmed that this antioxidative strategy based on polymer nanotherapeutics is a robust colon cancer treatment. However, treatment with a single antioxidative agent may not completely cure colon cancer. There are a large number of anticancer drugs that function by versatile mechanisms to eliminate cancer cells. Combination of these anticancer drugs with RNP^O is a promising strategy. Iri is used to treat lung, esophageal, gastric, and colon cancers. Iri interacts with cellular DNA topoisomerase I, causing the apoptosis and death of cancer cells. However, Iri efficiency is strongly suppressed by the cancer microenvironment. In particular, oxidative stress in the tumor environment, such as overproduction of ROS and activation of NF- κ B increases cancer cell resistance to Iri treatment.³² It was interesting in examining whether the ROS scavenging effect of RNP^O enhanced chemotherapy of Iri in CAC mice. Here, Iri (0.25 mg/kg, 2.5 mg/kg or 5 mg/kg) was given by oral gavage 5 times per week for 3 weeks, while RNP^O (2.5 mg/mL) was given to mice in free drinking water (**Figure 5.8A**).

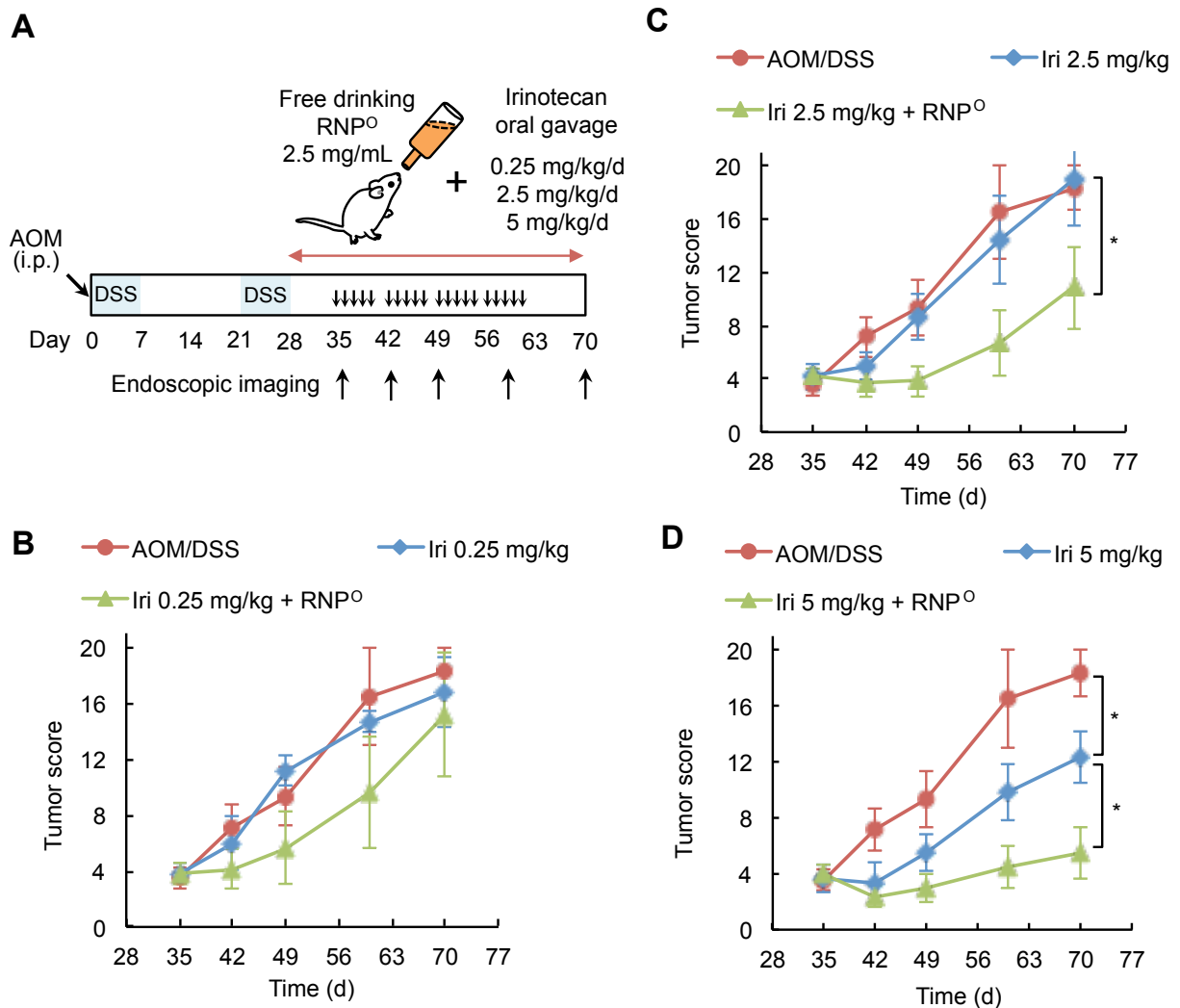


Figure 5.8. Oral administration of RNP^O enhances the anticancer effect of Iri. (A) Scheme of AOM/DSS-induced CAC and administration of Iri and RNP^O. (B–D) Combination effect of Iri and RNP^O against CAC development was evaluated by assessment of tumor scores: 0.25 mg/kg Iri (B), 2.5 mg/kg Iri (C), or 5 mg/kg Iri (D). The data are expressed as mean ± SEM, **P* < 0.05, *n* = 6 mice. The data are expressed as mean ± SEM, **P* < 0.05, *n* = 5 mice.

- It should be noted that 0.25 mg/kg of Iri is a very low dose treatment that did not suppress tumor growth on its own. A slight (but not significant) combination effect was observed when Iri (0.25 mg/kg) was combined with free drinking RNP^O (2.5 mg/mL) (Figure 5.8B). Interestingly, when higher dose of Iri (2.5 mg/kg) was administered in combination with free drinking RNP^O, a remarkable suppression of tumor growth was observed in mice treated with combination compared

to mice treated with Iri alone (**Figure 5.8C**). Furthermore, combination with Iri (5 mg/kg) and RNP⁰ completely inhibited tumor growth in CAC mice (**Figure 5.8D**). This result demonstrates that combination with free drinking RNP⁰ effectively improves the anticancer efficacy of Iri.

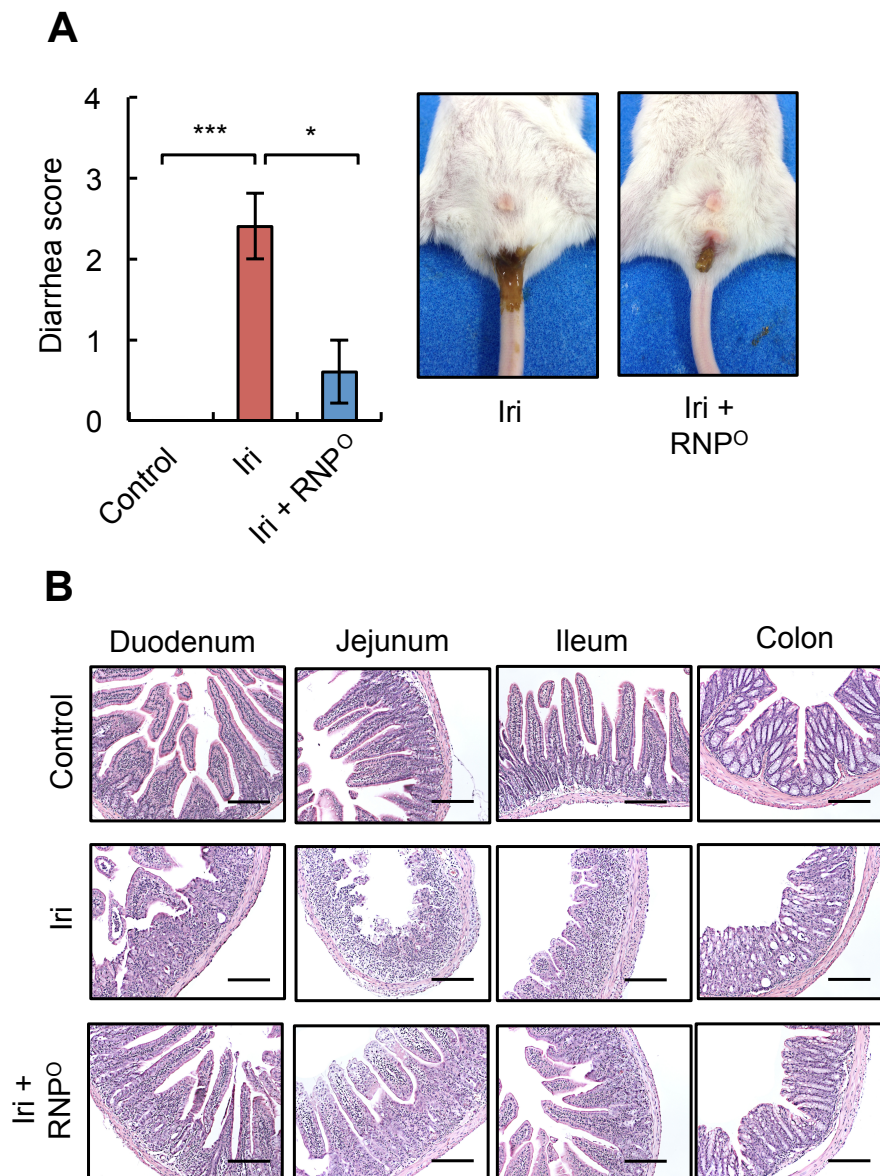


Figure 5.9. Oral administration of RNP⁰ reduces side effect of Iri on the GI tract. (A) Diarrhea score and (B) Histological assessment of intestinal sections by H&E staining. The data are expressed as mean ± SEM, * $P < 0.05$ and *** $P < 0.001$, $n = 5$ mice. Representative sections are shown for $n = 3$ mice. Scale bars = 100 μm .

- Since that high dose of Iri administration is known to cause severe adverse effects in the GI tract such as diarrhea and intestinal inflammation, I also investigated the efficacy of RNP^O against Iri-induced mucositis. Mice receiving Iri alone (50 mg/kg, daily intraperitoneally injection for 4 d) exhibited severe diarrhea scores, weight loss, and neutropenia. These adverse effects were remarkably reduced in RNP^O-treated mice (**Figure 5.9A**). Histological investigation of GI tract organs (duodenum, jejunum, ileum, and colon) showed a remarkable recovery of these tissues in RNP^O-treated mice compared to mice treated Iri alone (**Figure 5.9B**). Notably, superoxide levels were also suppressed in mice treated with Iri and RNP^O compared to mice treated with Iri alone, once again confirming that suitable ROS scavenging at inflammation sites is a robust strategy for tumor treatment. These results indicate that oral administration of RNP^O not only significantly enhances the anticancer efficacy of Iri against CAC development, but also effectively suppresses the severe adverse effects of Iri.

5.4. Discussion and Conclusions

- Despite important advances in detection, surgery, and chemotherapy, colon cancer is difficult to treat and has a high mortality rate.³³ Current clinical trials and treatment strategies use single agents and combination strategies, but many of these regimens have severe adverse effects and complicated administration processes.^{34,35} For many years, a number of anticancer drugs for colon cancer treatment have been developed and used alone and combination in clinical such as 5-FU, oxaliplatin, leucovorin, bevacizumab and Iri.^{36,37} Although they are effective in suppressing development of carcinoma to some extent, they have severe adverse effects that raise significant concerns among both physicians and patients, limiting their use.³⁸

- High doses of drugs are required to achieve sufficient delivery of anticancer drugs to treat CAC. However, high doses are associated with undesirable adverse effects, because almost all LMW drugs tend to metabolize in the upper GI tract or be absorbed into the bloodstream. LMW

TEMPOL is well-known as a stable nitroxide radical with ability to scavenge ROS. It has been used for therapeutic applications, including antioxidative stress and cancer therapies.^{39–41} However, LMW TEMPOL spreads to entire body after administration, especially internalizes in healthy cells and even in mitochondria, disturbing normal respiratory system, which causes severe adverse effects to healthy cells. Most of antioxidants investigated so far have the similar issue limiting their clinical application. This strategy is to covalently install ROS scavenging moiety to large molecular weight chains in order to avoid the possible internalization in healthy cells and mitochondria. For this objective, 2 types of nitroxide radical containing nanoparticles (RNPs) have been developed: pH-sensitive RNP^N and pH-insensitive RNP^O, viz., RNP^N disintegrates under acidic environments, while RNP^O does not disintegrate regardless of changes in pH. Nitroxide radicals are covalently conjugated to the matrix and confined in the core of these nanoparticles, which shows high biocompatibility, including long-term blood circulation via intravenous administration and low toxicity.⁴² In addition, RNPs have been studied as therapies for oxidative stress injuries such as cerebral and renal ischemia reperfusion injuries, hemorrhage,^{25,43,44} and cancer.³¹ Since the pH-disintegrative character of RNP^N is not suitable for CAC treatment via oral administration, I have developed an oral nanotherapeutics using RNP^O with therapeutic effects against CAC model mice in this study.

- Although many nanoparticles used in biomedical fields have been known by bio-benign materials, they cause more or less inflammation or toxicity.^{45,46} Though we have already confirmed the safety characteristics of orally administered RNP^O via gavage daily for 1 week, but further investigation is required for the long-term applications. Here, free drinking RNP^O significantly accumulates in GI tract after 1 week administration, especially in the small intestine, cecum and colon regions, while no blood uptake is observed, which prevents undesired adverse effects of nitroxide radicals to entire body even for the long-term administration (**Figure 5.2A**). After oral administration, RNP^O highly internalizes in cancer tissues compared to healthy colon tissues,

resulting in a high therapeutic effect and extremely low GI toxicity with this nanotherapeutics. In fact, even when a high dose of RNP^O was given orally for 1 month, no toxicities were observed in the GI tract or other organs (**Figure 5.2B and C**).

- In the chapter 3 and 4, I have confirmed that oral administration of RNP^O highly accumulates in the colonic mucosa and effectively scavenges ROS, leading to suppression of inflammation in mice with DSS-induced colitis without damaging the intestinal microflora.^{21,24} If RNP^O works against inflammation in CAC via the same mechanism, RNP^O may be an ideal nanomedicine for these types of diseases. As anticipated, I found that oral administration of RNP^O along with DSS treatment clearly suppressed inflammation in the colon, significantly preventing carcinoma progression in the CAC mouse model. It is not surprising, because inflammation is an important factor to promote cancer development. Simultaneous administration of RNP^O with DSS protected against the generation of inflammation, resulting in suppression of carcinoma propagation (**Figure 5.5 and 5.6**). It should be rather noted that administration of RNP^O after DSS treatment also effectively suppressed tumor progression in mice given free drinking water with 5 mg/mL RNP^O (**Figure 5.6**). It was confirmed that the stability of RNP^O in the GI tract and exposure of nitroxide radicals inside cancer cells are critical factors for achievement of an effective oral drug for colon cancer therapy (**Figure 5.3**). It has been reported that the decrease of inflammation in the tumor microenvironments prevents activation of NF- κ B to result in suppression of resistance of cancer cells from apoptotic tendency.⁴⁷ Because RNP^O clearly suppressed inflammation around tumor microenvironment, a combination treatment with RNP^O and conventional cancer drugs is a robust strategy. In this chapter, I also investigated the combination of oral RNP^O with Iri and found that the anticancer efficacy was significantly enhanced with the combination compared to treatment with Iri alone (**Figure 5.8**). It is also interesting to note that co-treatment with RNP^O significantly suppressed the adverse effects in GI tract caused by Iri treatment (**Figure 5.9**), indicating that a synergistic effect was successfully achieved.

- In summary, a novel antioxidative redox nanoparticle, RNP^O, has been developed for CAC mice. RNP^O possesses capacity to highly accumulate in colon area and selectively internalize in cancer cells. Long-term oral administration of RNP^O exhibited extremely low toxicity due to a lack of RNP^O absorption into the bloodstream and lower uptake by healthy intestinal cells. Oral administration of RNP^O protected against tumor progression and displayed an anticancer therapeutic effect to prevent tumor development in a CAC mouse model. In addition, co-treatment with RNP^O and Iri achieved a significantly enhanced anticancer effect with suppression of the severe adverse effects of Iri on the GI tract. Taken together, these results indicate that the combination of novel antioxidative nanotherapeutics with conventional anticancer drugs is a strategy for patients-friendly anticancer therapy.

5.5. References

1. Abraham C, Cho JH. *N Engl J Med* **2009**;361:2066–78.
2. Khor B, Gardet A, Xavier RJ. *Nature* **2011**;474:307–17.
3. Loftus EV Jr. *Gastroenterology* **2004**;126:1504–17.
4. Podolsky DK. *N Engl J Med* **2002**;347:417–29.
5. Grivnenkov SI. *Semin Immunopathol* **2013**;35:229–44.
6. Tenesa A, Dunlop MG. *Nat Rev Genet* **2009**;10:353–8.
7. Coussens LM, Werb Z. *Nature* **2002**;420,860–7.
8. Gommeaux J, Cano C, Garcia S, Gironella M, Pietri S, Culcasi M, et al. *Mol Cell Biol* **2007**;27:2215–28.
9. Cui X, Jin Y, Hofseth AB, Pena E, Habiger J, Chumanovich A, et al. *Cancer Prev Res* **2010**;3:549–59.
10. Seril DN, Liao J, Ho KL, Yang CS, Yang GY. *Carcinogenesis* **2002**;23:993–1001.
11. Douillard JY, Cunningham D, Roth AD, Navarro M, James RD, Karasek P, et al. *Lancet* **2000**;355:1041–7.
12. Mathijssen RH, Alphen RJ, Verweij J, Loos WJ, Nooter K, Stoter G, et al. *Clin Cancer Res* **2001**;7: 2182–94.
13. Chen S, Yueh MF, Bigo C, Barbier O, Wang K, Karin M, et al. *Proc Natl Acad Sci USA* **2013**;110:19143–8.

14. Davis ME, Chen Z, Shin DM. *Nat Rev Drug Discov* **2008**;7:771–82.
15. Hrkach J, Hoff DV, Ali MM, Andrianova E, Auer J, Campbell T, et al. *Science Translational Medicine* **2012**;4:128ra139.
16. Kim BYS, Rutka JT, Chan WCW. *N Engl J Med* **2010**;363:2434–43.
17. Bisht S, Feldmann G, Koorstra JB, Mullendore M, Alvarez H, Karikari C, et al. *Mol Cancer Ther* **2008**;7:3878–88.
18. Ma L, Kohli M, Smith A. *ACS Nano* **2013**;7:9518–25.
19. Bergin IL, Witzmann FA. *Int J Biomed Nanosci Nanotechnol* **2013**;3:163–210.
20. Park EJ, Bae E, Yi J, Kim Y, Choi K, Lee SH, et al. *Environ Toxicol Pharmacol* **2010**;30:162–8.
21. Vong LB, Tomita T, Yoshitomi T, Matsui H, Nagasaki Y. *Gastroenterology* **2012**;143:1027–36.
22. Sha S, Vong LB, Chonpathompikunlert P, Yoshitomi T, Matsui H, Nagasaki Y. *Biomaterials* **2013**;34:8393–400.
23. Grivennikov SI, Greten FR, Karin M. *Cell* **2010**;140:883–99.
24. Vong LB, Yoshitomi T, Morikawa K, Saito S, Matsui H, Nagasaki Y. *J Gastroenterol* **2014**;49:806–13.
25. Yoshitomi T, Hirayama A, Nagasaki Y. *Biomaterials* **2011**;32:8021–8.
26. Kirpotin DB, Drummond DC, Shao Y, Shalaby MR, Hong K, Nielsen UB, et al. *Cancer Res* **2006**;66:6732–40.
27. Becker C, Fantini MC, Neurath MF. *Nat Protoc* **2006**;1:2900–4.
28. Lima-Junior RC, Freitas HC, Wong DV, Wanderley CW, Nunes LG, Leite LL, et al. *Br J Pharmacol* **2014**;171:2335–50.
29. Kurita A, Kado S, Kaneda N, Onoue M, Hashimoto S, Yokokura T. *Cancer Chemother Pharmacol* **2003**;52:349–60.
30. Johansson ME, Sjovall H, Hansson GC. *Nat Rev Gastroenterol Hepatol* **2013**;10: 352–61.
31. Yoshitomi T, Ozaki Y, Thangavel S, Nagasaki Y. *J Control Release* **2013**;172:137–43.
32. Xu Y, Villalona-Calero MA. *Ann Oncol* **2002**;13:1841–51.
33. Terzic T, Grivennikov S, Karin E, Karin M. *Gastroenterology* **2010**;138:2101–14.
34. Kopec JA, Yothers G, Ganz PA, Land SR, Cecchini RS, Wieand HS, et al. *J Clin Oncol* **2007**;25:424–30.
35. Sobrero AF, Maurel J, Fehrenbacher L, Scheithauer W, Abubakr YA, Lutz MP, et al. *J Clin Oncol* **2008**;26:2311–9.

36. Hurwitz H, Fehrenbacher L, Novotny W, Cartwright T, Hainsworth J, Heim W, et al. *N Engl J Med* **2004**;350:2335–42.
37. Sargent D, Sobrero A, Grothey A, O'Connell MJ, Buyse M, Andre T, et al. *J Clin Oncol* **2009**;27:872–7.
38. Dobbelstein M, Moll U. *Nat Rev Drug Discov* **2014**;13:179–96.
39. Mitchell JB, Anver MR, Sowers AL, Rosenberg PS, Figueroa M, Thetford A, et al. *Cancer Res* **2012**;72:4846–55.
40. Nagasaki Y. *Ther Deliv* **2012**;3:165–79.
41. Soule BP, Hyodo F, Matsumoto K, Simone NL, Cook JA, Krishna MC, et al. *Free Radic Biol Med* **2007**;42:1632–50.
42. Yoshitomi T, Miyamoto D, Nagasaki Y. *Biomacromolecules* **2009**;10:596–601.
43. Chonpathompikunlert P, Fan CH, Ozaki Y, Yoshitomi T, Yeh CK, Nagasaki Y. *Nanomedicine (London)* **2012**;7:1029–43.
44. Marushima A, Suzuki K, Nagasaki Y, Yoshitomi T, Toh K, Tsurushima H, et al. *Neurosurgery* **2011**;68:1418–25.
45. Cho WS, Cho M, Jeong J, Choi M, Cho HY, Han BS, et al. *Toxicol Appl Pharmacol* **2009**;236:16–24.
46. Zhao J, Castranova V. *J Toxicol Environ Health B Crit Rev* **2011**;14:593–632.
47. Ben-Neriah Y, Karin M. *Nat Immunol* **2011**;12:715–23.

Chapter 6

Summary and Conclusion

Summary and Conclusions

- The oxidative stress induced by reactive oxygen species (ROS) has been implicated in a pathogenesis of various disorders and diseases. In fact, ROS are related to a large number of diseases such as cardiovascular and neurodegenerative diseases, inflammatory bowel disease, pulmonary disease, renal and cerebral ischemia-reperfusion injuries, as well as cancer. A high amount of ROS is generated at the inflammatory and cancerous sites. Suppressing overproduction of ROS in these sites becomes promising approach for treatments of many diseases. In this thesis, I described a novel antioxidative redox nanoparticle (RNP^O) possessing ROS scavenging capacity for therapies of ulcerative colitis and colitis-associated colon cancer. Oral administration of RNP^O highly accumulated in the colonic mucosa and effectively scavenged ROS, leading to suppression of inflammation in mice with DSS-induced colitis without damaging the intestinal microflora. Long-term oral administration of RNP^O exhibited extremely low toxicity due to a lack of RNP^O absorption into the bloodstream and lower uptake by healthy intestinal cells.

- This thesis is composed of six chapters. Summaries of each chapter are described as follow.

- **Chapter 1** described the general introduction of the present thesis concerning inflammatory bowel disease and current medications. In addition, the development and advantages of nanoparticle-based drug delivery systems are summarized.

- **Chapter 2** describes the design and synthesis of block copolymer MeO-PEG-*b*-PCMS by the radical polymerization reactions using MeO-PEG-SH as a telogen. Redox polymer MeO-PEG-*b*-PMOT was synthesized by converting chloromethyl groups were converted to TEMPOs. The preparation and characteristics of redox nanoparticles RNP^O were also described in this chapter.

- **Chapter 3** describes the specific accumulation of orally administered RNP^O *in vivo* as compared to LWM TEMPOL and commercial polystyrene latex particles. The biodistribution of orally administered RNP^O was also investigated. In addition, chapter 3 described the therapeutic effect of RNP^O on dextran sodium sulfate (DSS)-induced colitis mice model compared to LMW TEMPOL and mesalamine, a commercial anti-inflammatory drug. The results showed that 40-nm-diameter RNP^O with PEG shell showed significantly high accumulation and long retention in colon area compared to LMW TEMPOL and polystyrene latex particles with similar size. Higher accumulation of RNP^O in inflamed colon than normal colon was observed. Oral administration of RNP^O showed significantly

higher therapeutic effect on DSS-induced colitis mice as compared to LMW drugs.

- **Chapter 4** described the effect of RNP^O on intestinal bacteria. The results in this chapter showed that oral administration of RNP^O did not show the significant changes in microflora in healthy mice, indicating the innocuousness of this oral nanoparticle therapeutics against healthy colonic microflora. On the other hand, RNP^O treatment inhibited the number of commensal bacteria such as *E. coli* and *Staphylococcus* sp. increasing in the fecal samples of DSS-induced colitis mice.

- **Chapter 5** described the specific accumulation of orally administered RNP^O in colonic cancer tissues and effect of RNP^O on colitis-associated colon cancer (CAC) chemically induced by azoxymethan and DSS. Accumulation of RNP^O in cancer tissues was significantly higher than in normal tissues. In addition, nitroxide radicals were exposed inside cancer cells after cellular internalization, and no cellular uptake of RNP^O was observed in normal cells. The toxicity of long-term RNP^O treatment was also described in this chapter. Free drinking RNP^O also works effectively to retard tumor growth, even after tumor generation in CAC mice. Interestingly, combination with free drinking RNP^O effectively improves the anticancer efficacy of Irinotecan, an anticancer drug, and effectively suppresses its severe adverse effects on GI tract. On the basis of these results, oral administration of RNP^O presents a promising nanotherapeutics for treating patients with ulcerative colitis and colitis-associated colon cancer.

- Through this thesis, the author revealed a high potential of redox nanoparticles RNP^O as oral nanotherapeutics for treatment of not only inflammatory bowel disease, but also many kinds of ROS-related diseases. With the great potential, the author wishes that the redox nanotherapeutics in present studies would have a great contribution to the clinical applications in near future.

List of Publications

1. Long Binh Vong, Tsutomu Tomita, Toru Yoshitomi, Hirofumi Matsui, Yukio Nagasaki, An Orally Administered Redox Nanoparticle that Accumulates in the Colonic Mucosa and Reduces Colitis in Mice, *Gastroenterology*, **2012**, 143(4), 1027-1036.

2. Long Binh Vong, Toru Yoshitomi, Kazuya Morikawa, Shinji Saito, Hirofumi Matsui, Yukio Nagasaki, Oral nanotherapeutics: Effect of redox nanoparticle on microflora in mice with dextran sodium sulfate-induced colitis, *Journal of Gastroenterology*, **2014**, 49(5), 806-813.

3. Long Binh Vong, Toru Yoshitomi, Hirofumi Matsui, Yukio Nagasaki. Development of an oral nanotherapeutics using redox nanoparticles for treatment of colitis-associated colon cancer, *Biomaterials* (submitted).

4. Long Binh Vong, John Mo, Bertil Abrahamsson, Yukio Nagasaki. Specific accumulation of orally administered redox nanotherapeutics in the inflamed colon to suppress the inflammation with dose-response efficiency (*in preparation*).

Other Publications

1. Sha Sha, Long Binh Vong, Pennapa Chonpathompikunlert, Toru Yoshitomi, Hirofumi Matsui, Yukio Nagasaki, Suppression of NSAID-induced Small Intestinal Inflammation by Orally Administered Redox Nanoparticles, *Biomaterials*, **2013**, 34, 8393-8400.

2. Toru Yoshitomi, Sha Sha, Long Binh Vong, Pennapa Chonpathompikunlert, Hirofumi Matsui, and Yukio Nagasaki, Indomethacin-loaded redox nanoparticles improve oral bioavailability of indomethacin and suppress its small intestinal inflammation, *Therapeutic Delivery*, **2014**, 5 (1), 29-38.

3. Toru Yoshitomi, Kazuhiro Kuramochi, Long Binh Vong, Yukio Nagasaki, Development of nitroxide radicals-containing polymer for scavenging ROS from cigarette smoke, *Science and Technology for Advanced Materials*, **2014**, 15, 035002.

4. Md. Amran Hossain, Mayo Yamashita, Long Binh Vong, Yutaka Ikeda and Yukio Nagasaki, Silica-installed redox nanoparticles for novel oral nanotherapeutics- Improvement in intestinal delivery with

anti-inflammatory effects, *Journal of Drug Targeting*, 2014, 22(7), 638-647.

5. Yoshitomi T, Vong LB, Nagasaki Y. *Nanomedicine for treatment of oxidative stress injuries*. Book chapter of Post-genomic Approaches in Cancer and Nano Medicine, *River Publishers, in press*.

Patent

1) 長崎幸夫、吉富徹、ボンビンロン、松井裕史, “高分子化環状ニトロキシドラジカル化合物の潰瘍性消化管の炎症の処置剤”, 特願 2010-260471.

List of Presentations

Oral

1. Long Binh Vong, Tsutomu Tomita, Toru Yoshitomi, Hirofumi Matsui and, Yukio Nagasaki, "Orally Administered Redox Nanoparticle Accumulates in the Colonic Mucosa and Reduces Colitis in Mice", The 9th SPSJ International Polymer Conference, (IPC2012), Kobe, Japan (2012.12).

2. Vong Long Binh, 吉富 徹, 森川 一也, 齋藤 慎二, 松井 裕史, 長崎 幸夫, 4, 経口投与型レドックス反応性ナノ粒子による潰瘍性大腸炎治療とその腸内細菌へ及ぼす影響, 第66回日本酸化ストレス学会学術集会、ウイックあいち、名古屋 (2013.6.14).

3. Vong Binh Long、吉富 徹、松井 裕史、長崎 幸夫、Oral nanotherapeutics for inflammatory bowel disease: Mechanistic investigation of redox-active nanoparticle in colon mucosa、第30回日本DDS学会学術集会、慶応大学芝共立キャンパス、東京 (2014.7.30).

4. Long Binh Vong、Toru Yoshitomi、Hirofumi Matsui、Yukio Nagasaki、Orally Administered Redox Polymeric Nanoparticle That Internalizes in Cancer Tissues and Inhibits the Colitis、63th Fall Meeting of Polymer Society, Japan, Nagasaki University, Nagasaki (2014.9.25).

5. Long B. Vong, Toru Yoshitomi, Hirofumi Matsui, Yukio Nagasaki, Oral delivery of redox nanoparticles for colitis-associated colon cancer therapy, The 73rd Annual Meeting of the Japanese Cancer Association, Pacifico Yokohama, Yokohama (2014.9.27).

6. Long B. Vong, Toru Yoshitomi, Hirofumi Matsui, Yukio Nagasaki, ROS scavenging nanotherapeutics for prevention and treatment inflammation and cancer, 第 33 回 Cytoprotection 研究会, メルパルク京都 (2015.3.20).

Poster

1. Vong Binh Long, Toru Yoshitomi, Hirofumi Matsui, Yukio Nagasaki: Oral Redox Nanotherapy for Ulcerative Colitis Treatment, The 38th Annual Meeting & Exposition of the Controlled Release Society 2011, Gaylord National Hotel and Convention Center, Maryland, U.S.A. (2011.07.30-08.03).

2. Long Binh Vong, Toru Yoshitomi, Hirofumi Matsui, Yukio Nagasaki, Enhancement of therapeutic effect on ulcerative colitis by accumulation of redox nanoparticles in colonic mucosa, MANA International Symposium 2012, Tsukuba, Japan (2012.3.2 PB-11).

3. L. B. Vong, T. Yoshitomi, H. Matsui, Y. Nagasaki, Specific accumulation of novel redox nanoparticles in colonic mucosa-enhancement of therapeutic effect on ulcerative colitis. Soft-interface mini-symposium on Biomaterials science, Tsukuba, Japan (2012.03.17-19).

4. Long Binh Vong, Toru Yoshitomi, Hirofumi Matsui, Yukio Nagasaki, Development of Novel Redox Nanoparticles for Treatment of Ulcerative Colitis, UK-Japan Research Symposium: Molecular Mechanisms of Stress Response in Disease, Tsukuba Science Information Center, Tsukuba, Japan (2012.4.7).

5. ボンビン ロン、吉富 徹、松井 裕史、長崎 幸夫、潰瘍性大腸炎治療に対する経口レドックスナノ治療に関する研究、第 65 会日本酸化ストレス学会学術集会、徳島、P41 (2012.6.7).

6. Long Binh Vong, Tsutomu Tomita, Toru Yoshitomi, Hirofumi Matsui, and Yukio Nagasaki, "Redox nanoparticle improves chemotherapeutic effect and suppress its adverse effects", International Workshop on Soft Interface Science for Young Scientists (SISYS2012), Tsukuba, Japan (2012.11.22).

7. Long Binh Vong, Toru Yoshitomi, Hirofumi Matsui, Yukio Nagasaki, "The effect of orally administered redox nanoparticles in colonic mucosa of mice with colitis", PL-17, MANA International Symposium on 2013, Epochal Tsukuba, Japan (2013.2.27-3.1).

8. Long Binh Vong, Tsutomu Tomita, Toru Yoshitomi, Kazuya Morikawa, Shinji Saito, Hirofumi Matsui, and Yukio Nagasaki, Oral nanotherapeutics: The Effect of Redox Nanoparticle in the Colonic Mucosa of Mice with Colitis, 2nd International Conference on Biomaterials Science in Tsukuba (ICBS2013), Tsukuba, Japan, P123 (2013.3.19-22)
9. Long Binh Vong, Toru Yoshitomi, Hirofumi Matsui, Yukio Nagasaki, Orally Administered Redox Nanoparticle Prevents Colitis-Associated Colon Cancer by Suppressing the Inflammation, Tsukuba International Conference on Materials Science, University of Tsukuba, Tsukuba, Japan (2013.8.29-30).
10. Long Binh Vong, Toru Yoshitomi, Hirofumi Matsui, Yukio Nagasaki, Oral nanotherapeutics: Redox nanoparticles accumulate in colonic mucosa and suppress the inflammation in colitis mice、つくば医工連携フォーラム 2014、つくば国際会議場、つくば (2014.1.20).
11. Long Binh Vong, Toru Yoshitomi, Hirofumi Matsui, Yukio Nagasaki, Orally administered redox nanoparticles internalize in the inflamed tissue and prevent the colitis-associated colon cancer, MANA International Symposium on 2014, Epochal Tsukuba, Japan (2014.3.5).
12. Long Binh Vong, Toru Yoshitomi, Hirofumi Matsui, Yukio Nagasaki, Oral nanotherapeutics of redox nanoparticles for treatment of colitis associated colon cancer, 第 63 回高分子学会春季年会, 3Pc135、名古屋国際会議場、名古屋 (2014.5.30).
13. Long Binh Vong, Toru Yoshitomi, Hirofumi Matsui, Yukio Nagasaki, Oral nanotherapeutics for inflammatory bowel disease: Mechanistic investigation of redox-active nanoparticle in colon mucosa, The 30th Annual Meeting of the Japan Society of Drug Delivery System, Keio University, Tokyo (2014.7.30).
14. Long Binh Vong, Toru Yoshitomi, Hirofumi Matsui, Yukio Nagasaki, Oral redox polymeric nanotherapeutics for treatment of colitis-associated colon cancer, 2nd Functionality Organized Nanostructures、(FON'14)、日本未来館、東京 (2014.11.27).
15. Long Binh Vong, Toru Yoshitomi, Hirofumi Matsui, and Yukio Nagasaki, Oral Nanotherapeutics of Polymeric Redox Nanoparticle for Treatment of Colitis-Associated Colon Cancer, 10th SPSJ International Polymer Conference, Epochal Tsukuba, Tsukuba (2014.12.5).

16. Long Binh Vong, Toru Yoshitomi, Hirofumi Matsui, and Yukio Nagasaki, Combination therapy using ROS scavenging nanoparticles for effective treatment of colitis-associated colon cancer, MANA International Symposium on 2015, Epochal Tsukuba, Japan (2015.3.11).

Other presentations

1. Yukio Nagasaki, Vong Binh Long, Toru Yoshitomi, Hirofumi Matsui: Nanoparticle therapy-Protection and suppression of DDS-induced ulcerative colitis in mice, Digestive Disease Week 2011, McCormick Place, Chicago, Illinois, U.S.A. (2011.05.07-11.).

2. 長崎幸夫, Vong Binh Long, 吉富徹, 松井裕史: 「レドックスナノ粒子による DSS 潰瘍性大腸炎モデルのナノ治療」, 第 8 回 HO 研究フォーラム, 京都府立医科大学 (2011.08.26.).

3. Toru Yoshitomi, Long Binh Vong, Hirofumi Matsui, Yukio Nagasaki: Ulcerative colitis treatment by nitroxide radical-containing nanoparticle, 5th Biennial Meeting of SFRR Asia 2011, Kagoshima Citizens' Culture Hall, Kagoshima, Japan (2011.08.31-09.04).

4. 吉富徹, ボンビンロン, 松井裕史, 長崎幸夫: 「ニトロキシドラジカル含有ポリマーナノ粒子の経口投与方法による潰瘍性大腸炎治療」, 第 60 回高分子討論会, 津島キャンパス, 岡山大学 (2011.09.28-30).

5. 長崎 幸夫、Vong Binh Long、吉富 徹、松井 裕史、レドックス能を有するナノ粒子による潰瘍性大腸炎治療法の開発、第 39 回日本潰瘍学会学術集会、2011 年 11 月 19 日、つくば国際会議場 (2011.11.19).

6. 吉富 徹、Long Binh Vong、松井裕史、長崎幸夫、O2O-5 新規潰瘍性大腸炎治療薬として機能するラジカル含有ナノ粒子、第 33 回日本バイオマテリアル学会大会、京都 (2011.11.21- 22).

7. S. Sha, P. Chonpathompikunlert, L. B. Vong, T. Yoshitomi, Y. Nagasaki, Design of indomethacin-loaded redox nanoparticles for enhancement of bioavailability of indomethacin. Soft-interface mini-symposium on biomaterials science, 2012/3/17-3/19, Tsukuba, Japan (2012.03.17-19).

8. Toru Yoshitomi, Long Binh Vong, Hirofumi Matsui, Yukio Nagasaki, "Oral nanotherapy for

treatment of ulcerative colitis by redox nanoparticle", Nanobio Seattle, Seattle, U.S.A. (2012.7.23-24).

9. Sha Sha, Long Binh Vong, Pennapa Chonpathompikunlert, Toru Yoshitomi, Hirofumi Matsui and Yukio Nagasaki, "Develop a novel oral administration of indomethacin-loaded redox nanoparticles for enhancement of bioavailability and suppression of side effect", International Workshop on Soft Interface Science for Young Scientists (SISYS2012), Tsukuba, Japan (2012.11.22).

10. Toru Yoshitomi, Long Binh Vong, Hirofumi Matsui and Yukio Nagasaki, Oral Nanotherapy by Redox Nanoparticle, 29th International Conference of Photopolymer Science and Technology (ICPST-29), Chiba, Japan (2012.6.27).

11. 長崎幸夫、Long Binh Vong、吉富 徹、松井 裕史、「レドックスナノ粒子による潰瘍性大腸炎に対するナノ治療法の開発」、第 98 回日本消化器病学会総会、京王プラザ、東京 (2012.4.19).

12. 沙 莎、吉富 徹、Vong Long Binh、Pennapa Chonpathompikunlert、松井裕史、長崎幸夫、「非ステロイド系抗炎症薬内包レドックスナノ粒子による消化管傷害の抑制と バイオアベイラビリティの向上」、日本バイオマテリアル学会シンポジウム 2012、仙台国際センター、仙台 (2012.11.27).

13. 長崎幸夫、Long Binh Vong、吉富 徹、松井裕史、Novel Redox Polymer Drug-New Oral Nanotherapy for Ulcerative Colitis、第 85 回日本薬理学会年会 2012 年 3 月 14 日、京都国際会議場、京都 (2012.3.14).

14. 長崎 幸夫、Long Binh Vong、吉富 徹、富田 勉、松井 裕史、大腸粘膜に対する経口型レドックスナノ粒子の集積と潰瘍性大腸炎治療、第 28 回日本 DDS 学会学術集会、札幌、2-C-03 (2012.7.5).

15. 吉富 徹、Vong Binh Long、今泉夏香、長崎幸夫、潰瘍性大腸炎に対するナノ治療、nanotech2013-第 12 回国際ナノテクノロジー総合展・技術会議(東京ビックサイト、東京 (2013.1.30-2.1).

16. Sha Sha, Long Binh Vong, Pennapa Chonpathompikunlert, Toru Yoshitomi, Hirofumi Matsui,

Chapter 6: Summary and Conclusion

Yukio Nagasaki, Development of Redox Nanoparticles for Treatment of NSAIDs-induced Small Intestinal Inflammation, 2nd International Conference on Biomaterials Science in Tsukuba (ICBS2013), Tsukuba, Japan, P098 (2013.3.19-22).

17. Sha Sha, Pennapa Chonpathompikunlert, Long Vong Binh, Toru Yoshitomi, Hirofumi Matsui, Yukio Nagasaki, "Protection of NSAIDs-induced small intestinal inflammation by redox nanoparticle", PL-14, MANA International Symposium on 2013, Epochal Tsukuba, Japan (2013.2.27-3.1).

18. 岩淵大輝, 唐澤直義, 松坂 賢, Vong Long Binh, 吉富 徹, 長崎幸夫, 島野 仁、酸化ストレスを消去する腸管非解離型ニロキシドラジカル含有ナノ粒子 (RNP -O) を利用した動脈硬化を利用した動脈硬化抑制の試み、つくば医工連携フォーラム 2014、つくば国際会議場、つくば (2014.1.20).

19. Yukio Nagasaki, Toru Yoshitomi, Kazuhiro Kuramochi, Long Binh Vong, Development of nitroxide radicals-containing polymer for ROS-scavenging in cigarette smoke, MANA International Symposium on 2014, Epochal Tsukuba, Japan (2014.3.5).

20. Md. Amran Hossain, Mayo Yamashita, Long Binh Vong, Yutaka Ikeda, Yukio Nagasaki, Highly stable PEGylated silica nanocomposite - A new drug carrier for oral drug delivery, MANA International Symposium on 2014, Epochal Tsukuba, Japan (2014.3.5).

21. 池田 豊、Amran Md. Hossain、Vong Binh Long、長崎 幸夫、抗炎症機能を併せ持つ経口投与剤を目指したシリカ含有ナノ粒子の開発と評価、第 30 回日本 DDS 学会学術集会、慶応大学芝共立キャンパス、東京 (2014.7.30).

22. 池田 豊、Md. Amran Hossain、Long Binh Vong、長崎 幸夫、抗炎症作用を有した有機-無機融合ハイブリッド経口投与ナノ粒子の構築と評価、第 63 回高分子討論会、長崎大学、長崎 (2014.9.26).

23. 長崎幸夫、Long Binh Vong、吉富 徹、松井裕史、レドックスナノ粒子の経口投与による炎症誘起化学発生大腸がんの治療効果、第 42 回日本潰瘍学会、慶応大学、東京 (2014.10.31).

24. Yutaka Ikeda, Amran Md. Hossain, Long Binh Vong, Yukio Nagasaki, Construction of highly stable

nanoparticle with high drug loading and anti-inflammatory properties for efficient oral delivery, 7th International Workshop on Advanced Materials Science and Nanotechnology (IWAMSN2014), Ha Long City, Vietnam (2014.11.4).

Awards

1. “**Best Poster Award**” Long Binh Vong, Tsutomu Tomita, Toru Yoshitomi, Kazuya Morikawa, Shinji Saito, Hirofumi Matsui, and Yukio Nagasaki, 2nd International Conference on Biomaterials Science in Tsukuba (ICBS2013) Tsukuba, Japan (2013.3.19-22).
2. “**Excellent Poster Award**” Long Binh Vong, Toru Yoshitomi, Hirofumi Matsui, Yukio Nagasaki, つくば医工連携フォーラム、つくば国際会議場、つくば (2014.1.20).
3. “**Excellent Poster award**” Long Binh Vong, Toru Yoshitomi, Hirofumi Matsui, Yukio Nagasaki, 第63回高分子学会春季年会, 3Pc135、名古屋国際会議場、名古屋 (2014.5.30).
4. “**Excellent Poster Award**” Long Binh Vong, Toru Yoshitomi, Hirofumi Matsui, and Yukio Nagasaki, The 10th SPSJ International Polymer Conference, Epochal Tsukuba, Tsukuba (2014.12.5).